MEASUREMENT OF PAVEMENT PERMANENT DEFORMATION BASED ON 1 MM 3D PAVEMENT SURFACE MODEL

By

Shi Qiu

Bachelor of Science in Logistics Management
Beijing Jiaotong University
Beijing
2007

Master of Science in Management Science and Engineering
Beijing Jiaotong University
Beijing
2009

Submitted to the Faculty of the
Graduate College of the
Oklahoma State University
in partial fulfillment of
the requirements for
the Degree of
DOCTOR OF PHILOSOPHY
December, 2013

MEASUREMENT OF PAVEMENT PERMANENT DEFORMATION BASED ON 1 MM 3D PAVEMENT SURFACE MODEL

Dissertation Approved:

Dissertation Adviser Dr. Kelvin C. P. Wang

Committee Member Dr. Michael Phil Lewis

Committee Member Dr. Xiaoming Yang

Committee Member Dr. Joshua Qiang Li

Outside Committee Member Dr. Terry Collins

ACKNOWLEDGEMENTS

First of all, I am extremely grateful to my advisor, Dr. Kelvin C. P. Wang, for his valuable guidance and encouragement in helping me complete this dissertation. Dr. Wang's rigorous attitude and scientific spirit set a great model for my future career. Without his constructive criticism and patience, I would not accomplish the degree. I would also thank Dr. Wang's wife, Lily Liu, who offers my family countless assistance and helpful advice.

My thanks go to Dr. Terry Collins, Dr. Michael Phil Lewis, Dr. Xiaoming Yang, and Dr. Joshua Li for serving on my dissertation committee. Not only have I learnt useful knowledge from their classes but I have also obtained substantial and meaningful direction during my difficult times in writing the dissertation. Other faculty members and staff of the School of Civil and Environmental Engineering (CIVE), the Graduate College, and Oklahoma State University (OSU) are also appreciated. I have been feeling at home with their dedication and service.

I would also like to express my thanks to Dr. Danny Xiao, Mr. Aonan Zhang, Mr. Weiguo Gong, Dr. Vu Nguyen, Mr. Lin Li, and Mr. Justin Thweatt for their sincere help and wonderful collaboration. Under Dr. Wang's leadership in Arkansas and Oklahoma, valuable friendships were developed in the past four years.

Thanks also go to the University of Arkansas (U of A), where I started my study in the United States. Specifically I should thank Dr. Kelvin Hall and Dr. Jim Gattis from the U of A, who opened the door for me to enter the world of transportation engineering. In addition, I would

like to thank Mr. Mike Moravec from Federal Highway Administration (FHWA), from whom I received precious information about the state of the art of the U.S. transportation system. I also thank Dr. Sue McNeil from University of Delaware, who has initiated the summer infrastructure symposium (AISIM) for graduate students. Her insight and mindset affect me significantly. I met with professional friends, established my network, learnt cutting edge knowledge, and broadened my horizon with two participations to AISIM and communications with Dr. McNeil.

Special appreciation belongs to the Chinese Scholarship Council (CSC) and Beijing Jiaotong University (BJTU). BJTU's recommendation and CSC's financial support made the four years a reality. I am indebted to my advisor in China, Dr. Xuewei Li, who is a visionary and charismatic leader both administratively and academically. It is his decisive motivation that set my mind on pursuing this degree.

I sincerely thank all my family members, my wife, my father and mother, and my relatives who have been supporting me and serving the family over the years.

Last but not least, for those organizations and people who helped me but were not listed in this acknowledgement, I do appreciate their generous help and will always remember.

Name: SHI QIU

Date of Degree: DECEMBER, 2013

Title of Study: MEASUREMENT OF PAVEMENT PERMANENT DEFORMATION BASED ON 1 MM 3D PAVEMENT SURFACE MODEL

Major Field: Civil Engineering

ABSTRACT: Measurement of pavement permanent deformation is critical to highway agencies for both pavement design and rehabilitation. Since the AASHO Road Test in the late 1950s and early 1960s, field rut condition is monitored by agencies on a regular basis. Over the decades, rut depth has been the solely dominating pavement permanent deformation indicator extensively used, though it faces many criticisms for being incomplete to characterize rut. The premature data collection technology, lack of uniform practice standard, and unrealistic expectations have hindered the improvement of rut measurement.

Recently, two AASHTO draft standard documents PP70-10 and PP69-10 are published specifying data requirements and procedures for deriving new technical parameters, respectively. It is envisioned that the mature application of the 1 mm 3D pavement surface data collected by PaveVision3D Ultra system in companion with the new standards poses a significant opportunity to change the landscape of current rut measurement practice.

This research described in the thesis accomplishes the following tasks to provide substantial insights into the new rut measurement requirements. First, thirteen technical parameters covering multiple aspects of pavement ruts are derived based on PP69-10. The rut depth measures documented in PP69-10 are verified with ground truth values. Second, a thorough study of these rut attributes is conducted with 8,960 transverse profiles collected from National Highway Systems (NHS) in Arkansas. The interrelationships among different technical parameters are explored, and inferences regarding pavement performance are developed. Third, a comprehensive hierarchical system is constructed for overall permanent deformation evaluation. The standardized index provided by the proposed system can help highway agencies manage pavement performance in a more comprehensive and reasonable manner. Fourth, the impact of vehicle wandering on the accuracy of rut measurements is assessed. A methodology is developed and verified to reduce the adverse effect of unknown lane locations.

Overall, this thesis demonstrates findings of a timely study in rut measurement and characterization based on the latest standard protocols and data collection technology. The research provides insights and useful supplements to both practitioners and researchers in the transition to apply the most advanced 1 mm 3D laser imaging technology to comprehensive pavement survey.

TABLE OF CONTENTS

Chapter Page

Chapter Page

Chapter Page

Chapter Page

Chapter Page

Chapter Page

LIST OF TABLES

LIST OF FIGURES

CHAPTER 1 INTRODUCTION

1.1 Background

Pavement system is one of the most important infrastructure assets of the nation. Over the years, bulks of the pavements in the United States have suffered from various distresses, among which rut is a very typical and commonly seen one (1, 2). Pavement permanent deformation, also known as rut, has long been the interest of pavement engineers and State highway agencies due to its critical roles in pavement design and management. The earliest rut measurement dates back to the AASHO Road Test in the late 1950s and early 1960s (3, 4), when the rut depth was manually measured and integrated into the calculation of Present Serviceability Index (PSI). Since then, manual measurement of rut depth has been incorporated in many State agencies' annual or biannual pavement condition monitoring programs. In consideration of unsafe setting, insufficient repeatability, tedious process, and labor-intensive nature of manual survey, a number of automated devices have gradually been developed for rut measurement. Despite the efficiency and effectiveness of data collection which have been significantly improved during the past two decades, most of the rut data from the field remain incomplete, inaccurate and inconsistent. These limitations prevent pavement researchers from establishing sound scientific principles in materials modeling and performance prediction of pavement systems.

In recent years the successful integration of the high-performance sensors, inertial units and positioning technology has resulted in sophisticated automated systems for reliable and comprehensive data collection. Very recently, an innovative 3D laser imaging system PaveVision3D Ultra (3D Ultra for short) engineered by WayLink System Co. is capable of automatically acquiring both 2D and 3D laser imaging data from pavement surface and reconstruct the 3D virtual pavement surface at 1 mm resolution at 60 miles per hour. This system breaks the constraints of historical line-of-sight technique and provides fundamentally novel data sets for engineers. How to exploit the new data sets for the purpose of pavement management and modeling becomes a new challenge to pavement engineers.

1.2 Problems and Objectives

Measuring pavement permanent deformation is an important activity in pavement management. On one hand, highway agencies use various types of manual or automated instruments to collect rut data. On the other hand, multiple standards and protocols have been published by different organizations to guide the characterization of rut with the collected data. According to these standards, characteristics of rut from collected data are used to determine the serviceability of pavements, plan maintenance strategies, and build deterioration models for pavement design. However, because of the limitation of the technology, incomplete data requirements, and lack of uniform standards, most of the historical data from field are problematic, which have hindered the effective decision making and sound pavement modeling. Furthermore, for decades rut depth has been the only measure extensively collected and used in current practice despite of many studies indicating that depth alone is insufficient to capture overall properties of rut.

The study of measurement of pavement permanent deformation has never ceased. However, since Simpson and the LTPP program conducted a series of research projects in the late 1990s and early 2000s, the systematic study of measurement of pavement permanent deformation

has rarely been revisited (1, 2). As a matter of fact, in the past decade that automated methodologies for pavement data collection have undergone revolutionary changes. The mature applications of new technologies such as the 3D Ultra system have changed the landscape of transverse profiling. The advances in data collection technology provide pavement engineers opportunities to examine different performance indicators of permanent deformation with bulks of data.

A recent development in terms of evaluation of pavement permanent deformation is the release of the AASHTO Designation: PP69-10 *Standard Practice for Determining Pavement Deformation Parameters and Cross Slope from Collected Transverse Profiles* (PP69-10 for short) (5) and the AASHTO Designation: PP70-10 *Standard Practice for Collecting the Transverse Pavement Profile* (PP70-10 for short) (6). These two standards are attached in Appendices A and B, respectively. PP70-10 specifies rigorous technical requirements for transverse profiling and PP69-10 proposes a set of parameters such as percent deformation, rut cross-sectional area, and water entrapment depth for the assessment of pavement permanent deformation.

With the advance in new data collection technology and release of new standards, the lack of consistency and reliability in the current practice of State highway agencies needs to be addressed. Although it is apparent that these new data sets based on the new technology will benefit the entire research field and industry, the adaptation of properly designed standards and protocols is required for field deployment of the new data sets. The most significant challenge is to demonstrate the effectiveness of the new rut measurements and convince the pavement engineers as well as management to adopt the new systems. To deal with these challenges, the general objective of this research is to provide insights into the new parameters derived from PP69-10 and promote the application of multiple parameters in characterizing rut. The following specific objectives are identified for this dissertation:

- To review the state of art in rut measurement and summarize the limitations.
- To demonstrate the applicability of 3D Ultra for transverse profiling per PP70-10 requirement.
- To derive multiple rut parameters based on PP69-10 with transverse profiles collected by 3D Ultra.
- To evaluate the effectiveness of the new AASHTO protocol PP69-10.
- To compare the current rut depth measures to the new rut depth measures based on PP69-10.
- To explore the interrelations between the derived parameters according to PP69-10.
- To explore the intrinsic relations between the technical parameters and pavement performance.
- To develop a set of standardized scales for each rut attribute derived from PP69-10.
- To combine multiple parameters into one single index for rut evaluation.
- To establish a comprehensive evaluation system to serve different stakeholders.
- To study the impact of vehicle wandering on the results of data derivation and develop a methodology to mitigate this impact.

1.3 Layout of Dissertation

Multiple research tasks are accomplished in this dissertation and are organized into relevant chapters based on their objectives. Figure 1.1 illustrates the general structure and flow of this dissertation. This chapter is an overview of the entire dissertation. The problems and objectives of this research are presented.

An in-depth literature review is documented in Chapter 2. Sources pertinent to this dissertation such as mechanisms of permanent deformation, traditional methodologies to measure rut, and different approaches to obtain rut attributes are reviewed and summarized therein.

In Chapter 3, the characteristics of 3D Ultra system and the applicability of data sets collected by 3D Ultra are first presented. Pavement transverse profiles collected with 3D Ultra are utilized to characterize multiple attributes of permanent deformation according to PP69-10. The problems encountered in the implementation process of PP69-10 are discussed.

Chapter 4 analyzes the relations between the rut attributes. The traditional methods for measuring rut depth and cross slope are compared with the PP69-10 method. Abnormal attribute values are identified. The interrelations between different measures derived from PP69-10 are examined. The prediction models for new measures are developed. Inferences to pavement performance are drawn based on the results of statistical analyses.

A comprehensive evaluation system for pavement permanent deformation is established in Chapter 5. Each single attribute is assessed with a subjective survey. Based on the survey results, scoring functions are elicited for all attributes, respectively. Three comprehensive evaluation methodologies are employed to construct the comprehensive system for rut evaluation.

The impact of vehicle wandering on the accuracy of PP69-10 measures is investigated in Chapter 6. Three machine learning based methodologies are used to reduce the errors produced by unknown lane position.

Chapter 7 serves as concluding remarks and recommendations for future studies.

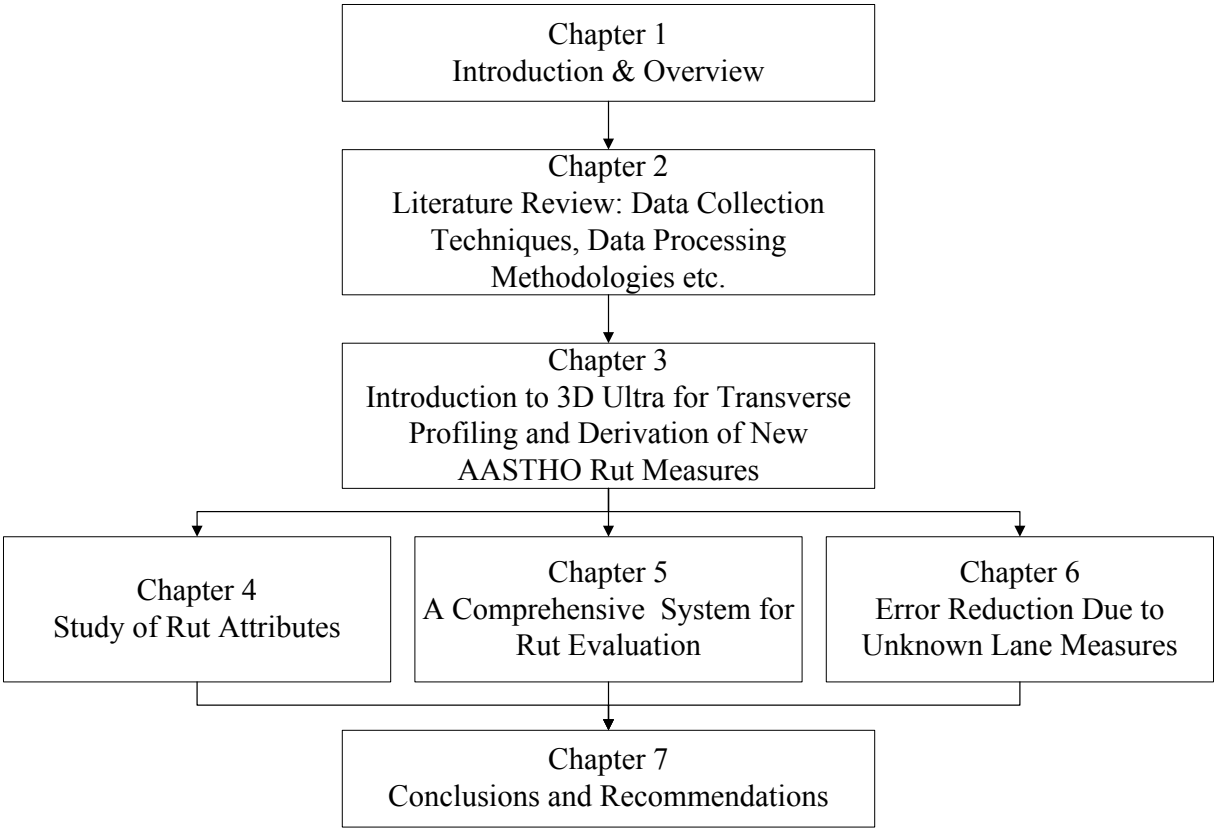

Figure 1.1 General Structure of This Dissertation

CHAPTER 2 LITERATURE REVIEW

2.1 Pavement Permanent Deformation

2.1.1 Definition

Rut is the longitudinal depression in the wheel-path of the asphalt surfaced pavements. As shown is Figure 2.1, rut is a very common and important distress in the nation's flexible pavement systems (1, 2, 7, 8, and 9). In the context of pavement engineering, "rut", "transverse deformation", and "permanent deformation" are interchangeable terms, all of which refer to this pavement depression phenomenon.

a. An Example of Pavement Rut on Highway

(Image taken by 3D Ultra on March 7th 2013, on US 65 North Bound near the junction of AR Highway 159)

b. An Example of Rut at Intersection with Pooled Water

(Image taken by Shi Qiu on, at Intersection of Hall of Fame and Washington St., Stillwater, OK)

Figure 2.1 Examples of Pavement Rut

2.1.2 Causes and Classifications

Most researchers agree that the primary cause of pavement rut is repeated loading whereas some holds an idea that the change of temperature is also a major contributor (8, 9, and 10). Systematically speaking, all factors that cause pavement deterioration considered in pavement design affect the formation and propagation of rut (9, 11, and 12). Internally, the thicknesses, materials, and other properties of the pavement surface and the sub-layers contribute to rut. Externally, environmental factors such as temperature and precipitation are also causes of rut in addition to heavy vehicles (9).

Based on its major mechanisms and physical characteristics, engineers categorize rut into different types (1, 9). Simpson and the LTPP program defined three types of ruts (1). The first type only involves the asphalt surface layer of the pavement. As illustrated in Figure 2.2a, it is the one-dimensional vertical compression of pavement surface. In this case, rare hump is accompanied with the downward depression on the surface. This type of rut is named post-construction densification. It normally results in low or moderate levels of damage to the pavement surface and is stable with time. The second type is the subgrade rut, in which deformation occurs in all layers of the pavements (Figure 2.2b). The third type is caused by lateral movement of the pavement surface layer. The uplift of surface are always associated with the downward depression in this category. Ruts are usually at moderate to high severity levels.

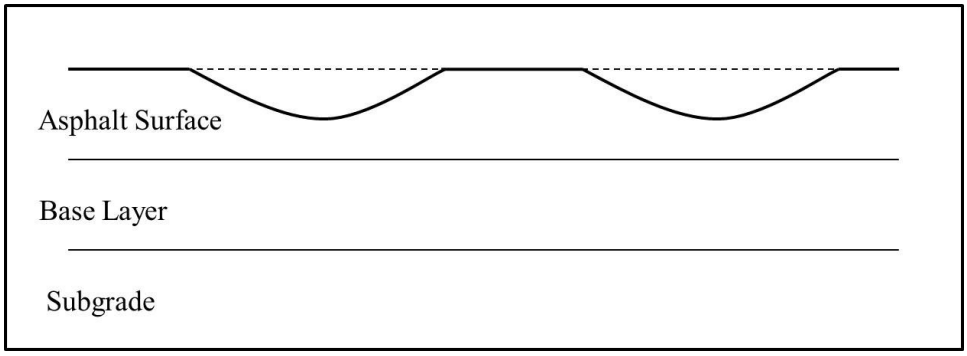

a. Type 1 Pavement Rut

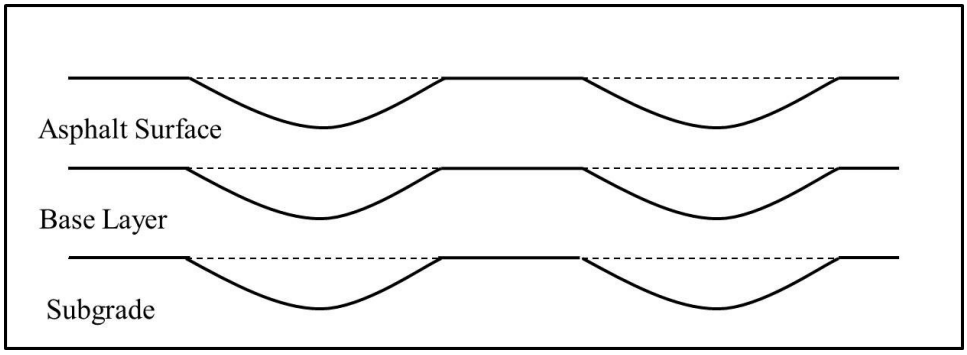

b. Type 2 Pavement Rut

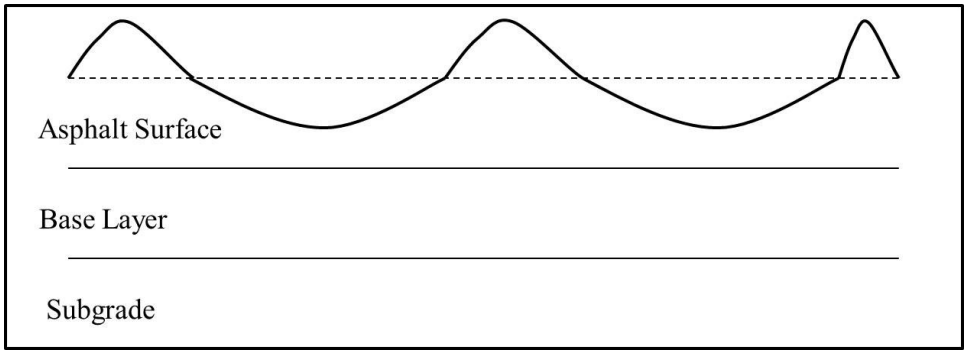

c. Type 3 Pavement Rut

Figure 2.2 Illustration of Three Types of Pavement Rut

(Figure modified based on Simpson (1), not to scale)

The normal nondestructive testing methods (NDT) are only able to measure pavement surface deformation. The rut underneath the surface is immeasurable unless pavement trenches (cores) are extracted. Due to the unavailability of trench data for in service pavements, rut generally denotes to the visible deformation on the asphalt surfaces in pavement management practice (13). Deformation in the layers other than the surface can be estimated by examining the shape of the surface (1, 2).

2.2 Significance of Rut Measurement and Analysis

Since the AASHO Road Test, collecting rut information from the field has become an important item in State highway agencies' annual or biannual pavement condition monitoring program. Rut plays significant roles in pavement research and pavement management practice:

First, rut condition is a straightforward and explicit indicator of soundness of pavement structure. Researchers can infer the cause and mechanism of the permanent deformation from the physical characteristics such as rut shape. Change of rut amount and severity level implies the propagation of deterioration in the pavement. Monitoring this process is significant in developing accurate prediction models (1, 2). In addition, rut is the depression in the wheel-paths, which are the portion of the pavements that bear the traffic loadings. The occurrence of rut may be frequently associated with other important pavement distresses such as fatigue cracking (9, 14). To prevent pavements from excessive deterioration, these distresses are the center of concern to pavement engineers.

Second, pavement engineers are prone to schedule maintenance and rehabilitation actions on the basis of rut performance (10). In many State agencies, the measured rut depth serves as a trigger for overlay or other pavement rehabilitation actions. Furthermore, understanding the rut type is critical to engineers in terms of selecting optimal countermeasures. For example, simple overlay would just be a temporary medication to the subgrade rut (1). Additionally, the

rehabilitation costs can be estimated from the physical rut information, which is helpful to funding allocation.

Third, the presence of rut harms pavement functionality. Pavement smoothness is reduced with the growth of rut, which is sensitive to the vehicles and pavement users. The new pavement design guide (MEPDG) incorporates rut depth into prediction models for International Roughness Index (IRI) (9). Rut could cause pool of water in the pavement wheel-path (Figure 2.1b), which is associated with driving safety (15). The excessive water on pavement surface may result in hydroplaning, which is extremely dangerous to the traffics (16). Meanwhile, the wheel-path water generates spray and splash, which are potential hazards.

Last, but not least, rut is an indispensable indicator in pavement design guide and a principal item in comprehensive pavement evaluation systems. The amount of rut depth is incorporated in the formula of calculating Present Serviceability Index and therefore included in the AASHTO 1993 pavement design guide (4, 14, and 17). MEPDG predicts rut depth as a criterion for life-long pavement failure indicator (9). Comprehensive pavement information systems such as Long-Term Pavement Performance program (LTPP) and Highway Performance Monitoring System (HPMS) require rut information for record (13, 18). Rut also deducts scores in the Pavement Condition Index (PCI) system (19).

2.3 Review of Relevant Studies

Permanent deformation is an important study area in pavement engineering. Substantial attentions have been paid to different aspects of rut related problems. The topics can be categorized into three major types:

- Rut modeling and prediction. Technically, these studies include methods based on mechanistic, or empirical approaches, or combination of both. Mechanistic studies

involve analysis of mechanics, usually the impact of different types of stress on plastic deformation of materials. For example, Park developed a non-linear infinite model to simulate the resilient response in low volume load-zoned pavements so as to evaluate propagation of rut (20). In empirical studies, different factors that affect rut are compared with the actual deformation measures. Omar tested the relation between different combinations of air voids and temperature and rut formation (21). Naiel modeled propagation of rut depth for different climate zones (12). Ali and Tayabji utilized the collected transverse profile data to predict the plastic deformation parameters of pavement layers (22). Also, some studies for mechanistic-empirical modeling were conducted. Al-Suleiman et al. examined the major contributions of rut based on their field and laboratory data (23). By comparing several methodologies on life-long rut depth prediction, Yang et al. found that empirical methods are more reliable than mechanistic models (24).

- Automated rut measurement devices and their reliability. Over the years, automated devices are developed for rut data collection and studies conducted to demonstrate and promote the applications of these technologies. For example, Obaidat et al. introduced a system with stereovision technology to quantify rut depth (11). Wang proposed a 3D laser system for measurement of rut and other pavement distresses (25). In papers published by Tsai et al. and Huang et al. 3D systems capable of collecting continuous transverse profiles were introduced (26, 27). The accuracy and precision of the new 3D systems were demonstrated in their studies.
- Technical parameters for rut characterization and their applications. Some researchers focused on the derivation of the technical parameters for rut characterization. Simpson conducted a series of studies on rut characterization, including selection of rut parameters, relating rut parameters to mechanism and so on (1, 2, and 28). Chen and Li

compared five different algorithms for rut depth calculation (29). Meanwhile, some researchers investigated the impact of rut attributes on pavement functionality. Fwa et al. evaluated skidding and hydroplaning phenomenon based on rut depth (16). Hou et al. discussed the selection of rut parameters from the perspectives of traffic safety such as hydroplaning (30).

In addition to the three major categories, some studies in other major research areas such as network optimization problems also involve rut. For example, Li introduced a topological ordering based cluster algorithm for the segmentation of homogenous rut sections (31). Also, some researchers contributed to developing techniques to rehabilitate pavements with rut (10). From these studies, it is found precise and accurate rut measurement is the precondition of reliable rut prediction models.

2.4 Rut Data Collection

2.4.1 Overview

A variety of manual and automated rut survey methodologies have been developed to assist pavement engineers monitoring rut condition. Table 2.1 lists most of the commonly used devices for rut data collection over the years. In practice, manual systems are limited to project level data collection because they are relatively static and have to interrupt traffic; however their accurate result is an exclusive advantage. Comparing to manual surveys, the advantages of the automated survey systems are evident: less labor consuming, safer work setting, more objectivity, higher efficiency and better repeatability. More noticeably, current automated systems for transverse profiling are able to work at traffic speed without lane closures. Generally, automated systems are more frequently used in network level surveys. In some applications, the manual systems are adopted for the calibration of automated devices.

Table 2.1 Summary of Common Devices for Rut Data Collection

Type	Device	Brief Introduction	Comments
Manual Systems	Straightedge and Gauge	Place the 1.8 m straightedge across the wheel-path, and then use the gauge to measure the maximum vertical or perpendicular distance between pavement surface and the straightedge.	ASTM standard and LTPP have different definitions for measuring rut depth.
	Stringline and Gauge	Use the 3.7 m stringline to stretch across the pavement lane. The stringline only touches the peaks of pavement. Then measure each wheel-path like straightedge method.	Adopted by LTPP program.
	Walking Profiler	A device looks and operates like a lawnmower. Measure elevation points of the transverse profile every 241 mm.	Developed by Australian Road Research Board.
	Dipstick Profiler	Two feet of the Dipstick are spaced 305 mm. Measure the transverse profile by stand one foot and rotate the other.	Adopted by LTPP program.
Automated Systems	3-Point Rut Bar (South Dakota Profiler)	3 acoustic sensors mounted along the rut bar of the van to detect the distances from the bumper to pavement surface. One sensor in the middle of the bumper and the other two over each wheel-path.	Can only cover partial lane per restriction of width, which in consequence may underestimate rut.
	5-Point Rut Bar	Similar to 3-Point rut bars, 5 acoustic sensors usually spaced 813 mm between two outside ones and 406 mm between the inside ones.	It has the same deficiency but more accurate than the 3-point rut bar. Number of sensor can further increase to improve accuracy.
	Rut Bars with Many Sensors	Up to 37 ultrasonic sensors to collect transverse profile data.	The 37-sensor version system is able to cover full lane, but exceeds the width limit by some States' law.
	Scanning Laser Rut Bar	Laser mounted on the rut bar scans along the bar to collect a continuous transverse profile.	The laser-based rut bar is the predominant method in current automated rut data collection.
	Optical Systems	A camera and a strobe mounted on the van. The camera takes picture of the shadow projected from a preset line. The line is the digitized to transverse profile.	Illumination has been updated to laser now. Ever adopted by LTPP program.

The basic mechanism of the automated transverse profilers is to measure the relative height (elevation) of a finite number of points on pavements surface. Various types of sensors with different physical principles can serve this purpose. As summarized in Table 2.1, the typically used sensors include point laser, scanning-line laser, acoustic, optical, and ultrasonic and so on. These sensors are mounted on either front or rear of the data collection vehicle. For point laser, ultrasonic, and acoustic systems, the number of sensors determines the number of elevation points that can be measured. This number is called the resolution of data in rut measurement

terminology. Regardless of vehicle wandering, the position of the collected elevation points along the transverse direction depends on the mounting location of the sensors. Usually, engineers' interests are centered on the middle points of both wheel-paths.

The systems equipped with point laser, acoustic, and ultrasonic sensors are only able to collect low resolution pavement transverse profiles. The maximum number of elevation points ever developed and used in the field is 37 with ultrasonic sensor. However, a 3.7 m wide bar needs to be mounted in this case, which is too wide and causes severe safety issues on in-service roadways. By contrast, the optical scanning laser systems are capable of obtaining significantly more elevation points. In 2004, a promising laser system was claimed to have a resolution of 1,280 points per transverse profile (32). Generally, the laser technology based systems achieve a better accuracy and repeatability.

A questionnaire survey was conducted in 2004 to investigate the state of practice of rut measurement (32). 46 out of 56 responding State or Province agencies in both US and Canada used automated rut bar systems to collect rut data, 32 of which adopted the 3-point or 5-point rut bars while the rest used similar systems with more sensors. A more recent telephone interview was carried out by Texas DOT in 2007 (29). According to the responses from 24 State agencies, 13 of them used a 37 sensor ultrasonic rut bar; 5 of them used a scanning laser profiler with collected points from 960 to 1,280; and 5 of them used a point laser rut bar. Only one agency applied manual measurement.

2.4.2 Classification of Devices

Based on their output information, the data collection systems can be categorized into two types. The Type 1 devices measure a very limited number of elevation points. The rut depth is a direct measure from the Type 1 devices. Commonly seen devices include the straightedge/stringline and gauge, 3-point and 5-point rut bars. As shown in Figure 2.3a, the straightedge and gauge only

measures the maximum rut depth. Figure 2.3b shows the 3-point and 5-point rut bars to identify the maximum rut depth in both wheel-paths of the pavements. As illustrated in Figure 2.2, the pavement surfaces with occurrence of rut can present various forms of shapes that substantially deviate from the original true plane. The 3-point and 5-point rut bars are difficult to capture the actual maximum rut depth due to irregular rut shape and vehicle wandering. Therefore, Type 1 devices are no longer regarded as a reliable and repeatable rut measurement instrument.

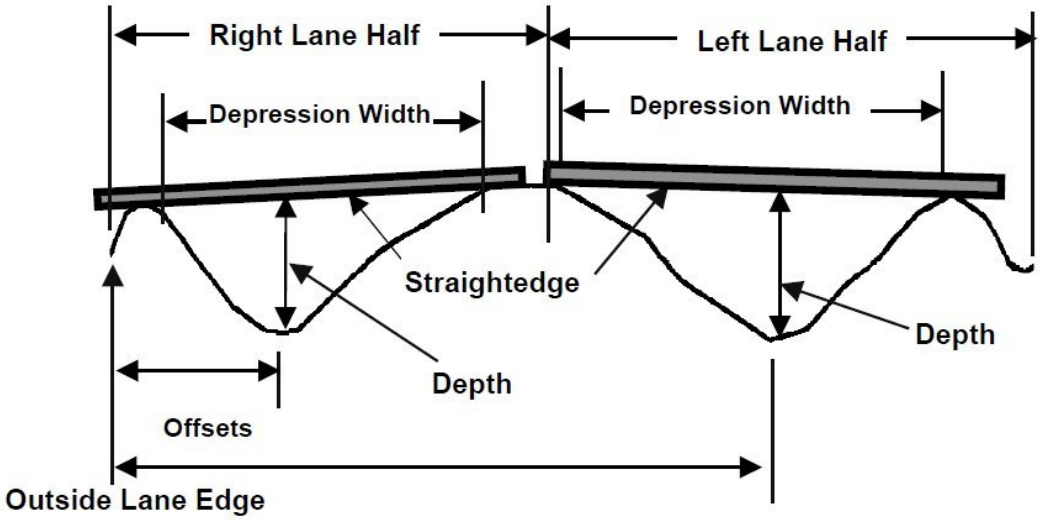

a. Illustration of Straightedge Rut Depth Measures

(Figure adopted from Elkins et al. (33))

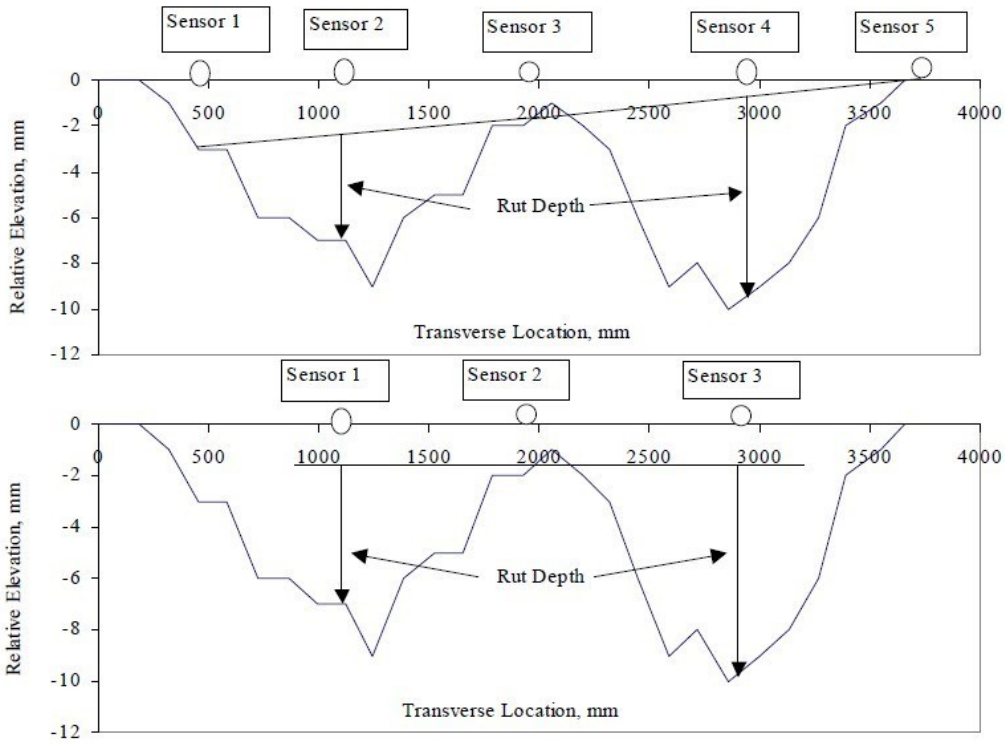

b. Illustration of 5-point and 3-point Rut Bars for Rut Depth Measures

(Figure adopted from Simpson (2))

Figure 2.3 Illustration of Type 1 Rut Measurement Devices

The Type 2 devices are able to measure significantly more elevation points, which are adequate to generate transverse profiles. This type of devices includes some manual devices such as walking Profiler (Figure 2.4a), the rut bars equipped with more sensors, and some line-laser-based continuous transverse profilers (Figure 2.4b). Research demonstrates that if a minimum of 9 elevation points along the transverse direction can be acquired with proper interval, the transverse profile is able to be interpolated with an acceptable accuracy (1). The collected transverse profile needs to be post-processed to further acquire useful rut information.

a. Illustration of Walking Profiler (Photo adopted from the manufacture's brochure (http://www.arrb.com.au/Equipment-services/Walking-Profiler-G2.aspx))

b. Illustration of Automated Rut Bars (Photo adopted from manufacture's presentation (http://pavement.engineering.asu.edu/wordpress/wp-content/uploads/2013/02/Robson.pdf))

Figure 2.4 Illustration of Type 2 Rut Measurement Devices

2.5 Rut Characterization

2.5.1 Pavement Transverse Profile

The current prevailing systems collect pavement transverse profiles for rut analysis. According to Sayers and Karamihas (34), *a profile is a two-dimensional slice of the road surface, taken along an imaginary line*. Conventionally, the profiles taken along the longitudinal and transverse direction of the pavement are collected for analysis. As illustrated in Figure 2.5, *transverse profile is the intersection between the road surface and a reference plane perpendicular to the road surface and to the lane direction* (35). A true transverse profile can only be obtained by taking a trench of the pavement surface layer, which is too costly and therefore unrealistic in practice. As an alternative, pavement engineers use the above introduced Type 2 devices to measure the transverse profile.

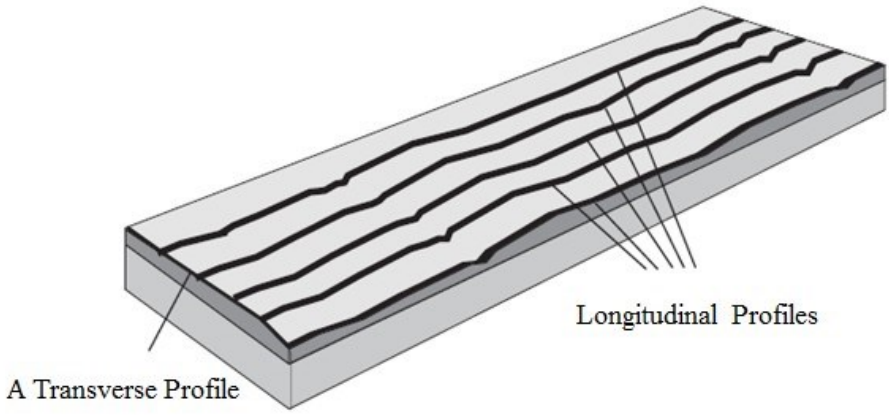

Figure 2.5 Illustrations of Pavement Profiles

(Figure modified from Sayers and Karamihas (34))

A transverse profile has three dimensions, the length, the height, and the width. Theoretically, an ideal transverse profile should be a continuous line which has a length of a

pavement lane width. However, existing data collection technologies are only able to collect a limited number of elevation points along the pavement transverse direction. It is evident that the more points a system can collect the higher resolution the data have. For those systems which cannot collect a sufficient number of points, interpolation is a necessary step to obtain a continuous transverse profile. If the gap between two consecutive points is small enough, then no further interpolation is required. The height of the transverse profile is the elevation of the points collected. Theoretically, the points of a perfect pavement surface should be on a straight-line. The variations of height represent the distortion of the pavement surface. The width of a transverse profile usually depends on the measurement device. Currently, a high resolution profiler can collect 1 mm wide transverse profiles. However, the width of a transverse profile is not specified in any standard.

2.5.2 Rut Parameters

A complete transverse profile contains valuable information such as cross slope of the pavement, rut shape and amount, and other distresses. However, it is unrealistic to directly use transverse profile to make engineering judgment. Therefore, pavement engineers introduce technical parameters such as rut depth and rut width to characterize the condition of permanent deformation and infer its mechanisms (22).

There are various standards, protocols, or publications that are relied on to standardize the data reduction from transverse profile data. Pavement engineers can therefore reduce the transverse profiles to a handful of simplified technical values or indices. For the purpose of comparison, some of the commonly used rut parameters are summarized in Table 2.2.

Table 2.2 Commonly Used Technical Parameters for Rut Evaluation

Technical Parameters	Definition and Data Processing Methodology	Degree of Wide Use/Application of Standard
Rut Depth (Two Methods)	Straightedge method: the concept is similar to that of the manual surveys in Table 2.1. Only the 1.8 m straightedge is a fictive one.	The most widely used parameter, required by almost every standard.
	Stringline method: the concept is similar to that of the manual surveys in Table 2.1. Only the 3.7m stringline is a fictive one.	
Rut Width (Two Methods)	Straightedge method: the rut width is the horizontal distance or straight-line length between two points on which the straightedge rests where the rut depth was obtained.	Used along with rut depth but is not always collected.
	Stringline method: the rut width is the horizontal distance or straight-line length between two peaks where the stringline touches the pavement surface around the location of the maximum rut depth is occurred.	
Rut Cross-Sectional Area (Three Methods)	Positive area: the area between a straight-line which connects two end points of the transverse profile and the pavement surface above the line.	Not very common in most of the protocols, but is proposed by LTPP.
	Negative area: the area between a straight-line which connects two end points of the transverse profile and the pavement surface below the line.	
	Fill area: uses a stringline to stretch across the profile and measure the area between the stringline and pavement surface.	
Cross slope (Two Methods)	Regression line method: the slope of the regression line through the transverse profile (Need at least seven points equally spaced across the profile).	Used in some European countries.
	Edge points method: the slope of the straight-line connects two edge points of the transverse profile.	

2.5.2.1 Rut Depth and Width

Rut depth is the universally used indicator for rut measurement. In the light of manual survey, two methods are developed to derive rut depth based on collected transverse profiles: the straightedge and stringline methods.

The straightedge method stems from the manual straightedge and gauge method. Physically, by placing the straightedge on the left or right half of the lane, the rut depth is taken. A 1.2 m straightedge was the prevailingly used method in AASHO and early LTPP program (3, 13). However, it was uncovered that a straightedge less than 1.8 m in length is inadequate to rest across the entire wheel-path (28). Therefore, by placing a fictive 1.8 m straightedge on left and

right wheel-path of the collected transverse profiles, the rut depth measures of the two wheel-paths are calculated, respectively. There are two different measures of rut depth can be obtained from the straightedge method. The first one is the LTPP standard, which is also proposed by Simpson. As shown in Figure 2.6a, the rut depth is defined as the largest vertical distance between the pavement profile and the straightedge. However, the ASTM standard defines the rut depth as the length of the perpendicular line from the lowest point of the profile to the straightedge, as can be seen in Figure 2.6b (36). It is apparent that ASTM standard can lead to a smaller value of rut depth.

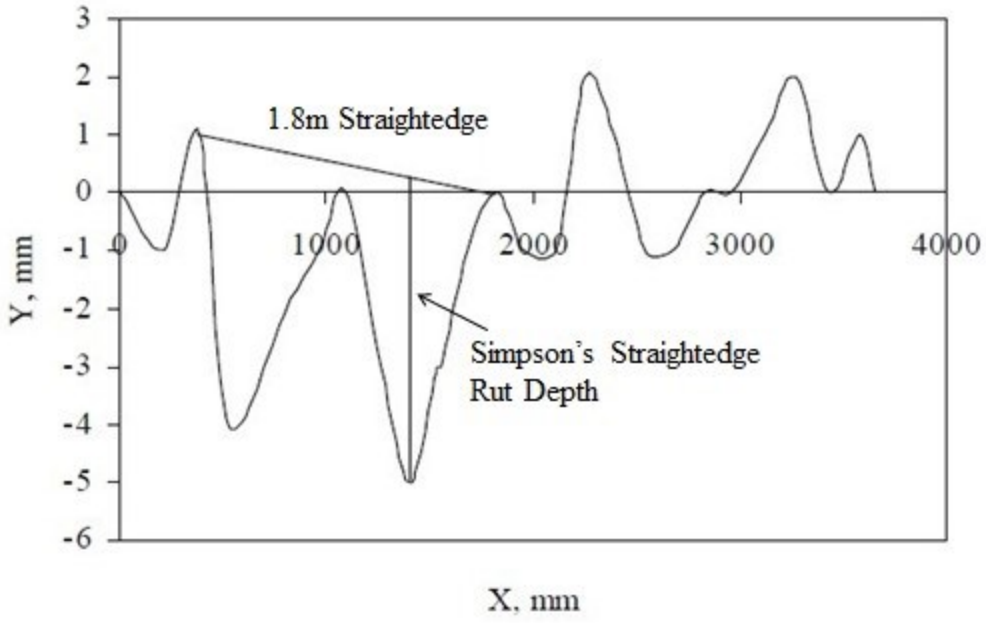

a. Rut Depth Measurement by 1.8 m Straightedge with Simpson's Method

(Figure modified from Simpson (2))

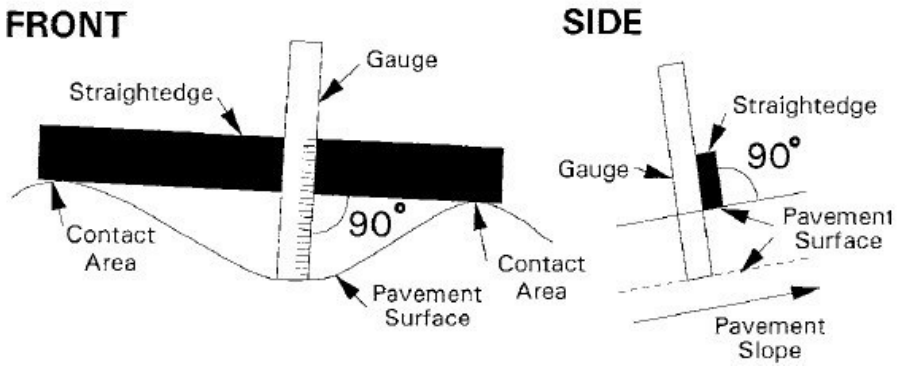

b. Rut Depth Measure by Straightedge with ASTM Method

(Figure adopted from ASTM E1703 (36))

Figure 2.6 Comparison of Two Rut Depth Measures

As illustrated in Figure 2.7, the rut width is determined by the two points where the straightedge rests. There are two different methods for rut width quantification. The first one is the straight-line length of the line connecting two points. The second one is the difference of the transverse location between the two points, as defined by Simpson (2). Apparently, the second measure of rut width cannot be greater than the measure from the first.

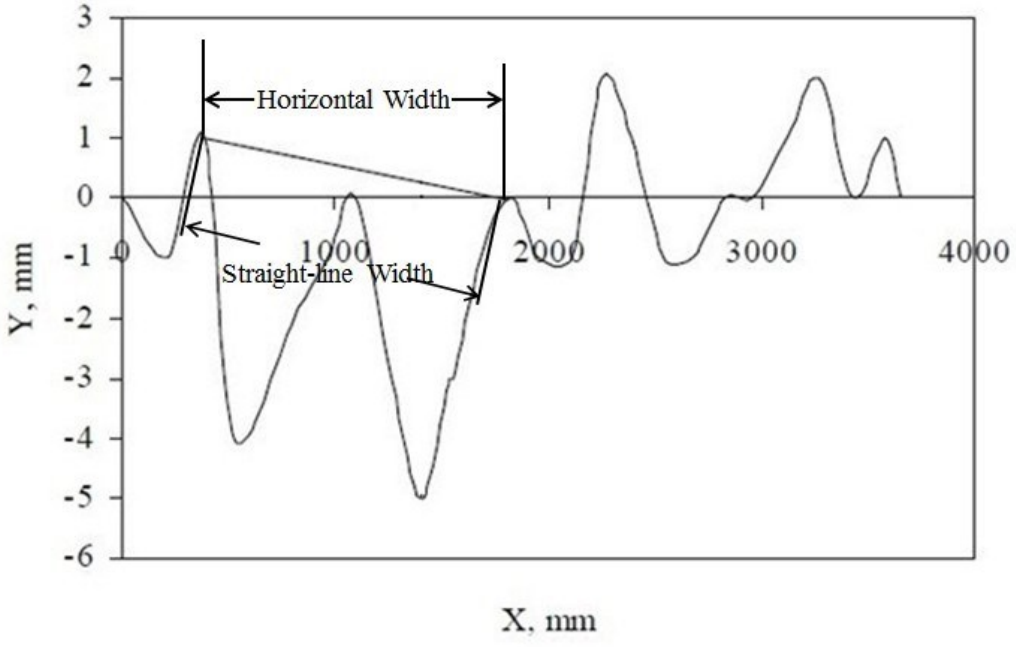

Figure 2.7 Illustration of Two Rut Width Measures

(Figure modified from Simpson (2))

The stringline method is called tensioned wire method in Europe. In manual survey, the length of the stringline should not be shorter than the pavement lane width. Being different from the straightedge, the stringline touches all the peak points of the transverse profile disregarding the location of wheel-path. The maximum vertical distance between the profile and the stringline in each half side of the lane is taken as left and right rut depth measures, respectively. The rut width is the length of the portion of the stringline between two peaks where the stringline touches the pavement surface around the location of the maximum rut depth is occurred. Similar to straightedge method, rut width can also be calculated differently. As shown in Figure 2.8, the stringline method may produce the same results with the straightedge in some cases; however, the results can be different with certain shapes of transverse profiles, in which the middle humps are skewed.

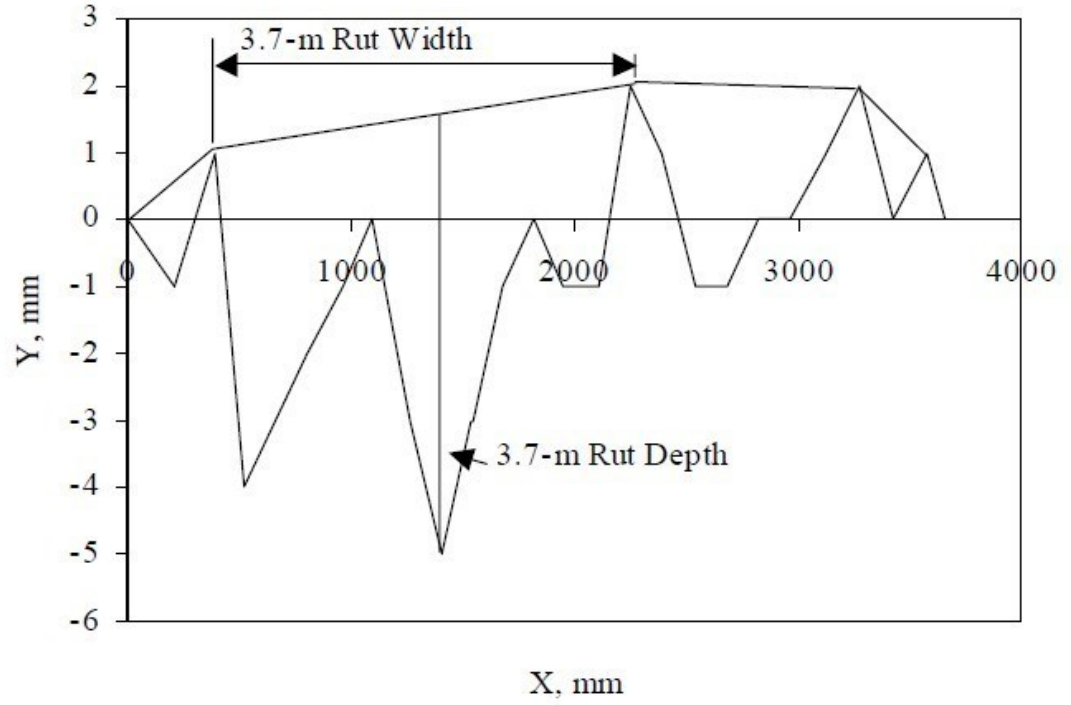

Figure 2.8 Illustration of Stringline Method for Rut Depth and Width Measurement

(Figure adopted from Simpson (2))

Note that the two edges of transverse profile must be leveled by rotating one side to the same level of the other side before all straightedge and stringline rut depth analyses (2).

2.5.2.2 Other Attributes

As listed in Table 2.2, the cross slope describes the general shape of the transverse profile. It is an indicator of driving safety and water run-off. The comparison of the measured cross slope with the original design scheme is meaningful. However, the cross slope is rarely reported in current practice due to device inadequacy. Rut cross area is a two-dimensional measure of rut depression; however it is also seldom used in practice because of technology constraints. In addition to those

listed parameters, some other indices such as radius of curvature and water height are occasionally used in studies.

2.6 Limitations in Current Practice

Even though rut data collection technologies, especially automated data instruments, and standards for rut characterization were updated several times over the years, some limitations in current practice are summarized as follows:

- Lack of operating standard for data collection. The parameters of rut are very sensitive to the survey device (35). However, many in-service instruments are inadequate in producing high quality data. The most significant problems are the total width of coverage and resolution. These limitations bring up inaccuracy and weak repeatability. Studies reveal that the discrete transverse profile measurements of limited points result in loss of information, always underestimating rut depth (1, 9). The lack of uniform operating standard in data collection leads to incomparable and unreliable data. For example, the AASHTO R48-10 rut depth protocol requires a minimum of five sensors (37). However, data demonstrate that the 3-point and 5-point rut bars produce unreliable results and need to be obsolete.
- Lack of practicing standard for data processing. Various protocols and standards proposed different methodologies for rut depth measurement. However, most of these standards do not provide standardized algorithms or specific procedures to derive rut parameters on computer systems. Difference in details of the computation process may produce different results, which causes low repeatability of data. Also, agencies use different protocols, which produce different results as well. This inconsistency prevents historical data comparison, which affects agencies and pavement engineers' trust in the data quality.

- Lack of a standardized evaluation system. Based on current rut depth measurement, the average value of left and right wheel-path rut depth measures are recorded; while in some cases the maximum value or both numbers are reported. This is an undesired practice because important information can be lost and the resulting information can be biased. In addition, when the rut depth measures are interpreted for pavement performance evaluation, the agencies tend to categorize the rut depth values into a few grades. The five-grade and three-grade systems are commonly used (35). However, inaccurate results are produced under this kind of systems. For example, if the threshold depth for "good" and "fair" condition is 15 mm, a 14.9 mm rut depth and a 15.1 mm rut depth are categorized into two separate levels despite their actual difference is small.
- Traditional process. Various technical parameters are introduced for pavement deformation characterization but rut depth is the only universally used parameter in the past decades (28, 35). Although researchers and agencies have been realizing that only using rut depth is insufficient for pavement modeling and evaluation of rut mechanisms, this custom remains unchanged for years.

2.7 Summary

Relevant studies of pavement rut are reviewed in this chapter. Basics of pavement permanent deformation and its measurement are outlined. Specifically, systematic comparisons of different automated systems, rut characterization methodologies using data produced with different instruments and protocols are summarized. The reviews present a holistic picture of this study area. The weaknesses in current rut measurement practice are summarized.

Note that only the methodologies currently in use for rut measurement are evaluated in this literature review. The recent development the draft AASHTO Standard Practice PP69-10 specifies a dozen of technical parameters for rut characterization for the first time. The in-depth

discussion of this protocol is proposed in Chapter 3. Furthermore, the introduction to statistical and modeling methodologies used in this research and their literature reviews are presented in their respective sections.

CHAPTER 3 NEW AASHTO MEASURES OF PERMANENT DEFORMATION

3.1 General

Recently, two important developments are prone to change the current rut measurement systems. One is the publication of two AASHTO draft standards: The AASHTO Designation: *PP70-10 Standard Practice for Collecting the Transverse Pavement Profile* (PP70-10 for short) (6) and AASHTO Designation: *PP69-10 Standard Practice for Determining Pavement Deformation Parameters and Cross Slope from Collected Transverse Profiles* (PP69-10 for short) (5). The other is the field application of 1 mm 3D pavement surface model produced with PaveVision3D Ultra (3D Ultra in short) system on pavement transverse profiling. From data collection to extraction of parameters, these two developments may fundamentally change how pavement ruts are measured and analyzed. In this chapter, the new technology for transverse profiling, derivation of the new rut parameters, and evaluation of new standard PP69-10 are proposed.

3.2 PaveVision3D Ultra System

Data collection is the foundation of rut characterization. Recently, the landscape of data collection based on the line-of-sight technique is changed with the invention of the PaveVision3D Ultra (3D Ultra in short) system.

Digital Highway Data Vehicle (DHDV), developed by the WayLink Systems Corporation, has been evolved into the sophisticated system to conduct full lane data collection on roadways at highway speed up to 60 mph (about 100 km/h).

With the latest 3D Ultra, the resolution of surface texture data in vertical direction is about 0.3 mm and in the longitudinal and transverse direction is approximately 1 mm at 60 mph data collection speed, which cannot be achieved with any other 3D systems today. The 3D line rate of the new 3D Ultra can be as high as 28,000 per second by using custom circuit boards and multiple high performance 3D cameras. Figure 3.1 shows the exterior appearance of the DHDV equipped with the 3D Ultra technology. Like most of the data collection systems, DHDV consists of its hardware and software system.

Figure 3.1 A DHDV with PaveVision3D Ultra

3.2.1 Hardware System

With the high power line laser projection system and custom optic filters, DHDV can work at highway speed during daytime and nighttime and maintain image quality and consistency. 3D Ultra is the latest imaging sensor technology that is able to acquire both 2D and 3D laser imaging data from pavement surface through two separate left and right sensors. Each sensor in the rear of the vehicle consists of two lasers and five special-function cameras. For the two lasers, one is for

providing 2D visual illumination and the other one is for providing the 3D data illumination. For the five cameras, four cameras are for capturing 3D laser illumination and the other one is for capturing 2D laser illumination. The working principle of camera and laser is shown in Figure 3.2. In addition, a video camera is mounted at the front of the vehicle for Right of Way (ROW) data collection.

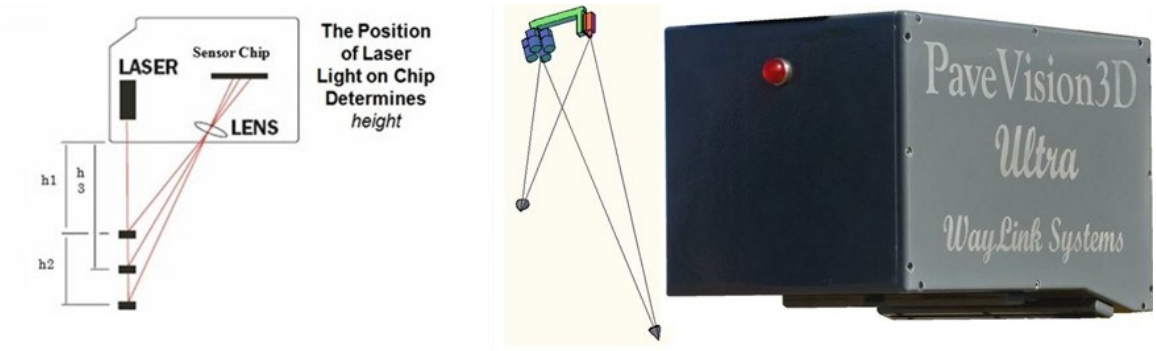

Figure 3.2 Working Principles of Sensors in 3D Ultra

Furthermore, the positioning data collections (including high-frequency differential GPS receiver, Distance Measurement Instrument, and Inertial Measurement Unit (IMU)) are incorporated into the 3D Ultra to provide geographical references of the collected data. Before every data collection, a system calibration is also mandatory to ensure precision and accuracy. The major calibration items include the distance measurement calibration, 3D height and flatness calibration, 3D sensor alignment calibration, 2D and 3D offset adjustment, and so on.

3.2.2 Software System

The 3D Ultra system installs two key software applications, which are the 3D Automated Distress Analyzer (ADA3D) and the Multimedia based Highway Information System (MHIS).

3D Automated Distress Analyzer (ADA3D) is the primary data processing tool. By implanting the sophisticated algorithms, ADA3D is currently capable of conducting automated

rut, cracking, roughness, and texture analyses at 1 mm resolution in real time at highway speed. Semi-automated distress analysis is also feasible. Different protocols are coded in ADA3D.

MHIS-3D Deluxe is a comprehensive application interface to view the collected data sets and the automated processed distress data. It provides the users with a 2D and 3D graphical representation of all the data sets collected with 3D Ultra DHDV. MHIS does not analyze the distress per se; instead, it is an auxiliary tool to visualize and display all the collected data sets, including 3D, 2D, and Right of Way (ROW) images. In addition, MHIS-3D Deluxe can also assist the users to edit and add various distresses. An example of MHIS interface with displayed 3D pavement surface image is illustrated in Figure 3.3.

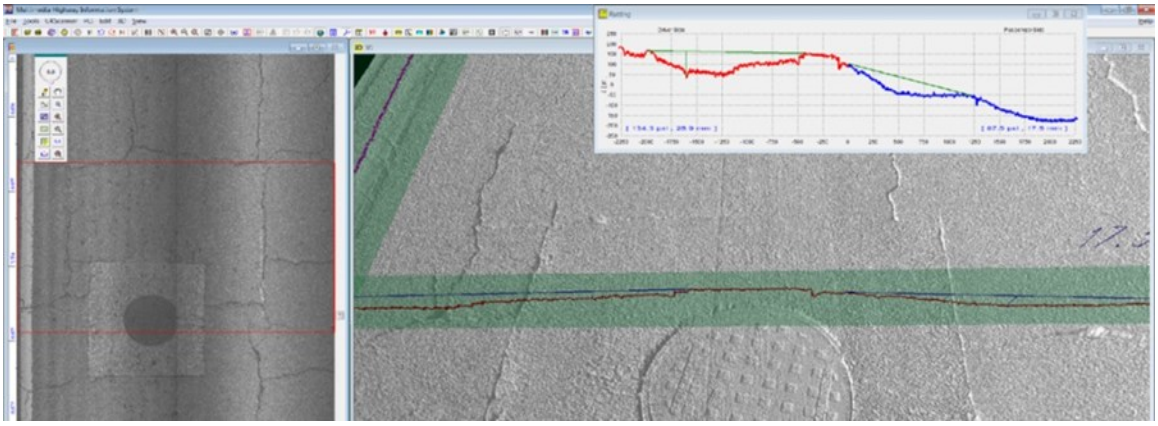

Figure 3.3 MHIS Interface with Displayed 3D Pavement Surface

3.3 Data Collection with 3D Ultra

3.3.1 PP70-10 Requirements

Recently, the AASHTO Designation: PP70-10 *Standard Practice for Collecting the Transverse Pavement Profile* (PP70-10 for short) was released to provide a practicing standard for transverse profile data collection (6). The minimum technical requirements of transverse profiles for analysis are specified in PP70-10. Some key requirements are summarized as below:

- The transverse measurement width should be at least 4,000 mm (13 ft), which is sufficient to cover the whole lane with vehicle wandering.
- The collected elevation points on the transverse profile should not be separated more than 10 mm (0.4 in.), which means at least 400 points need to be collected if equally distributed.
- The vertical resolution should not exceed 1 mm (0.04 in.).
- The longitudinal interval of collected transverse profiles should not exceed 3.0 m (10 ft) in network-level data collection and 0.5 m (1.5 ft) in project-level data collection.

This standard is meaningful to transverse profiling as it quantifies the minimum technical requirements for the transverse profiling systems. Different systems meeting the minimum requirements may produce consistent transverse profiles for practice and research.

3.3.2 3D Ultra for Transverse Profiling

In this research, 3D Ultra system is used to collect pavement transverse profiles for all analyses. 3D Ultra simultaneously takes both 2D and 3D images at about 1 mm resolution. For a detected pavement section, the same numbers of 2D and 3D images are produced. Both 2D and 3D images have 4,096 pixels transversely and 2,048 pixels longitudinally; each pixel corresponds to a 1 mm point on the actual pavement surface. Thus, each image represents an area with fixed transverse width of 4,096 mm (161 in.) and longitudinal length of 2,048 mm (80 in.). Computationally, each image is a matrix A with 2,048 rows and 4,096 columns, as shown in Equation 3.1.

$$A = (a_{i,j})_{2048\times4096} = \begin{pmatrix} a_{1,1} & a_{1,2} & \cdots & a_{1,4096} \\ a_{2,1} & a_{2,2} & \cdots & a_{2,4096} \\ \vdots & \vdots & \ddots & \vdots \\ a_{2048,1} & a_{2048,2} & \cdots & a_{2048,4096} \end{pmatrix} \quad (3.1)$$

3.3.2.1 3D Data

For 3D images, the values of the elements $a_{i,j}$ in the matrix A can be used to express two different types of information. The first type is called range data, which are the relative elevations (heights) of the pavement surface. Each $a_{i,j}$ stands for a pixel, the value of which is the relative height of its corresponding point on the pavement surface. After calibration, each pixel represents 0.3 mm of the actual pavement surface elevation. This elevation value is the most valuable information to transverse profiling. In 3D images, each row in the matrix A composes a transverse profile, which is constituted of an array with 4,096 elements. Each image contains 2,048 transverse profiles with a gap of 1 mm between each other. In the ith transverse profile, two attributes are concerned, one is the subscript j the relative location on the transverse profile and the other is the $a_{i,j}$, the relative elevation of the point (i, j). An example of 4,096 mm transverse profile is illustrated in Figure 3.4. It can be seen that the high resolution has reached to a level where the surface textures are clearly displayed.

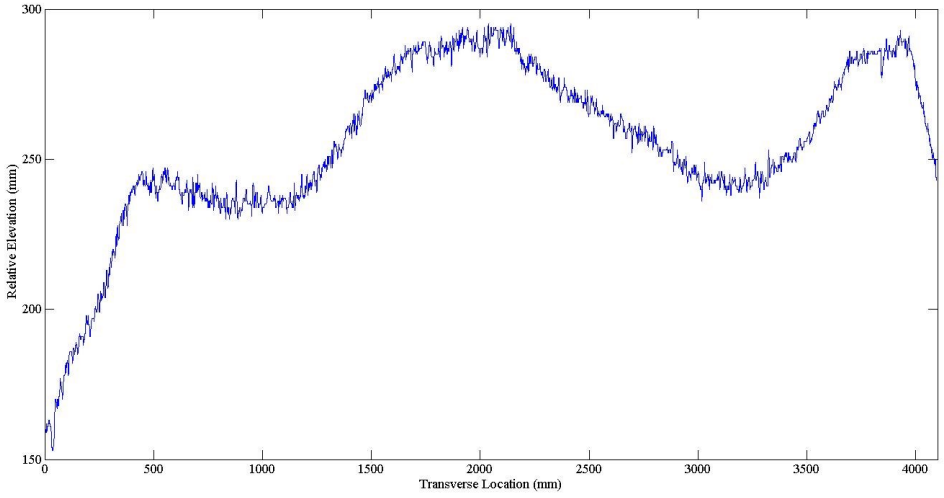

Figure 3.4 An Example of 4,096 mm Transverse Profile Collected by 3D Ultra

Since the area of interest of the sensor is limited, when the DHDV travels on a rough surface at highway speed, excessive vehicle bouncing or extreme pavement deterioration may prevent the reflected laser line from reaching the sensor ("out of the range"). Figure 3.5a illustrates the normal scenario and Figure 3.5b is the exaggerated illustration of the bounced vehicle. As a result, blank points can be recorded in the sensor and "0"s are produced accordingly in the 3D image matrix A. These "0"s are defined as outlier values of the raw data. The outlier removal is further discussed in Section 3.3.4.

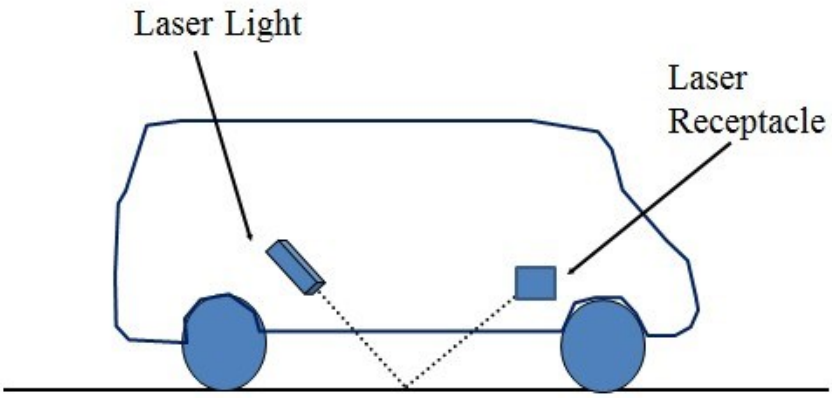

a. Normal Scenario

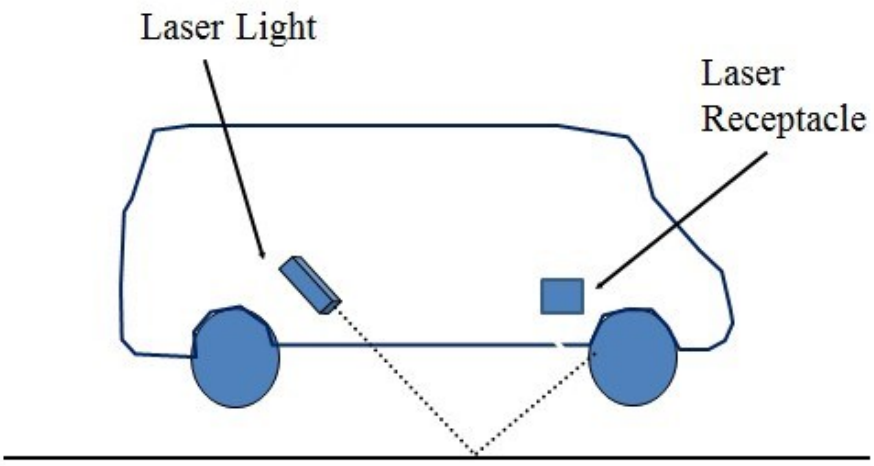

b. Bounced Vehicle

Figure 3.5 Illustration of Generation of Outlier Values in Data Collection

The second use of the 3D data is to produce the 3D intensity image, as illustrated in Figure 3.6a. This intensity image can be used for cracking detection and other analyses. However, since this intensity image is produced with the range information, some characteristics without significant height difference such as thin or worn-out lane markings are not very distinctive from the pavement surface on the 3D intensity image. In transverse profiling, 3D intensity image serves as an auxiliary tool for lane marking identification.

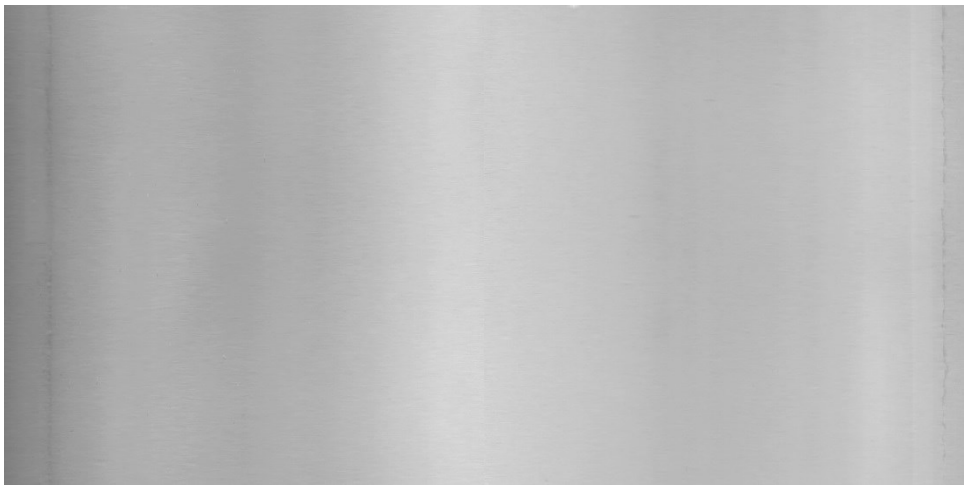

a. An Example of 3D Intensity Image

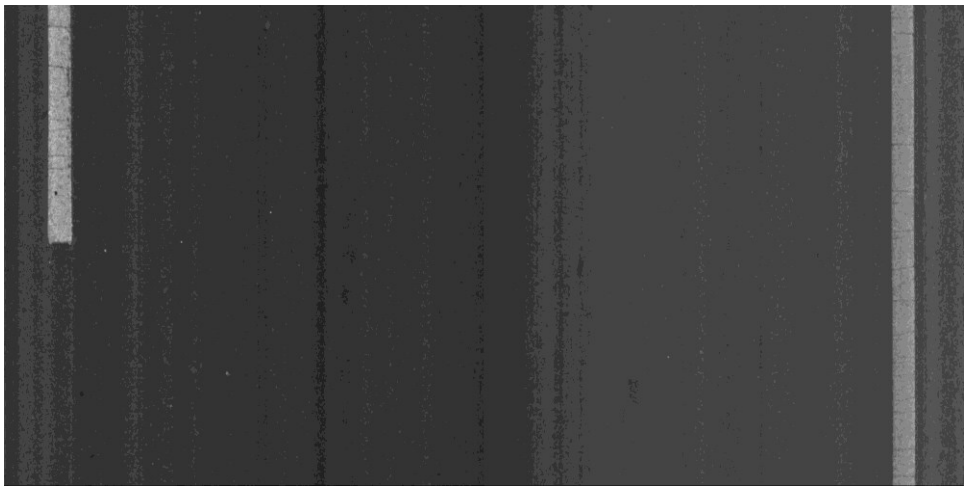

b. An Example of 2D Grayscale Image

Figure 3.6 Examples of 3D and 2D Images Collected by 3D Ultra

3.3.2.2 2D Data

2D images are directly produced through the 2D line camera and laser sub-system. Since there is no height information contained in 2D images, they are not useful for direct transverse profiling. However, the 2D images are helpful to the detection of pavement lane markings by matching with 3D intensity images. Figure 3.6b shows a 2D image which is taken with the same geographical

position of the shown 3D image in Figure 3.6a. It can be seen that the pavement markings are more visible in 2D images than in 3D intensity images.

3.3.3 Summary

3D Ultra exceeds all requirements for data collection specified in PP70-10 and is determined to be adequate for transverse profiling. The major advantages of using 3D Ultra system include:

- High resolution data can be used for both pavement management activities and research.
- Data quality does not change with data collection speed. Data collected from a network survey can also be used in project level analysis, which is of practical significance.
- Sufficient data resolution requires no further interpolation in terms of obtaining a satisfactory transverse profile.
- Visible images (2D and 3D) are available to extract lane markings, which allow the exact determination of wheel-path and lane location in transverse profiles.

3.4 Implementation of PP69-10

3.4.1 Introduction to PP69-10

The recent AASHTO Designation: PP69-10 *Standard Practice for Determining Pavement Deformation Parameters and Cross Slope from Collected Transverse Profiles* (PP69-10 for short) is used to characterize pavement permanent deformation with three types of indicators: surface deformation condition, rut related attributes and water entrapment condition.

The attributes are interconnected and mutually affected but with different emphases (2).The deformation percent can be treated as a preliminary indication of pavement deterioration (5). Rut depth is one of the criteria determining pavement distress level and failure indicator of design in the next generation pavement design guide (MEPDG) (9). Rut cross-sectional area is

helpful in determining optimal techniques and estimating costs for maintenance (38). The pool of water in wheel-path may result in hydroplaning and spray and splash, which are all latent safety hazards (1, 7, and 8). In addition, undrained water on the pavement surface would accelerate pavement damage. A collection of standardized procedures are specified in PP69-10 to derive the pavement deformation parameters.

In brief, PP69-10 has the following important features:

- The transverse profile data used for PP69-10 must meet the technical requirement specified in PP70-10.
- Multiple technical parameters for rut characterization can be extracted from a transverse profile.
- The quantification of all attributes is based on the set of predefined procedures. The entire process solely is feasible through computer programs. No human interventions are necessary except the lane extraction process.
- The position of the wheel-paths, which is determined by the lane location, is critical in this protocol as all rut related attributes are scanned based on the elevations of wheel-paths.

Wheel-path location, longitudinal reporting sample interval, and data consistency are explicitly addressed in PP69-10, which were not clearly defined in previous protocols. In companion with PP70-10, PP69-10 has the potential to become a real practicing standard for the evaluation of pavement permanent deformation.

3.4.2 Terminologies

To aid the derivation of these parameters from the collected transverse profiles, some basic and relevant terminologies are defined in PP69-10. The following ones are important and frequently referenced in this research (5):

- Lane: The pavement surface between inside edges of inside (left) and outside (right) lane markings. If the lane marking is absent, an equivalent portion of the surface is accounted. Note that the lane location is invisible from solely the transverse profiles.
- Centerline: The centerline is an imaginary line located at the middle of the lane which divides the lane into two halves with equal width. It should be always parallel to the lane markings.
- Wheel-path: There are two wheel-paths on each lane. A wheel-path is a longitudinal strip of the pavement 0.75 m (30 in.) wide. The inside (left) wheel-path is centered 0.875 m (35 in.) from the centerline towards the adjacent lane (left) and outside wheel-path is centered 0.875 m (35 in.) from the centerline towards the shoulder (right). Note that this wheel-path definition is completely different from the LTPP wheel-path definition (13). It is emphasized the wheel-path coordinates are depended on centerline location in PP69-10 but not right edge as per LTPP (5, 13).
- The Five Spots: The Five Spots are used to determine rut related attributes. They are new concepts introduced by the new protocol. Each spot has two attributes, the elevation and the location. Spot 1 is located on the centerline of the pavements. Its elevation is the average elevation of data points in the center 75 mm (3 in.) of the pavement lane. Spot 2 and Spot 4 represent the elevations of inside (left) and outside (right) wheel-path, respectively. Their elevations are the average elevations of the lowest 10% data points in their respective wheel-paths. Their locations are the midpoints of their respective 10%

data points. Spot 3 and Spot 5 represent the inside (left) edge and outside (right) of the pavement lane. Their elevations are averaged from the data points within 100 mm (4 in.) from the pavement edges, respectively. They are located 50 mm (2 in.) from the edges of the lane, respectively. In the transverse profiles collected by 3D Ultra, each mm corresponds to a data point, which makes the determination of the Five Spots straightforward. In a specific transverse profile with the known lane location, the locations of Spot 1, Spot 3, and Spot 5 remain constant. By contrast, the locations Spot 2 and Spot 4 vary by the wheel-path elevations. Note that the elevations of the Five Spots are averaged from a series of points; therefore they may not sit on the transverse profile.

The above definitions are paraphrased and interpreted in the thesis' study for the purpose of concision and convenience in understanding. Comprehensive and rigorous definitions are contained in PP69-10. According to PP69-10, the identification of the wheel-path is the foundation of the entire process since the generation of most parameters is based on the location of wheel-paths and the Five Spots. An example of the lane, wheel-path, centerline, and Five Spots of the pavements is illustrated in a 3.6 m (12 ft) lane in Figure 3.7. Note that the illustration of the Five Spots is not true but a symbol in this example. The actual Five Spots only can be visualized on a cross-sectional profile and is presented in next section where the rut attributes are analyzed (Figure 3.11). In addition, note that the "left" and "right" are the relative directions from the perspective of crews or passengers who travel forward along the pavement section.

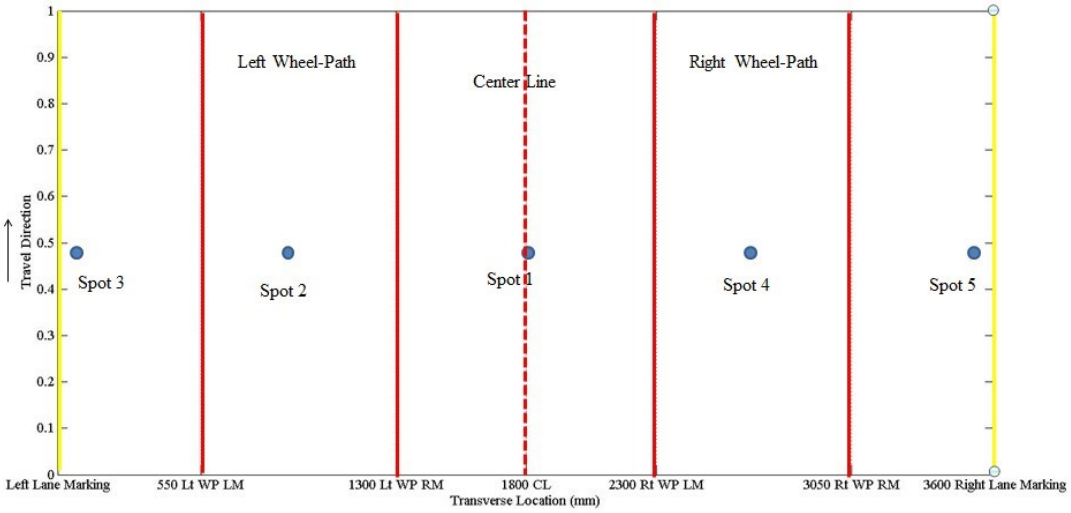

Figure 3.7 Illustration of Lane, Wheel-path, Centerline, and Five Spots in PP69-10

3.4.3 ADA3D Preparation

Following the procedures specified in PP69-10, the calculation algorithms of the deformation attributes are coded with C++ programming language and integrated into ADA3D. ADA3D is able to conduct transverse profiles analysis in semi-automated or fully automated manner.

3.4.3.1 Data Preprocess

To ensure accurate results can be produced with the given algorithms, all transverse profiles need to be preprocessed before analyzing.

Since the outlier values may pose significant impacts on the results, the first step is to remove the outliers presented in the collected transverse profiles. As introduced in Section 3.2, the outlier values are the "0"s in the transverse profile array due to the loss of laser illumination. The positions of the "0"s are first detected and the linear interpolation is applied to approximate the substituted values of these "0"s in the array. The linear interpolation for outlier removal is

applied according to Equation 3.2. The Figure 3.8a illustrates a profile with outliers and Figure 3.9b is the same profile after linear interpolation applied at "0"s.

$$y(x) = y(x_0) + \frac{y(x_1) - y(x_0)}{x_1 - x_0}(x - x_0) \tag{3.2}$$

where x is the location or subscript of a "0";

$y(x)$ is the approximated value for a "0";

x_0 is the location of the predecessor of the first "0" in a series successive of "0"s;

x_1 is the location of the successor of the last "0" in a series of successive "0"s;

$y(x_0)$ and $y(x_1)$ are the elevation value of x_0 and x_1, respectively.

Due to the existing of pavement textures and other anomalies such as cracking and potholes, these noise points should be filtered for rut characterization. As suggested by PP69-10, the second step of data preprocess is to smooth the collected transverse profiles. By applying the symmetric Moving Average Filter (MAF) according to Equation 3.3, the major effects of the "noise points" can be suppressed. The greater size the filter is the smoother profiles are obtained. PP69-10 suggests a 50 mm (2 in.) MAF for the calculation of rut and deformation related parameters and a 200 mm (8 in.) MAF for water related analysis. However, the symmetric MAF only allows the filter size being odd numbers. Therefore, the 51 mm and 201 mm MAF are applied for the two types of demands, respectively. For the convenience of representation, 50 mm and 200 mm MAF are used in the thesis. The same profile after applying 50 mm MAF and 200 mm MAF are shown in Figures 3.8c and 3.8d, respectively. Note that the example profile as shown is wider than a lane; the data at both edges are not valid.

$$y'[i] = \frac{1}{m}\sum_{j=-(m-1)/2}^{(m-1)/2} y[i+j] \tag{3.3}$$

where $y[\,]$ is the input profile;

$y'[\,]$ is the output profile from the filter;

m is the size of the filter.

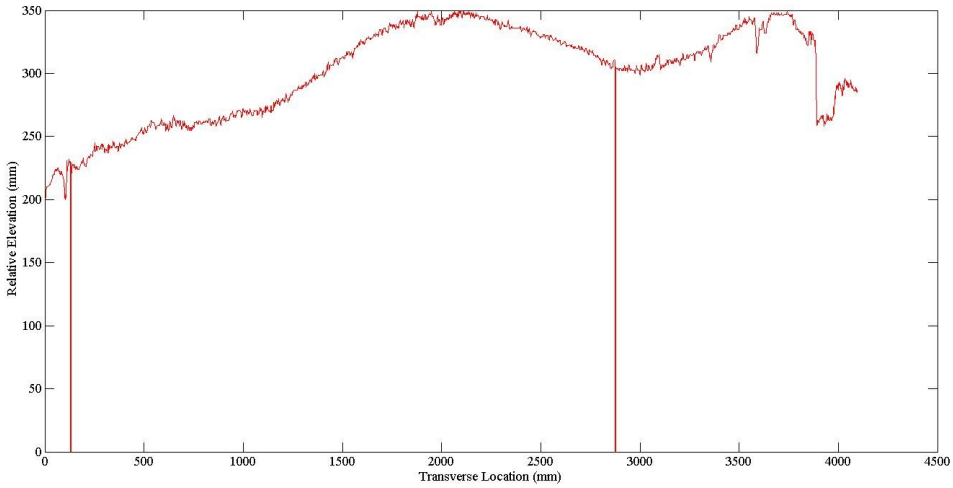

a. An Example of Transverse Profile with Outlier Values

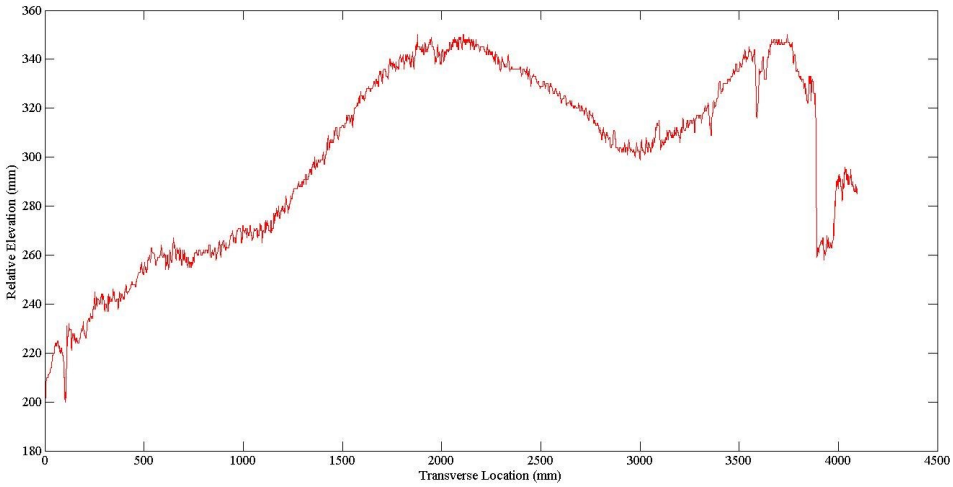

b. An Example of Transverse Profile with Outlier Values Removed

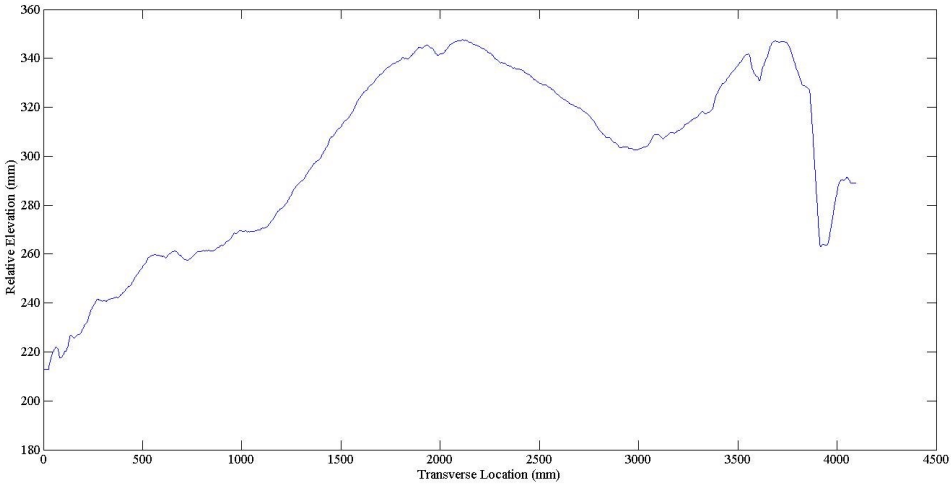

c. An Example of Transverse Profile with applying 50 mm MAF

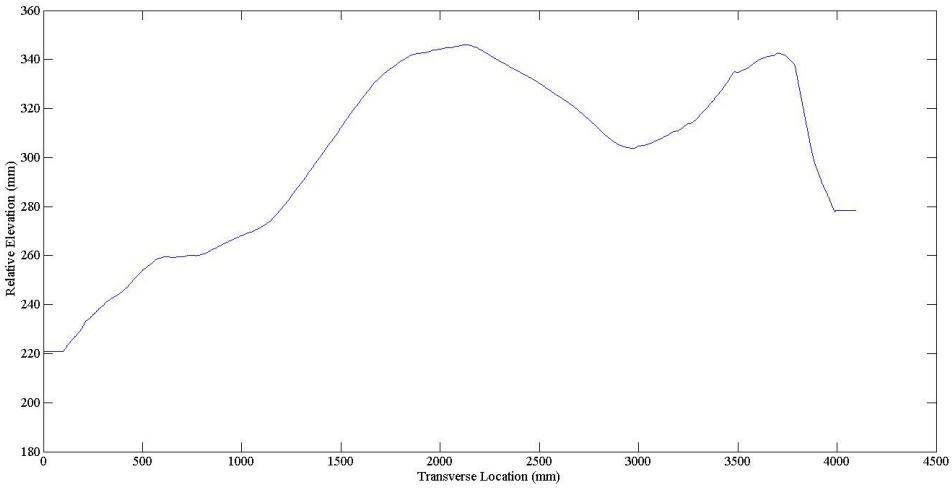

d. An Example of Transverse Profile with applying 200 mm MAF

Figure 3.8 Examples of the Preprocess of Transverse Profiles

3.4.3.2 Identifying Lane Marking Position

As required in PP70-10, the collected transverse profile must have a wider transverse coverage than the actual traveled lane. Further, the extraction of all rut attributes must be within the lane

limit per PP69-10. Therefore, an indispensable step before performing data analysis is to extract the lane marking locations.

For data collected with 3D Ultra, the 3D intensity image is first matched with the 2D intensity image by their distinctive features and then utilized to locate the exact lane location for 3D height matrix. In these visible images, the lane location is determined by two parameters: Left Margin (LM) and Right Margin (RM), which are the distances from left and right edges of the image to their nearest inner lane markings or actual pavement edges, respectively, as shown in Figure 3.9. Generally, each image only needs one pair of LM and RM measures. These two parameters are essential inputs in ADA3D calculation for the rut related parameters. After identifying LM and RM, the subscripts of centerline and wheel-path coordination are accordingly acquired for transverse profiles in the 3D height image (Figure 3.10). This lane identification can be conducted automatically with embedded image recognition technique or semi-automatically with human intervention. Thus, in this research, if the extraction of LM and RM is performed with human intervention, the transverse profile analysis is defined as semi-automated. On the other hand, if the lane identification is automated conducted, the entire analysis is a fully automated process.

To assure sufficient accuracy, the LM and RM are semi-manually measured with the assistance of ADA for all collected images in this study unless there are other intended purposes (e.g. Chapter 6). For those images without lane marking on the left side (gaps on broken markings), the lane width from adjacent images is referenced with the RM to approximate the LM. For those pavements without right lane markings, the lane to shoulder separating line is taken as the right boundary.

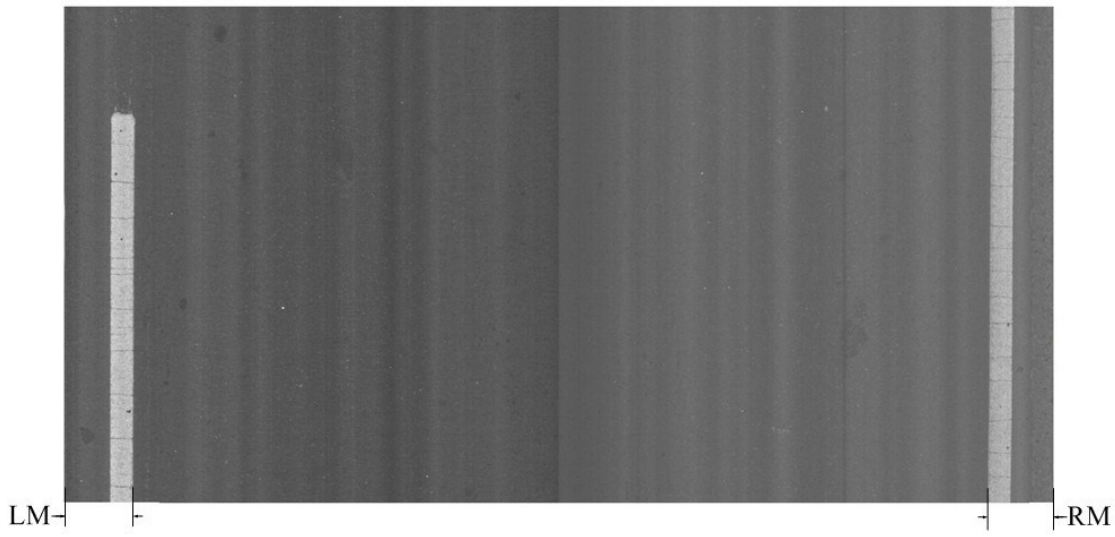

Figure 3.9 The Acquisition of Left Margin (LM) and Right Margin (RM)

3.4.4 Rut Parameters Calculation

In this section, the derivation of all technical parameters according to PP69-10 is outlined. The entire process is performed on an example transverse profile in which LM and RM are 297 mm and 270 mm, respectively (Figure 3.9). The width of the lane is 3,529 mm. The aforementioned preprocess procedures are implemented before the profile is used for rut characterization. All procedures presented in this section can be implemented by ADA3D in real time; however, the graphical examples shown in the text are generated from MATLAB 2010b (39).

3.4.4.1 Cross Slope and Percent Deformation

The derivation of cross slope (CS) and percent deformation is illustrated in Figure 3.10 and Equation 3.4-3.7.

The calculation of the percent cross slope (CS) involves two steps (Equation 3.4). First, the average elevation of each half lane separated by the centerline is calculated, respectively. The difference of these two values is divided by half of the lane width multiplied by 100. Note that

PP69-10 does not specify which half lane average elevation should be subtracted from the other. To keep consistent with other protocols and the latter definition in deriving water attributes, in this study, the elevation of the left side (profile AC) minuses the elevation of the right side (profile CB) is executed. Therefore, if the cross slope is greater than zero (positive), the average elevation of the left half lane is higher than that of the right half lane, and vice versa. The CS of this example profile is -0.74.

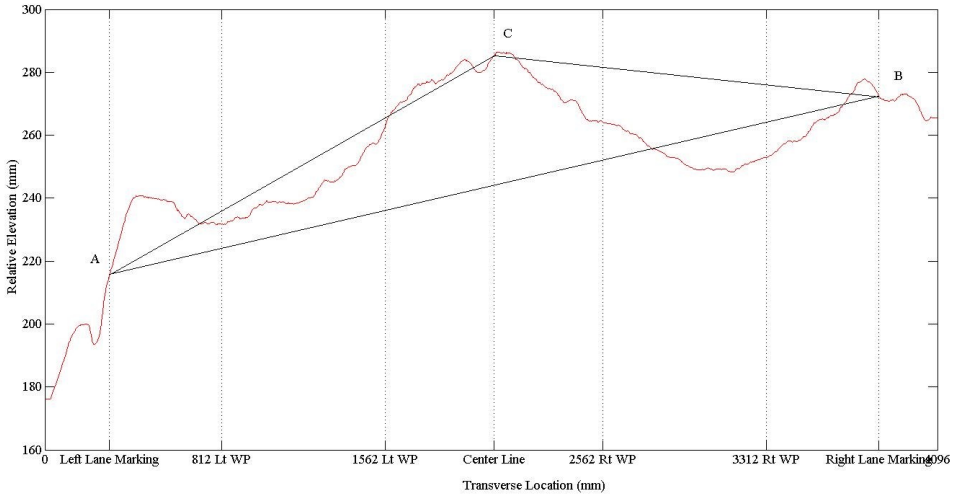

Figure 3.10 Illustration of Derivation of Cross Slope and Percent Deformation

$$Cross\ Slope\ (CS) =$$

$$(Mean\ Elev.of\ Profile\ AC - Mean\ Elev.\ of\ Profile\ BC) * 100/(1/2 * Lane\ Width) \quad (3.4)$$

$$Total\ Percent\ Deformation\ (TDF) =$$

$$(Profile\ Length\ of\ AB - Straightline\ Length\ of\ AB)/Straightline\ Length\ of\ AB\ *\ 100 \quad (3.5)$$

$$Left\ Percent\ Deformation\ (LDF) =$$

$$(Profile\ Length\ of\ AC - Straightline\ Length\ of\ AC)/Straightline\ Length\ of\ AC\ *\ 100 \quad (3.6)$$

$$Right\ Percent\ Deformation\ (RDF) =$$

$$(Profile\ Length\ of\ BC - Straightline\ Length\ of\ BC)/Straightline\ Length\ of\ BC * 100 \quad (3.7)$$

The calculation of the percent deformation defined in PP69-10 (Equation 3.5) consists of four steps. First, the length of the pavement transverse profile between the two edge points is computed. The profile length is approximated by summing the section length between each two adjacent points. Second, the straight-line distance of the pavement is measured. Third, the straight-line length is subtracted from the profile length. After dividing the result by the straight-line length and multiplying by 100, the percent deformation is obtained. For this research, the total percent deformation (TDF) is acquired based on this procedure. Considering the usage of deformation percent parameter, two additional parameters the left percent deformation (LDF) and right percent deformation (RDF), which are used in latter studies, are derived following similar computational processes (Equation 3.6 and 3.7). The TDF, LDF, and RDF in this example profile are 0.358, 0.411, and 0.252, respectively.

As the values of deformation are too small to distinguish in percent unit, Total Deformation Permillage (TDP), Left Deformation Permillage (LDP), and Right Deformation Permillage (RDP) are proposed in the research to substitute TDF, LDF, and RDF, respectively. The permillage unit has a magnitude smaller than the percent unit. Under the unit of permillage, the deformation parameters are more distinctive with two decimals. Thus, the TDP, LDP, and RDP in this example profile are 3.58, 4.11, and 2.52, respectively.

3.4.4.2 Rut Related Attributes

Being different from the traditional rut depth and width quantification methodology, a completely new approach is proposed in PP69-10 to extract rut related parameters. Two types of rut based on their location of occurrence are defined. The first one is the normal rut, which is the depression in the wheel-path. The second one is the center depression, which occurs in the middle of the two wheel-paths. In this study, the emphasis of the discussion is on normal rut attributes since the

center depression is rarely seen from a large numbers of observations. However, it is also worthwhile pointing out that center depression is mutually exclusive to normal rut as defined in PP69-10.

Two attributes of rut are introduced in PP69-10, the rut depth and rut cross-sectional area. Figure 3.11 is shown with the following procedures to derive rut related parameters. The calculation formulas for rut depth and rut cross-sectional area are given in Equation 3.8-3.11.

$$Left\ Rut\ Depth\ (LRD)\ =\ |Spot\ 2| \tag{3.8}$$

$$Right\ Rut\ Depth\ (RRD)\ =\ |Spot\ 4| \tag{3.9}$$

$$Left\ Rut\ Area\ (LRA)\ =\ Area\ between\ Straightline\ AB\ and\ Profile\ AB \tag{3.10}$$

$$Right\ Rut\ Area\ (RRA)\ =\ Area\ between\ Straightline\ CD\ and\ Profile\ CD \tag{3.11}$$

The Five Spots are used to determine the rut depth by applying the following procedures:

First, the original profile (Figure 3.10) is counterclockwise rotated a cross slope to reach a leveled profile (Top/Blue profile in Figure 3.11) (It might not be significant visually as the cross slope is only -0.74 in this example). In this leveled profile, the Spot 3 is set to 0. Then, the profile is rotated about Spot 3 until Spot 1 reaches 0. The rotated profile (Left middle and right bottom/Black profile in Figure 3.11) is used to characterize left rut information. At this time, the absolute value of Spot 2 is the rut depth for the left wheel-path (LRD). Based on the profile where Spot 1 is 0, the profile is further rotated about Spot 1 until Spot 5 reaches 0. This new profile (Right middle and left bottom/Green profile in Figure 3.11) is used for right rut characterization. At this time, the absolute value of Spot 4 is the rut depth for the right wheel-path (RRD). In this example profile, the LRD and RRD are 11.92 mm and 30.94 mm, respectively.

The black and green profile is also used for left and right rut cross-sectional area calculation, respectively. Scanning from the location of Spot 2 and Spot 4, when three values equal to or greater than 0 are encountered, the first reached point of the three points is identified as a rut edge. This scanning is applied to both sides of the Spot 2 and Spot 4. For each occurrence of rut depth, there are two rut edges (A and B for left rut and C and D for right rut in Figure 3.11). The area between the straight-line connecting two rut edges and the profile is defined as the rut cross-sectional area. Note that the rut edge may be located on the other side of the pavement centerline. In calculation, the area is approximated using basic integral calculus methods (Equation 3.12). In this example, the Left Rut Cross-Sectional Area (LRA) and Right Rut Cross-Sectional Area (RRA) are 11,317.44 mm^2 and 30,245.65 mm^2, respectively.

$$A = \int_a^b f(x)dx = \sum_{i=a}^{b-1}(f(x_{i+1}) + f(x_i))/2 \quad (3.12)$$

where A is the one-sided rut cross-sectional area;

a and b are the left and right rut edge of one-sided rut respectively;

$f(x)$ is the elevation at the point x.

In addition to the specified rut depth and rut cross-sectional area by PP69-10, another pair of attributes of practical significance, the rut width, is further obtained based on the definition of rut depth and rut cross-sectional area in this research. As shown in Figure 3.11 and Equation 3.13 and 3.14, the rut width defined in this research is the length of straight-line that connects two rut edges. The rut width is calculated based on the rotated profiles (Black and Green profile in Figure 3.11) which are used to determine the rut cross-sectional area. As a matter of fact, according to this definition, the straight-line length rut width is the same as the rut width calculated based on transverse location. In this example, the Left Rut Width (LRW) and Right Rut Width (RRW) are 1045.96 mm and 1,552.47 mm, respectively.

$$Left\ Rut\ Width\ (LRW)\ =\ Length\ of\ Straightline\ AB \tag{3.13}$$

$$Right\ Rut\ Width\ (RRW)\ =\ Length\ of\ Straightline\ CD \tag{3.14}$$

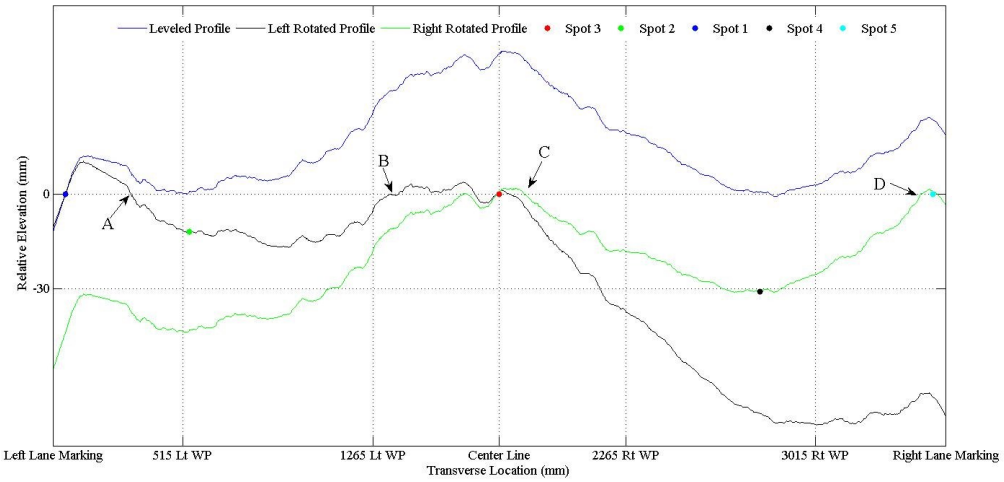

Figure 3.11 Illustration of Derivation of Rut Related Parameters

Theoretically, if there is rut on the pavement, the Spot 2 and Spot 4 should be negative as they have the average lowest elevations, which are the depressions in the wheel-paths. However, in practice, when there is no rut or the rut shape is abnormal, it is possible that the values of Spot 2 and Spot 4 are positive instead of negative. Though PP69-10 does not specify it, the rut depth is set to 0 when the Spot 2 or Spot 4 emerges positive values in this research. In addition, when the rut depth is 0, the rut cross-sectional area and rut width are correspondingly setting to 0.

3.4.4.3 Water Entrapment Attributes

Water entrapment attributes are identified by applying a scanning procedure defined in PP69-10. All profiles for water entrapment analysis are smoothed by 200 mm (8 in.) moving average filter (MAF) from the original denoised profiles. The basic mechanism is to scan from one end of the filtered profile for a pair of points, a lowest point and a nearest lip point from this lowest point.

According to PP69-10, a lowest point in the scanning is a point with *filtered elevation not equal to or at lower elevation than any previous point plus 2 mm (0.08 in.)*. Based on the acquired lowest point, the scanning continues until meeting with three sequential points which are lower than their predecessors. The highest point of these three points is the lip point associated with the lowest point. Every time when such a pair of points is identified, a water entrapment point is identified and recorded. The scanning should be proceeded until the other side of the profile is reached. All water entrapment points and their properties are reported.

Per PP69-10, the beginning point of the scanning is determined by the cross slope of the profile. The scanning starts from left to right (from Spot 3 toward Spot 5) when the cross slope is positive and zero. For negative slopes, the scanning is inversely conducted (from Spot 5 toward Spot 3). Note that the definition of the cross slope here is incongruent with the previously calculated cross slope according to PP69-10. The 200 mm filtered elevations of Spot 3 and Spot 5 are used to determine the properties of the cross slope. If the Spot 3 elevation is greater than Spot 5, the slope is defined a positive and vice versa. When the Spot 3 elevation equals to Spot 5, the slope is zero.

In practice, a profile may present none water entrapment point or a few water entrapment points. PP69-10 defines the water entrapment depth as the elevation difference between a lip and a lowest point. In this research, three water entrapment attributes are investigated based on the above scanning methodology: Total Water Entrapment Depth (TWD), Total Water Entrapment Width (TWW), and Total Number of Water Entrapment Points (TNW). TWD is the sum of the water entrapment depth of all found water entrapment points. A water entrapment width is the absolute value of the location difference between a lowest point and its corresponding lip point. TWW is the sum of the water entrapment width of all found water entrapment. These attributes are illustrated in Figure 3.12 and equations given in Equation 3.15-3.17. In this example, there are

2 water entrapment points. Their depths are 7.86 mm and 35.33 mm, from left to right, respectively. Their widths are 296.72 mm and 933.68 mm, from left to right, respectively. Therefore, the TWD, TWW, TNW of this profile are 43.19 mm, 1,230.41 mm, and 2, respectively.

$$Total\ Water\ Number\ (TNW)\ =\ Number\ of\ Water\ Lips\ or\ Lowest\ Points \tag{3.15}$$

$$Total\ Water\ Depth\ (TWD) =$$

$$\sum(Elevations\ of\ All\ Water\ Lips\ -\ Elevations\ of\ All\ Lowest\ Points) \tag{3.16}$$

$$Total\ Water\ Width\ (TWW) =$$

$$\sum|Locations\ of\ All\ Water\ Lips\ -\ Locations\ of\ All\ Lowest\ Points| \tag{3.17}$$

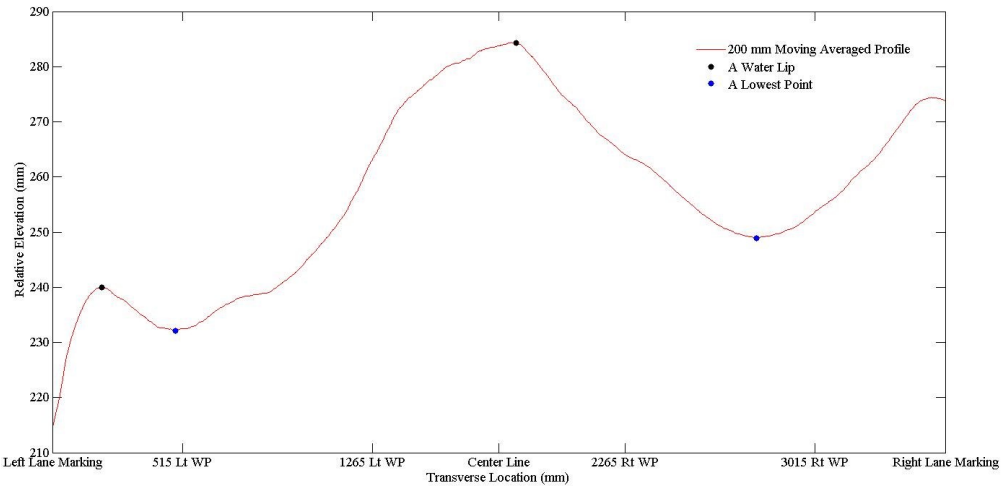

Figure 3.12 Illustration of Derivation of Water Related Parameters

3.4.5 Attribute Summary

The attributes proposed in PP69-10 are presented and tested in the research. Some attributes and procedures are slightly modified from PP69-10 for ease of automated implementation. In addition

to the seven parameters defined in PP69-10, six extra attributes are proposed in this study based on the definition of attributes and implementation procedures in PP69-10. The total thirteen attributes and their acronyms are listed in Table 3.1. The attributes with "*" are not part of PP69-10 and newly proposed in this research.

Table 3.1 List of Derived Parameters from PP69-10

No.	Attribute	Acronym	Illustration
1	Total Deformation Permillage	TDP	Figure 3.10
2	Left Deformation Permillage*	LDP	
3	Right Deformation Permillage*	RDP	
4	Left Rut Depth (mm)	LRD	Figure 3.11
5	Right Rut Depth (mm)	RRD	
6	Left Rut Width (mm)*	LRW	
7	Right Rut Width (mm)*	RRW	
8	Left Rut Cross-Sectional Area (square mm)	LRA	
9	Right Rut Cross-Sectional Area (square mm)	RRA	
10	Total Number of Water Entrapment Points*	TNW	Figure 3.12
11	Total Water Entrapment Depth (mm)	TWD	
12	Total Water Entrapment Width (mm)*	TWW	
13	Cross Slope	CS	Figure 3.10

3.5 Evaluation of PP69-10

3.5.1 General

PP69-10 defines multiple technical parameters to characterize pavement permanent deformation, which is significant to practitioners and researchers. Procedures to derive these technical parameters are explicitly addressed in the standard, which make the computerized process feasible, consistent, and efficient. As stated in PP69-10, if the procedures are adopted by agencies with data collected from adequate devices, a uniform data report can be produced. In general, the objective *balance between extreme calculation complexity and resultant accuracy* is reached (5).

3.5.2 Advantages

The new AASHTO protocol PP69-10 is tested with bulks of data with both semi-automated and automated process. In summary, the advantages of this provisional protocol are:

First, the physical significance of all attributes defined in the protocol is realistic and practical. Each parameter represents one aspect of pavement deformation characteristics. With these attributes, agencies and pavement engineers can focus on different characteristics of permanent deformation.

Second, the procedures defined in the protocol are explicitly designed for computerized calculation. Real-time data processing is therefore feasible. With minimum human intervention, the repeatability of parameter derivation is assured.

Third, based on a large-scale test of transverse profiles, attributes derived from PP69-10 are consistent and reasonable. The defined algorithms in the protocol are able to capture a majority of the characteristics of the attributes.

Last but not least, for data collection systems based on the companion of PP70-10, the raw data quality is assured for a more consistent result.

3.5.3 Potential Improvements

Meanwhile, several issues which may affect the rigor of this protocol:

First, there are two cross slope definitions involved in this standard. One is the cross slope of the profile, which is defined in *Section 6.4* of PP69-10 and is used to level the profile in *Section 6.7* of PP69-10. The other one is the cross slope for water entrapment depth calculation, which is defined in *Section 6.9* of PP69-10. They two definitions are incongruent with each other. The former definition derives cross slope from average elevations; however, the latter one is

based on elevation of two edge points (Spot 5 and Spot 3). Furthermore, the concept of positive and negative cross slope is defined in *Section 6.9* of PP69-10, but not for the former one, resulting in the inconsistency.

Second, in the definition of rut in *Section 6.7* of PP69-10, the absolute value of Spot 2 and Spot 4 are taken as left and right rut depth, respectively. However, a few cases are encountered that the elevation of Spot 2 or Spot 4 is positive, which physically means there is no rut depth. Under this case, taking the absolute value of them would overestimate the rut depth. It is suggested that taking the absolute value only if Spot 2 or Spot 4 has non-positive values. Otherwise the rut depth should set to zero. This recommendation also applies to center depression.

Third, by applying the scanning method in *Section 6.8* of PP69-10, the rut cross-sectional area may be obtained when the rut depth is zero. It is suggested that when there is no rut depth, the rut cross-sectional area directly goes to zero.

Fourth, it is noticed that PP69-10 may underestimate the rut depth. The reason is that the elevation Spot 2 and Spot 4 are obtained on the original profile before the suggested rotations are performed, as can be seen in Figure 3.11. Because of the cross slope, the lowest 10 percent points in the wheel-path of the original profile (Figure 3.10) might not correspond to the 10 percent deepest deformation points in the wheel-path of the analyzed profile (Black and Green profile in Figure 3.11). This underestimation can be avoided by acquiring Spot 2 and Spot 4 on the rotated profiles (Black and Green profile in Figure 3.11). However, it is found that underestimation of rut depth due to this definition may not be significant. The rut cross-sectional area and rut width are minimally affected.

Fifth, some important parameters such as the rut width and the deformation on both wheel-paths are not formally defined in this protocol. Though it is not difficult for users to

develop them, it would be better for this protocol to explicitly include all these measures so that consistency and clarity are assured.

Last but not least, the specific quality assurance requirement or tolerance for errors in measurement should be included in the protocol so that data quality and data consistency can be checked based on a standard.

3.6 Summary

In this chapter, multiple rut parameters are derived with new data sets according to the new AASHTO protocols, a first in the industry. The introduction to the PaveVision3D Ultra system, detailed procedures to derive multiple rut parameters, and evaluation of the PP69-10 protocol are presented. It is significant that a set of parameters can be consistently produced with the new protocols. The advance of new data collection technology, the specification for data collection, and standard for computerized rut characterization are important milestones on the measurement of pavement permanent deformation.

However, some challenges still remain. The fully automated data derivation is still premature due to the difficulties in lane detection. Some potential improvements in protocols are desired. More importantly, field users are not accustomed to these new parameters. Research should be carried out to overcome the challenges so as to promote the application of multiple parameters in practice.

CHAPTER 4 CASE STUDIES OF RUT ATTRIBUTES

4.1 Introduction

AASHTO protocol PP69-10 outlines a set of procedures to derive three types of rut attributes. These parameters are scientifically defined, can be consistently derived, and are significant in field practice. However, one of the challenges is that pavement engineers and agencies have little knowledge and experiences on these newly derived parameters (28). To help pavement engineers and agencies get accustomed to and make use of these new attributes, answers to these questions are sought in this chapter:

- What is the relation between the existing measures and new measures?
- How to connect the traditional rut depth measures and new measures?
- What are the reasonable value ranges of the new parameters derived from PP69-10?
- What are the relations between different new parameters?
- What inferences can be drawn from analysis of multiple parameters?

4.2 Data Acquisition

4.2.1 Network Data Collection

Bulks of transverse profiles are analyzed to observe the inherent characteristics of the different rut attributes. The data used in this research are collected with PaveVision3D Ultra under Arkansas

State Highway and Transportation Department (AHTD) Project TRC1103. Two asphalt surfaced national highway systems (NHS) sections: US Highway 65 North Bound (US 65 N) and US Highway 70 East Bound (US 70 E) in Arkansas are used for analysis. Data collections were conducted on March 7th and March 5th, 2013 for the two roadway sections, respectively. The weather condition of both days was sunny and the pavement surfaces were dry.

The section length of US 65 N is about 110 km (70 miles). The beginning point is near Lake Village (GPS: 33.331598, -91.291864) and the end point is about 10 miles to Pine Bluff (GPS: 34.160522, -91.828583). The section length of US 70 E is about 95 km (60 miles). The beginning point is south of Brinkley (GPS: 35.146316, -90.156416) and the end point is about 2 miles to the border of West Memphis (GPS: 35.147073, -90.25943). Figure 4.1 shows the locations for two data collections on Google map. The US 65 N is a divided highway and the US 70 E is undivided. Except necessary lane shift, data are collected for the outmost lanes. Urban streets and rural highways are traversed in both sections.

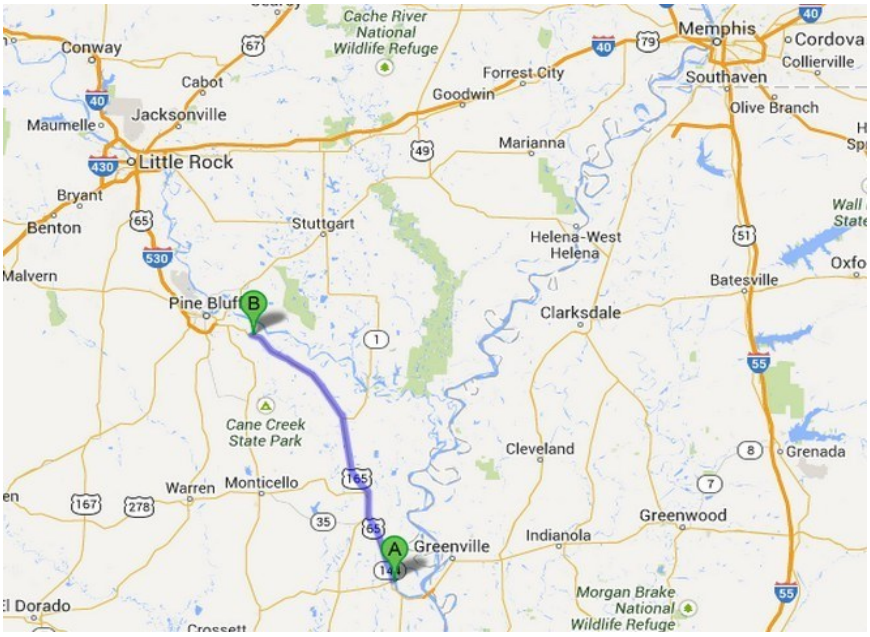

a. Data Collection for US 65 N (A to B)

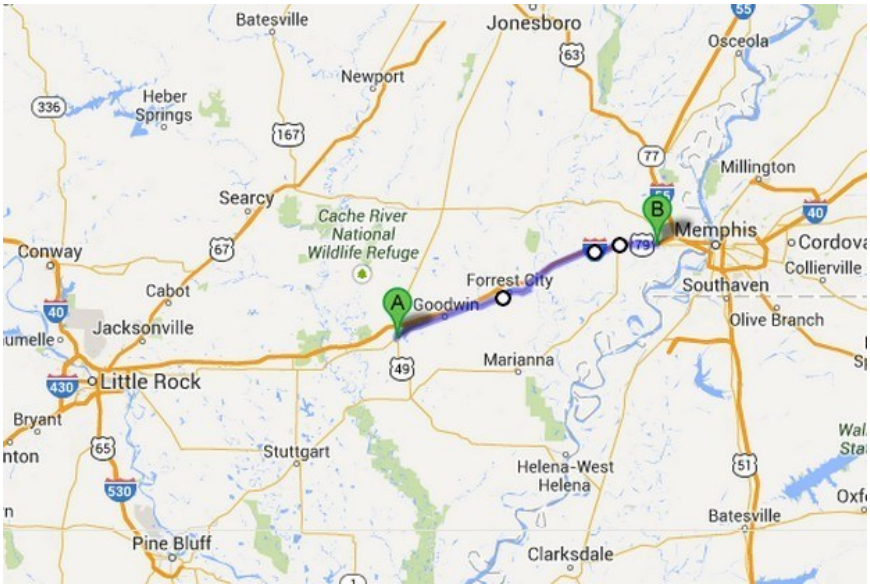

b. Data Collection for US 70 E (A to B)

Figure 4.1 Data Collection Map

(Source: Screenshot of Google Map)

4.2.2 Selection of Transverse Profiles

Data from regular pavement sections where the full lane is covered are used for transverse profiles selection. When the lane shift, merging or diverging occurs, the traveled lane may not be fully covered or its width is abnormal. These sections are therefore excluded from analysis.

Technically, millions of transverse profiles are available for analysis. However, it would be redundant to analyze every transverse profiles since the pavement performance is similar between adjacent sections. To characterize a wide range of pavement condition, for about every 200 m (656 ft) pavement sections, twelve successive profiles with a longitudinal interval of about 500 mm (20 in.) are randomly selected. More specifically, three successive images are randomly selected from about every 100 images, and the 1st, 501st, 1001st, and 1501st profile of each image

are selected, respectively. In total 8,960 profiles are analyzed: 4,920 for US 65 N and 4,040 for US 70 E.

To ensure the accuracy of data reduction, semi-automated lane positioning is conducted for all these transverse profiles in this research. In the analyzed sections, the width of the pavement ranges from 2,865 mm (9.37 ft) to 3,653 mm (11.98 ft) with an average of 3,452 mm (11.33 ft). The distribution of the pavement width for these selected profiles is shown in Figure 4.2. The performances of these transverse profiles, the derived attributes according to PP69-10, are listed in Appendix C on the basis or of the geographical order for US 65 N and US 70 E, respectively.

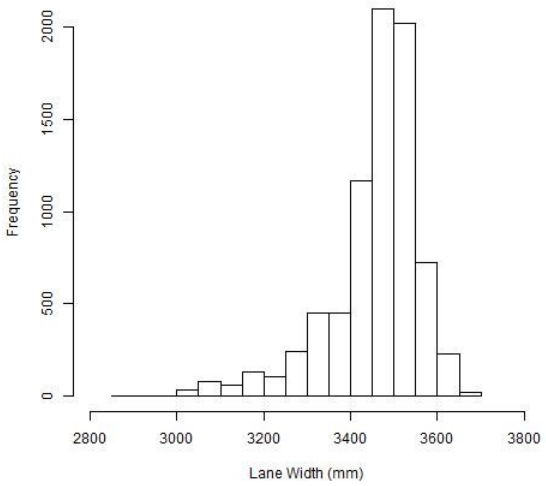

Figure 4.2 Distribution of Lane Width in the Study Sections

4.3 Methodology Review

Statistical analysis is the major tool for exploring the relations between parameters. In this chapter, three statistical techniques are involved.

4.3.1 Correlation Analysis

Correlation analysis is a statistical tool to examine the linear relationship between two variables (40, 41). Suppose there are two variables x and y, the Pearson correlation coefficient r is calculated as Equation 4.1.

$$r_{x,y} = corr(x, y) = \frac{s_{x,y}}{\sqrt{s_{x,x} s_{y,y}}} \tag{4.1}$$

where $s_{x,y} = cov\ (x,\ y)$ is the covariance of x and y,

$s_{x,x}$ and $s_{y,y}$ are the variance of x and y, respectively.

Correlation analysis reveals the strength of the linear relationship between two variables. The correlation coefficient r ranges from -1 to 1, with 1 being a perfect positive linear correlation, -1 being a perfect negative linear correlation, and 0 being no linear correlation. Usually, an absolute value of coefficient greater than 0.7 indicates a strong correlation; the absolute value of 0.4-to- 0.7 reflects a moderate correlation; and the absolute value less than 0.4 is a weak correlation (41).

When there are m $(m > 2)$ variables are encountered, a correlation matrix M is conventionally used to exhibit the correlations between paired data sets. The correlation matrix $M_{n\times n}$ is a symmetrical matrix with elements $r_{i,j}(i = 1,2, \dots, n, j = 1,2, \dots, n)$, as shown in Equation 4.2. The diagonal elements are 1 because they are correlations of themselves. Calculation of correlation matrix is available in most mathematical software (39, 42).

$$M = \begin{pmatrix} 1 & r_{1,2} & \cdots & r_{1,n} \\ r_{2,1} & 1 & \cdots & r_{2,n} \\ \vdots & \vdots & \ddots & \vdots \\ r_{n,1} & r_{n,2} & \cdots & 1 \end{pmatrix}_{n\times n} \tag{4.2}$$

4.3.2 Hypothesis Test

Hypothesis test is a commonly used method to examine the difference between sample mean and population mean (40). In most practices, the null hypothesis H_0 denotes the sample mean and population mean are equal, or namely, there is no statistically significant difference between the two means. The alternative hypothesis H_1 denotes the opposite from null hypothesis.

The evaluation of hypothesis test can be judged by either a test statistic or a p-value. A test statistic, usually the Student's t-test for single variable test, is obtained from Equation 4.3 (40). Based on the nature of the test, a p-value can be derived. When drawing a conclusion, a significance level α, which is the probability of an incorrect judgment, needs to be predetermined. If the test statistic is in the rejection region, which means the probability of the test statistic is located in the tails of the distribution, the null hypothesis H_0 is rejected. Likewise, if the p-value is less than or equal to the predefined significance level α, the null hypothesis is rejected at significance level α (40). In practice, p-value is more frequently used due to its adaptability. The assumption for t-test is that the populations of the variables are mound-shaped distributed. There are two types of errors in hypothesis test. Type 1 error means the null hypothesis H_0 is falsely rejected and Type 2 error is that the false null hypothesis is accepted.

$$t = \frac{\bar{x} - \mu}{s/\sqrt{n}} \tag{4.3}$$

where $\bar{x}$ is the sample mean;

s is the sample standard deviation;

μ is the population mean;

n is the sample size.

When there are two sample sets X and Y, the statistic paired t-test is used to compare the means of two samples (41). The calculation follows Equation 4.4. The null hypothesis H_0 denotes the means of X and Y are equal and the alternative hypothesis H_1 denotes their means are statistically different. Other procedures and inferences are the same as the single variable hypothesis test.

$$t = (\bar{X} - \bar{Y})\sqrt{\frac{n(n-1)}{\sum_{i=1}^{n}(\hat{X}_i - \hat{Y}_i)^2}} \tag{4.4}$$

where $\hat{X}_i = (X_i - \bar{X})$ and $\hat{Y}_i = (Y_i - \bar{Y})$;

$\bar{X}$ and $\bar{Y}$ are means of X and Y, respectively;

n is the sample size.

4.3.3 Linear Regression Analysis

Linear regression analysis is a basic tool for trend-line fitting problems or predictions. Typically, the regression analysis is used to examine the change of a dependent variable (response variable) with independent variables (predictor variables). The general form of regression is shown in Equation 4.5 (40). The principal method for linear regression analysis is the least square method (40). The essence of the method of least square is to minimize the random error ϵ in Equation 4.5. The indicator sum of square errors (SSE) is defined to represent this error (Equation 4.6). When the SSE is minimized, the ϵ in Equation 4.6 is removed and the y becomes $\hat{y}$, which is the predict value of y.

$$y = \beta_0 + \beta_1 x_1 + \beta_2 x_2 + \cdots + \beta_k x_k + \epsilon \tag{4.5}$$

where y is the response variable;

$\beta_0, \beta_2, \cdots \beta_k$ are coefficients to be determined;

$x_1, x_2, \cdots x_k$ are predictor variables;

ϵ is the random error.

$$SSE = \sum(y_i - \hat{y}_i)^2 \tag{4.6}$$

where y_i is the actual response variable;

$\hat{y}_i$ is the estimated response variable.

The coefficient of determination R^2 is conventionally used as an indicator to evaluate the strength of the linear regression model. As shown in Equation 4.7, R^2 value ranges from 0 to 1. A higher value of R^2 means that more variation is explained by the regression model, which indicates the prediction is more robust, and vice versa.

$$R^2 = \frac{SSR}{SSR+SSE} \tag{4.7}$$

where $SSR = \sum(y_i - \bar{y})^2$, is the variation explained by regression;

$\bar{y}$ is the mean of the response variables.

4.4 Comparison of Different Rut Depth Measures

4.4.1 Problems

Since the first application of the rut measurement in the AASHO Road Test, rut depth has been the only widely used and the most important indicator for pavement permanent deformation (1, 10). As reviewed in Chapter 2, the straightedge and stringline methods, especially the straightedge method, are the traditionally dominating approaches to deriving rut depth from transverse profiles. In PP69-10, the rut depth is the only indicator that is comparable with the traditional rut depth measure. However, the rut depth calculation in PP69-10 is very different

from the traditional method. For field application of the new measures, the following questions may be asked: what is the relation between the traditional rut depth and the PP69-10 rut depth? Are the values from the methods close to or distinct from each other? Is it feasible to convert the traditional rut depth to the new PP69-10 rut depth or vice versa?

Commonly used traditional methodologies for rut depth calculation include the 1.2 m (4 ft) straightedge, 1.8 m (6 ft) straightedge, and the 3.7 m (12 ft) stringline. Simpson compared the differences of the three measures based on a large sample of LTPP data (28). It was found that 1.2 m straightedge is inaccurate and is discarded in later analysis. Rut depth measures from 1.8 m straightedge and 3.7 m stringline are highly correlated with correlation coefficients 0.9639 and 0.9555 for left and right wheel-path, respectively. In this research the rut depth from 1.8 m straightedge method is compared with those derived according to PP69-10.

4.4.2 Rut Depth Measures from Straightedge Method

The concept of straightedge method for rut depth calculation is presented in Chapter 2. Computer programs are coded to attempt to automatically implement Simpson's rut depth calculation algorithms with 1.8 m straightedge method (28):

The first end of the straightedge is placed at each point up to, but not including, the half-lane mark. This point will be referred to as (x_s, y_s)*. The slope is calculated between* (x_s, y_s) *and each subsequent point up to and including the point* (x_p, y_p)*, where* $x_p = x_s + 1800$*. The end point* (x_e, y_e) *of the straightedge is the point with the largest slope from* (x_s, y_s)*. The rut depth is the largest vertical distance between the line connecting* (x_s, y_s) *and* (x_e, y_e) *and each of the points between* (x_s, y_s) *and* (x_e, y_e)*.*

The transverse profiles collected by 3D Ultra are used to derive straightedge rut depth measures. The profiles are preprocessed according to the description in Section 3.4.3 with

applying a 200 mm (8 in.) Moving Average Filter (MAF). Before applying the Simpson's procedures, the profiles are leveled by shifting two filtered end points to the same elevation.

However, it is found the errors are frequently observed with the provided methodology. A typical example of problematic rut depth measurement is shown in Figure 4.3. There are two problems in this example. First, the line connecting two points with largest slope from each other traverses into the transverse profile, which is impossible in real world; second, the fictive straightedge does not capture the actual largest rut depth. In summary, these errors are identified caused by irregular shapes of transverse profiles and the nature of the method.

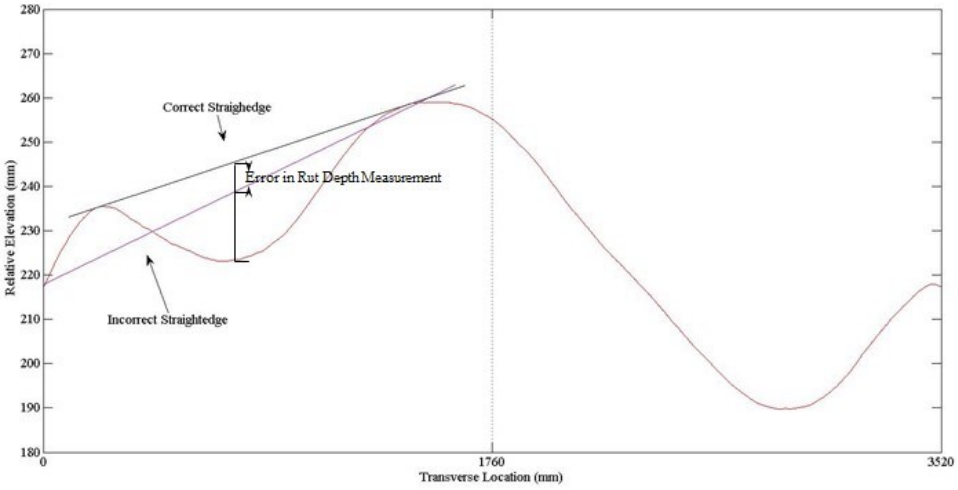

Figure 4.3 An Example of Erroneous Straightedge Rut Depth Measurement

Since the reliability and accuracy of placing fictive straightedge for rut depth measurement are not satisfied with automated process, human intervene is used to assure the correction of placing straightedge. Based on the correctly placed fictive straightedge, the rut depth is calculated by the coded program according Simpson's definition (28). Thus, this acquisition of straightedge rut depth measurement is conducted semi-automated. To be consistent with PP69-10 measures, the transverse profiles for analysis are filtered with 50 mm MAF.

4.4.3 Comparison of Rut Depth Measures

One fourth of selected transverse profiles are semi-automated analyzed per definition of Simpson's straightedge method. The first of every four consecutive profiles in the original data set are selected for this research. In total 2,240 transverse profiles are sampled. The derived rut depth measures are compared with PP69-10 rut depth measures from the same set of transverse profiles. The correlation matrix for left straightedge depth (SLRD), right straightedge depth (SRRD), left PP69-10 rut depth (LRD), right PP69-10 rut depth (RRD) is provided in Table 4.1.

Table 4.1 Correlation Matrix of the Two Rut Depth Measures

	LRD	**RRD**	**SLRD**	**SRRD**
LRD	1.00	0.67	0.97	0.67
RRD	0.67	1.00	0.68	0.98
SLRD	0.97	0.68	1.00	0.69
SRRD	0.67	0.98	0.69	1.00

In addition to the correlation matrix, paired t-tests are employed to check if the mean values of the data sets are statistically different. The p-values of the two tailed paired t-test are all 0.00 and are not listed in a table.

First, it can be seen that for both straightedge and PP69-10 measures, the correlation of left and right rut depth measures are moderate. The p-values indicate that the left and right rut depth measures are statistically different. These findings are in concert with Simpson's and Ali and Tayabji's conclusions (22, 28). It is observed that the right rut depth is much greater than left rut depth. The mean difference is 13 mm and 12 mm for straightedge and PP69-10 method, respectively.

With respect to the comparison of straightedge measures and PP69-10 measures, both left and right rut depth measures show strong correlation. The correlation coefficients are 0.97 and

0.98 for left and right rut depth measures, respectively. In other words, the rut depth measures from PP69-10 can be converted to semi-automated straightedge measurements.

The plots of the measures for left and right rut depth are given in Figure 4.4. Linear regression models are developed as shown in Equation 4.8 and 4.9. Their R^2 values are 0.94 and 0.96, respectively. The results indicate it is robust to use the straightedge rut depth measures to predict PP69-10 rut depth measures.

$$LRD = 1.01\ SLRD - 1.2,\ R^2 = 0.94 \tag{4.8}$$

$$RRD = 1.05\ SRRD - 1.42,\ R^2 = 0.96 \tag{4.9}$$

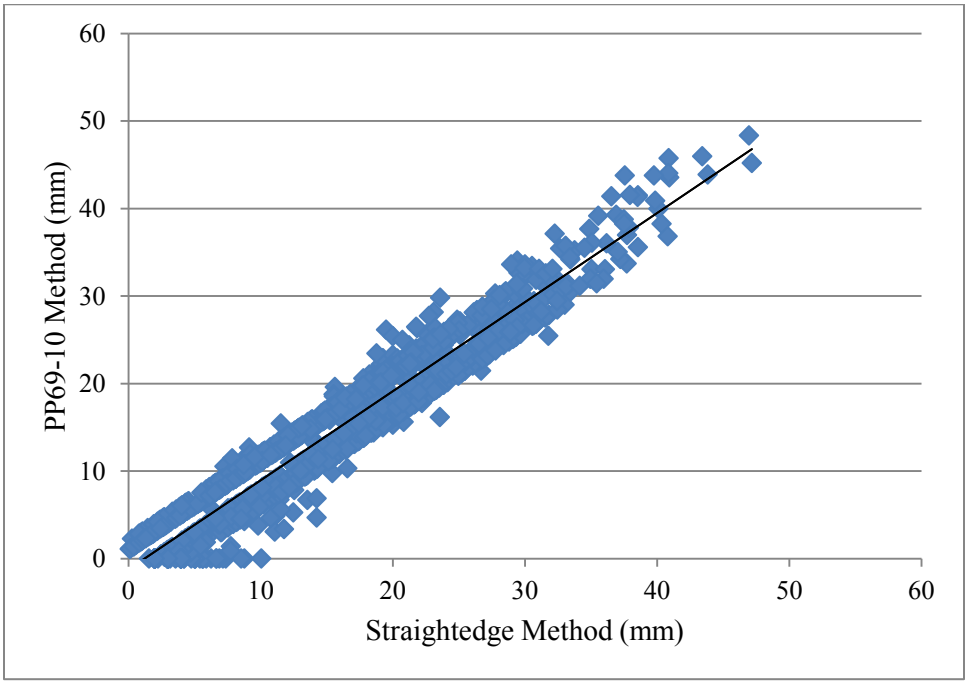

a. Left Rut Depth

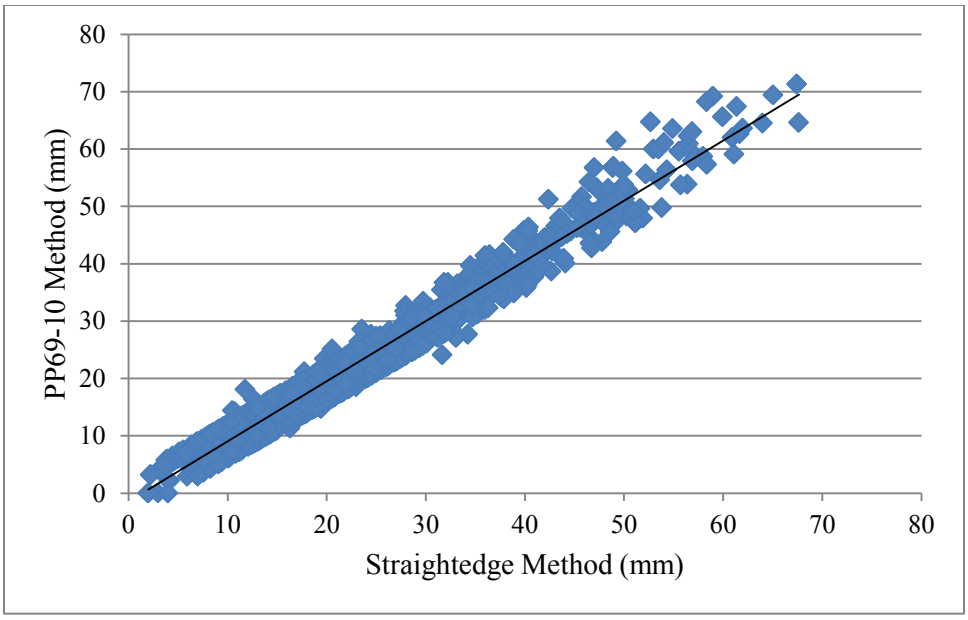

b. Right Rut Depth

Figure 4.4 Plot of Rut Depth Measures with Straightedge and PP69-10 Method

4.4.4 Summary

Strong correlation relation is observed between the rut depth measures from the straightedge and PP69-10 methods. As the straightedge rut depth measures are derived from semi-automated method, the accuracy of automated PP69-10 rut depth measures is validated. It is also demonstrated that scanning methodology proposed in PP69-10 is more robust and reliable than the traditional method in terms of automation. With the established regression relationship, the agencies without the capability of conducting PP69-10 analysis are able to use the proposed equations to convert rut depth measures with traditional straightedge method to PP69-10 rut depth measures.

4.5 Analysis of PP69-10 Attributes

4.5.1 General

Examining the relations between different measures derived with PP69-10 is significant to pavement engineers. First, the distribution and statistical summary of the parameters can assist pavement engineers in getting accustomed to using the parameters. Second, the relations reveal the interconnection among the parameters. Inferences regarding pavement performance can be made based on these interrelations. Last, it is significant for Pavement Management Systems (PMS) to convert existing measures to new measures deriving with PP69-10 for more consistent data sets in decision making.

4.5.2 A Geometric Model of Rut

Practically, permanent deformation cannot grow infinitely and attributes such as rut depths and water entrapment depths should be within reasonable ranges. During the research process, unusually large values are observed in the deformation permillage attributes. To identify the relationships among rut parameters or attributes, the calculation of deformation permillage is simplified remodeled in Figure 4.5. Rut depth, rut width, and lane width are modeled as independent variables and the deformation permillage is the dependent variable, as shown in Equation 4.10.

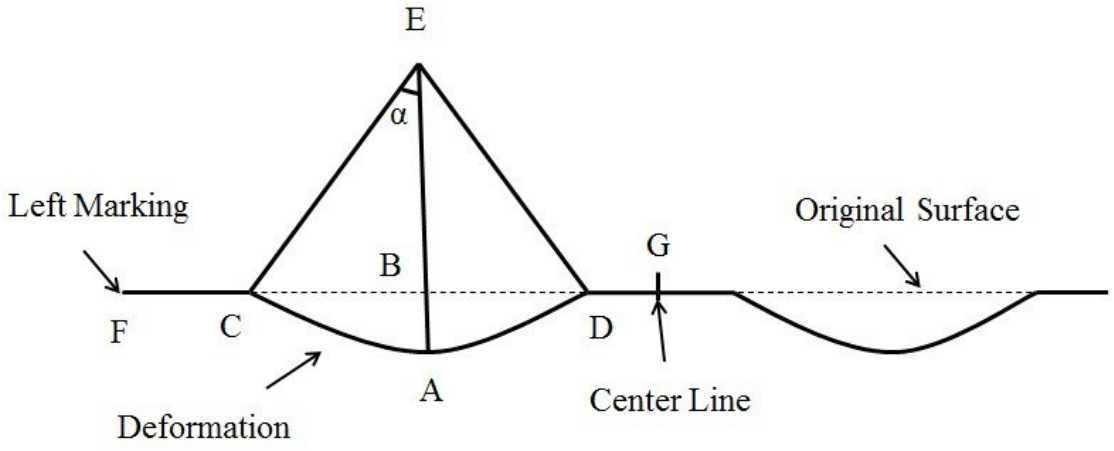

Figure 4.5 Model for Observing Abnormal Deformation Values

In this model, the profile length is the sum of length of FC, arc length of CAD, and length DG. The straight-line length of FG represents a half lane width. Length of AB is the rut depth and straight-line length of CD is the rut width. A is the deepest location of the rut and is located at the center of arc CD. E is assumed the center of the circle to which arc CD belongs and therefore CE, AE, and DE are assumed the radius of the circle and straight-line EBA is perpendicular to straight-line CBD. The depression is assumed symmetric on both wheel-paths so that the TDP, LDP, and RDP have the same value. Given the rut width and depth, the arc length of CAD is obtained. Based on this model, the deformation can be expressed with a function of rut width, rut depth, and lane width, as shown in Equation 4.10.

$$DP = \left(\frac{\pi \alpha w}{90\,(\tan \alpha)} + \frac{\alpha \pi d}{45} - 2w\right)\frac{1000}{l} \tag{4.10}$$

Where $\alpha = 180 - 2\tan^{-1}\frac{w}{2d}$;

DP is the deformation permillage (TDP, LDP, or RDP);

w is the rut width on a wheel-path;

d is the rut depth on a wheel-path;

l is the full lane width ($l \geq 2w$).

Different combinations of one sided rut depth and rut width, and full lane width values are substituted into Equation 4.10 to test the range of the deformation permillage. To be conservative, all of the tested scenarios assume significant amount of rut depth. The test results are shown in Table 4.2.

Table 4.2 Modeled Deformation Permillage

Lane width (l, mm)	**Rut depth (d, mm)**	**Rut width (w, mm)**	**Deformation permillage**
3600	100	1500	9.86
3600	80	1500	6.47
3600	80	1300	7.28
3500	100	1500	10.14
3500	80	1500	6.65
3500	80	1300	7.49
3400	100	1500	10.44
3400	80	1500	6.84
3400	80	1300	7.71

The maximum deformation permillage is 10.44 when the rut depth is 100 mm with the associated 1,500 mm rut width on a 3,400 m wide lane, which is an extreme example in actual pavement. More testing is performed in other scenarios with heavy rut and different combinations of rut width and pavement width, the deformation permillage ranges from 6.47 to 10.14. It is assumed that any deformation permillage with a value greater than 10 is defined as an abnormal value. Thus, if an abnormal value is seen in the attributes, the profile is subject to further investigation.

Based on the observation from substantial amount of data processing, three possible situations are prone to produce abnormal attributes:

- Wrong measurement of lane position. When the lane positioning is semi-automated conducted, the range of the attribute values generally appears reasonable and realistic. These unusual values are always observed in the results of the fully automated data analysis. It is found that errors in lane positioning can contribute to generation of outliers. As can be seen in Figure 3.9, if the right most portion of the profile is included in the lane, the RDP and TDP can be unusually high. This is apparent in the narrow pavements where no shoulder exists.
- Incomplete removal of outlier values on the raw transverse profiles. Take the Figure 3.8a as an example, the deformation permillage would be dramatically high with the existing of outlier values in the transverse profile. In very rare occasions, system errors could cause the undetected outlier values in the raw profile that affect the final results. As long as the outliers are correctly removed, the data ranges should be reasonable.
- Dramatic deformation on pavement surface. It is also a possibility that the profile per se is significantly damaged and surface excessively distorted so that a high deformation permillage is produced. In this case, human intervention is beneficial to examine the deterioration of the pavement.

In a network survey, generally, isolated abnormal values in deformation measures are mostly triggered by the first and second causes. If consecutive abnormal values are observed, the possible reason for abnormal deformation may be due to the third source. Also, when center depression is shown, alert should be given for a further examination.

4.5.3 Statistical Description

With the 8,960 transverse profiles selected from the Arkansas project, the thirteen attributes used for characterizing pavement permanent deformation according to PP69-10 are calculated and summarized. Before conducting descriptive and quantitative analysis, the abnormal profiles are removed. Based on the definition given in Section 4.5.2, a profile with any deformation permillage larger than 10 is deleted from the data set. In total 131 profiles (1.5%) are removed from the 8,960 profiles and 8,829 profiles remain for further investigation.

To observe the patterns and ranges of the data sets, histograms and basic statistics are presented in Figure 4.6 and Table 4.3.

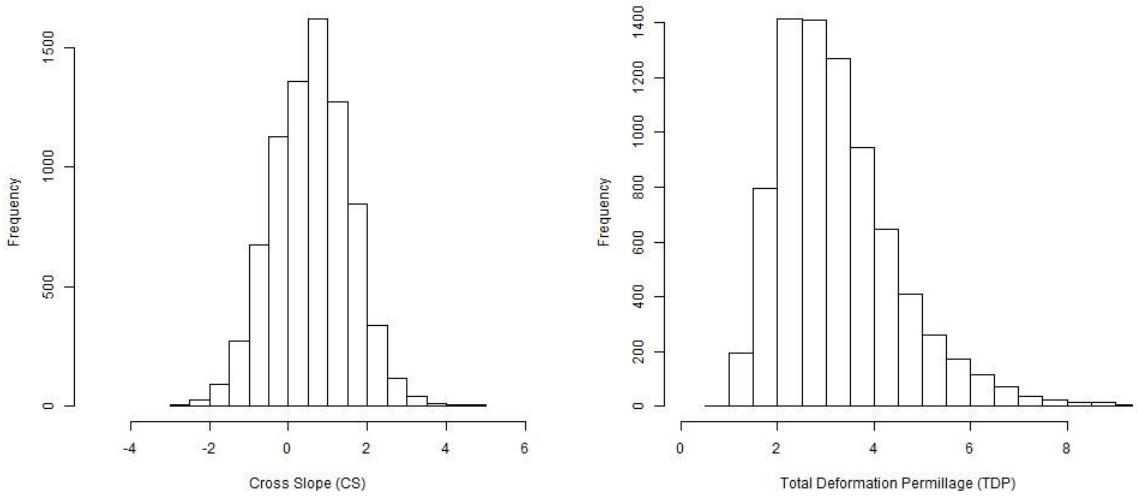

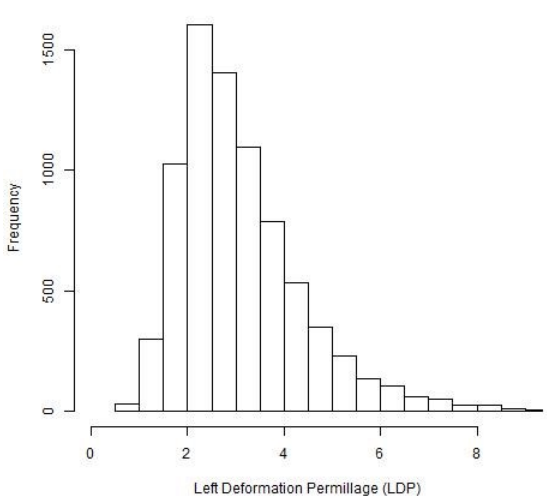
Frequency
0
500
1000
1500
0
2
4
6
8
Left Deformation Permillage (LDP)

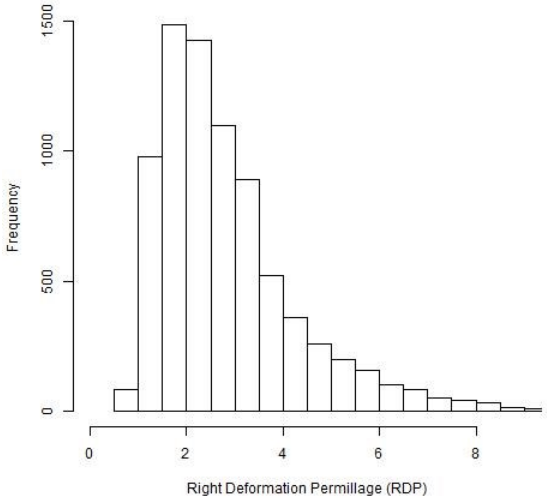
Frequency
0
500
1000
1500
0
2
4
6
8
Right Deformation Permillage (RDP)

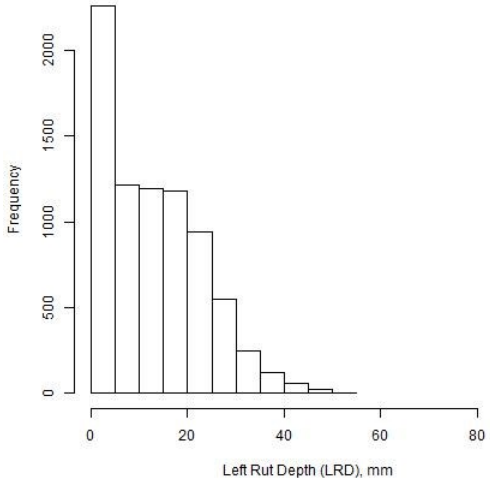
Frequency
0
500
1000
1500
2000
0
20
40
60
80
Left Rut Depth (LRD), mm

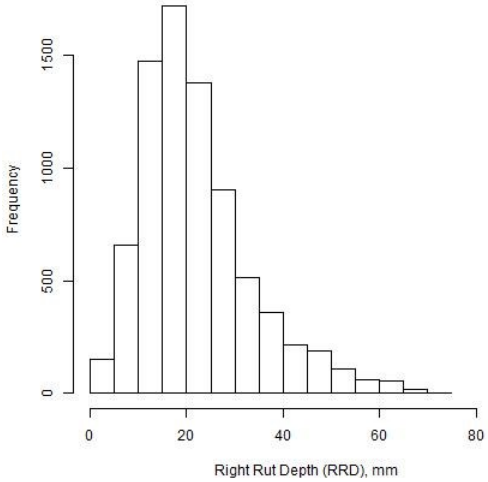
Frequency
0
500
1000
1500
0
20
40
60
80
Right Rut Depth (RRD), mm

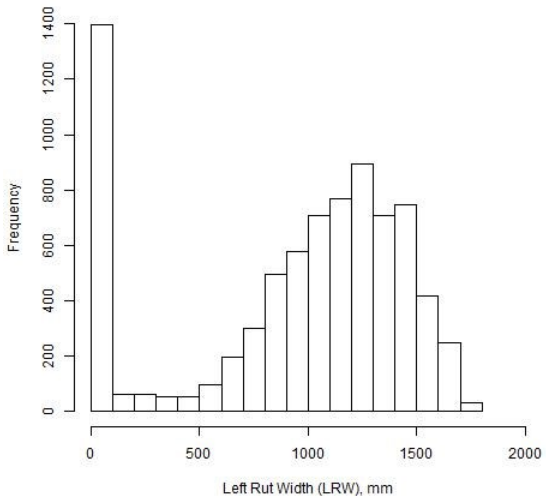
Frequency
0
200
400
600
800
1000
1200
1400
0
500
1000
1500
2000
Left Rut Width (LRW), mm

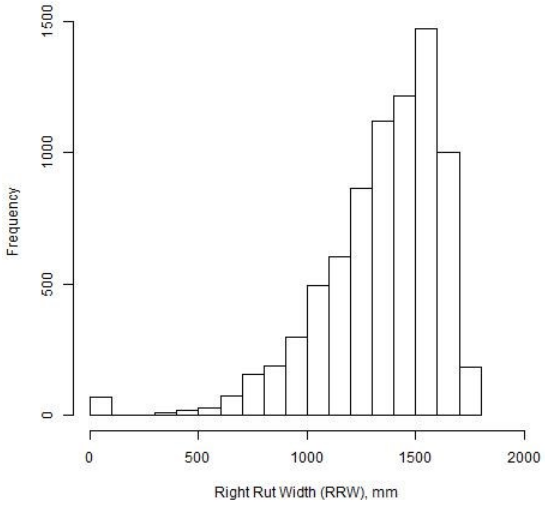
Frequency
0
500
1000
1500
0
500
1000
1500
2000
Right Rut Width (RRW), mm

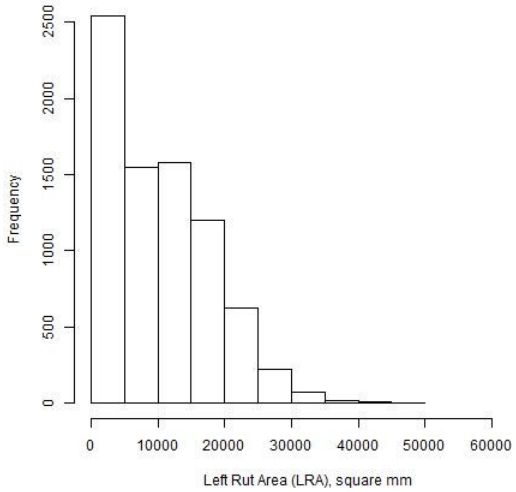
Frequency
0
500
1000
1500
2000
2500
0
10000
20000
30000
40000
50000
60000
Left Rut Area (LRA), square mm

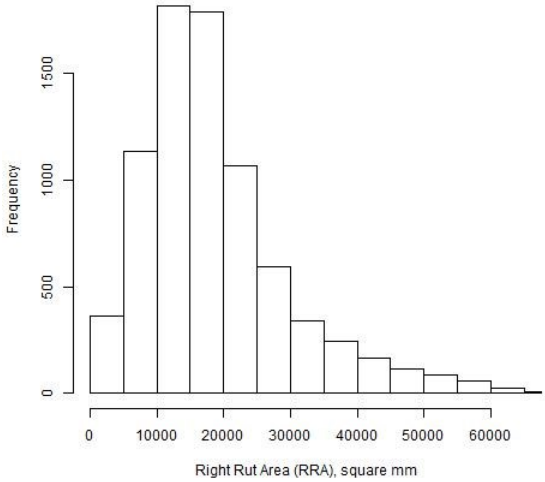
Frequency
0
500
1000
1500
0
10000
20000
30000
40000
50000
60000
Right Rut Area (RRA), square mm

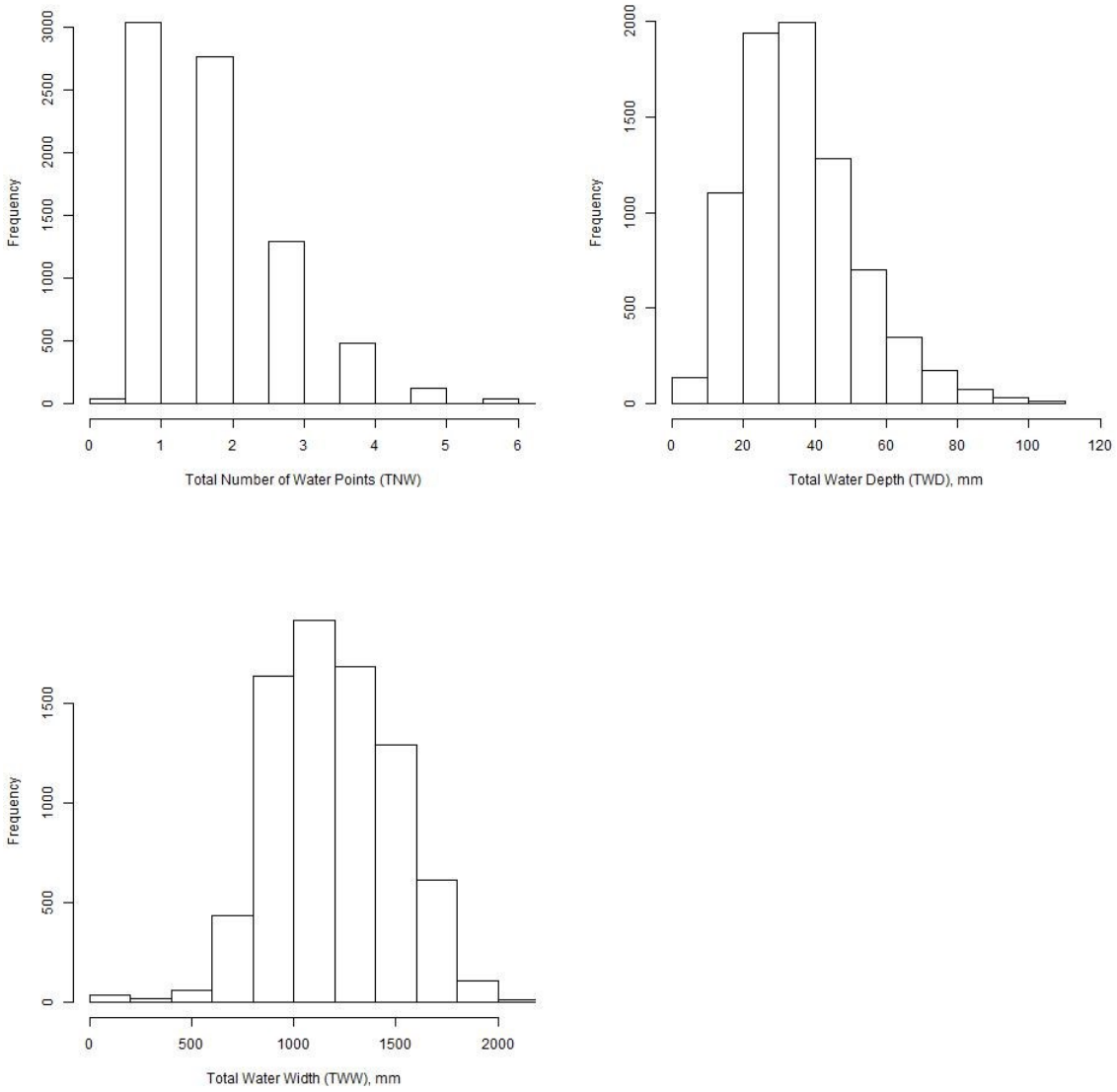

Figure 4.6 Histograms of the Attributes

Table 4.3 Statistics of the Attributes

	Mean	Max	Min	Median	Std. Dev.
CS	0.59	4.80	-2.88	0.61	0.98
TDP	3.26	9.81	0.98	3.03	1.24
LDP	3.11	9.98	0.77	2.82	1.31
RDP	2.85	9.98	0.66	2.48	1.45
LRD (mm)	12.79	52.52	0.00	11.80	10.32
RRD (mm)	21.99	71.37	0.00	19.64	11.56
LRA (sq mm)	10058.62	45210.79	0.00	9365.69	8076.05
RRA (sq mm)	18695.05	67967.50	0.00	16508.70	11019.85
LRW (mm)	940.44	1755.00	0.00	1087.00	519.43
RRW (mm)	1341.01	1767.00	0.00	1398.00	282.12
TNW	1.97	8.00	0.00	2.00	1.05
TWD (mm)	36.01	110.13	0.00	33.66	16.43
TWW (mm)	1194.39	2193.00	0.00	1177.00	296.64

Histograms and the statistics data show that all the attributes are slightly skewed. All deformation parameters, rut depths, rut cross-sectional areas, total water width, and total water depth are right skewed whereas rut widths, total number of water entrapment points, and cross slope are left skewed. The ranges of three deformation parameters are close to each other. Total deformation permillage has higher mean and median values than those of the left and right deformation. The rut depth measures are generally congruent with the conclusion from Section 4.4 and Simpson's research (28), where right rut depth is much higher than the left rut depth in terms of mean and median values. However, it is found that their standard deviations are close to each other, 10.32 mm and 11.56 mm for left rut depth and right rut depth, respectively. The rut width and rut cross-sectional area measures show the same trend in terms of mean and median values. However, their standard deviations have a larger difference. It is interesting to notice that both the average and median values of right deformation (RDP) are less than those of left deformation (LDP). This difference implies that the shape of right rut is more regular than that of the left wheel-path. In other words, the right wheel-path deformation is caused mainly by normal

downward pavement depression; however, the left wheel-path may contain irregular deformation such as lateral movement. The median and mean rut width measures are greater than 750 mm, which means the rut width is usually larger than the wheel-path width. The average points of water entrapment are about 2 and the mean total water entrapment depth is about 36 mm, which is close to the sum of mean left rut depth and mean right rut depth measures, which is about 34 mm. It can be inferred from this comparison that the wheel-path depressions are major contributors to water entrapment. The distribution of cross slope is of little practical significance in this research due to the lack of ground truth data.

4.5.4 Interrelationship among Parameters

In addition to the statistics and distribution of parameter ranges, pavement engineers are interested in understanding the relationships among the new parameters derived from PP69-10 and the traditionally measured parameter rut depth.

4.5.4.1 Correlation Analysis

The correlation analysis is used to examine the interrelationships. As shown in Table 4.4, only a handful of correlation coefficients are high (greater than 0.7) in the correlation matrix. The correlations between the following five pairs of parameters are high:

- Total Deformation Permillage (TDP) and Left Deformation Permillage (LDP)
- Total Deformation Permillage (TDP) and Right Deformation Permillage (RDP)
- Left Rut Depth (LRD) and Left Rut Cross-Sectional Area (LRA)
- Left Rut Width (LRW) and Left Rut Cross-Sectional Area (LRA)
- Right Rut Depth (RRD) and Right Rut Cross-Sectional Area (RRA)

Table 4.4 Correlation Matrix of All PP69-10 Attributes

	CS	TDP	LDP	RDP	LRD	RRD	LRA	RRA	LRW	RRW	TNW	TWD	TWW
CS	1.00	0.04	0.12	0.00	0.27	0.07	0.17	0.22	0.23	0.34	0.02	0.00	0.09
TDP	0.04	1.00	0.89	0.91	0.57	0.61	0.52	0.53	0.28	0.02	0.29	0.51	0.24
LDP	0.12	0.89	1.00	0.65	0.58	0.48	0.52	0.44	0.30	0.09	0.32	0.38	0.21
RDP	0.00	0.91	0.65	1.00	0.48	0.66	0.44	0.57	0.24	0.03	0.29	0.47	0.20
LRD	0.27	0.57	0.58	0.48	1.00	0.42	0.94	0.38	0.68	0.03	0.22	0.44	0.25
RRD	0.07	0.61	0.48	0.66	0.42	1.00	0.37	0.95	0.14	0.45	0.17	0.64	0.18
LRA	0.17	0.52	0.52	0.44	0.94	0.37	1.00	0.33	0.77	0.01	0.22	0.43	0.28
RRA	0.22	0.53	0.44	0.57	0.38	0.95	0.33	1.00	0.14	0.61	0.18	0.58	0.20
LRW	0.23	0.28	0.30	0.24	0.68	0.14	0.77	0.14	1.00	0.02	0.18	0.21	0.29
RRW	0.34	0.02	0.09	0.03	0.03	0.45	0.01	0.61	0.02	1.00	0.13	0.13	0.07
TNW	0.02	0.29	0.32	0.29	0.22	0.17	0.22	0.18	0.18	0.13	1.00	0.08	0.36
TWD	0.00	0.51	0.38	0.47	0.44	0.64	0.43	0.58	0.21	0.13	0.08	1.00	0.38
TWW	0.09	0.24	0.21	0.20	0.25	0.18	0.28	0.20	0.29	0.07	0.36	0.38	1.00

These high coefficients between total deformation and deformations of two wheel-paths demonstrate that the total deformation is affected by the left or right deformation. The rut depth has a very strong correlation with the rut cross-sectional area: left and right correlation coefficients are 0.94 and 0.95, respectively. This indicates that it is promising to use the rut depth measures to estimate the rut cross-sectional area measures.

Three parameters only have weak correlations with any other parameters: cross slope (CS), total number of water entrapment points (TNW), and total water width (TWW). It is straightforward that the TNW is not correlated with any other parameters as it is a discrete measure and other measures are physical measures. However, it is difficult to explain the low correlations for CS and TWW. With respect to the water entrapment depth (TWD), it has moderate correlation with TDP, RDP, LRD, RRD, LRA and RRA, where RRD is the greatest 0.64. This result is understandable that both rut depth measures contribute to TWD to some extent and so does the deformation of the pavements. Right rut depth has a greater impact on the cumulative water depth. The reason these coefficients are only moderately high is explained by the inherent properties of water entrapment. Many local water entrapment points are not generated by major rut depression but the texture variation or other forms of deformation.

4.5.4.2 Estimating New PP69-10 Parameters with the Existing Measures

Based upon literature review, rut depth is the only measure for most of the State agencies, which means it is the only retrievable technical parameter for analysis and comparison in past and current Pavement Management Systems (PMS). The relationship between traditional straightedge method and new PP69-10 method for rut depth measures is developed in Section 4.4. For the purpose of prompting the application of PP69-10, it is necessary and meaningful to establish quantitative relationships between the rut depth and the other newly proposed attributes in PP69-

10 such that the parameters like rut cross-sectional area and deformation permillage can be estimated by rut depth measures.

Based on the physical significance of the attributes, linear regression is employed to use rut depth measures to predict the new attributes. The regression analysis is conducted based on the attributes of the 8,829 transverse profiles. The relationships among rut depth, rut width, rut cross-sectional area, deformation, and water entrapment attributes are generated.

Rut depth and rut width (Equation 4.11 and 4.12):

$$LRW = 34.24\,LRD + 502.67,\ R^2 = 0.46 \tag{4.11}$$

$$RRW = 11.04\,RRD + 1098.1,\ R^2 = 0.20 \tag{4.12}$$

Rut depth and deformation permillage (Equation 4.13-4.15):

$$LDP = 0.074\,LRD + 2.172,\ R^2 = 0.34 \tag{4.13}$$

$$RDP = 0.084\,LRD + 1.008,\ R^2 = 0.44 \tag{4.14}$$

$$TDP = 0.045\,LRD + 0.049\,RRD + 1.602,\ R^2 = 0.49 \tag{4.15}$$

Rut depth and rut cross-sectional area (Equation 4.16 and 4.17):

$$LRA = 738.53\,LRD + 615.88,\ R^2 = 0.89 \tag{4.16}$$

$$RRA = 901.81\,RRD - 1131.2,\ R^2 = 0.90 \tag{4.17}$$

Rut depth and total water depth (Equation 4.18):

$$TWD = 0.787\,LRD + 0.337\,RRD + 14.396,\ R^2 = 0.45 \tag{4.18}$$

The relations between rut depth and water width and number of water points are not established due to their weak physical connections. It can be seen that the rut cross-sectional area measures can be satisfactorily approximated by the rut depth measures. The R^2 values are close to 0.9 for both wheel-paths. Therefore, it is promising for agencies to estimate the rut cross-sectional area with collected rut depth. The R^2 values for total water depth (TWD), total deformation (TDP), right deformation (RDP), and left rut width (LRW) are moderate, which demonstrates that it is feasible but need to be cautious when use rut depth measures to predict those values. For the prediction with low R^2 values, it is not recommended to conduct the estimates. In addition, these regression analysis results are consistent with the analyses addressed in the Section 4.5.4.1.

4.5.5 Pavement Performance and Rut Measures

4.5.5.1 General

Rut is a surface depression mainly caused by repeated traffic loadings. It is a direct indictor of the pavement performance. PP69-10 proposes a dozen parameters for characterizing permanent deformation; however, the users need to exploit these parameters to make engineering inferences. It is recommended that examining rut data statistically is an important approach to identifying the potential mechanisms of the rut (1, 10). In this section, the network rut data is used to analyze the cause of permanent deformation. Interrelations between four rut attributes: rut depth, rut width, rut cross-sectional area, and deformation are investigated.

To diminish the effect of undesired data, the transverse profiles without left or right rut (rut depth, rut width, and rut cross-sectional area are 0) are further removed from the sample data set. In the 8,829 profiles, there are 1,084 of them has no rut on left wheel-path, 81 of them has no

rut on right wheel-path, and 15 of them has rut depth on neither wheel-paths. In total 1,150 profiles (13%) are removed and 7,679 remain for this analysis.

The statistical summary of the reduced data set is presented in Table 4.5. Table 4.6 shows the correlation between the concerned attributes with new data set.

Table 4.5 Statistical Summary of Non-Zero Rut Attributes

	LDP	**LRD (mm)**	**LRA (sq mm)**	**LRW (mm)**
Mean	3.29	15.38	12114.52	1133.38
Median	3.02	14.46	11559.11	1175.00
Std. Dev.	1.31	9.41	7318.50	326.48
	RDP	**RRD (mm)**	**RRA (sq mm)**	**RRW (mm)**
Mean	3.02	23.19	19758.13	1352.02
Median	2.67	20.83	17243.76	1410.00
Std. Dev.	1.49	11.99	11478.81	263.64

Table 4.6 Correlation Matrix of Non-Zero Rut Attributes

	LDP	**RDP**	**LRD**	**RRD**	**LRA**	**RRA**	**LRW**	**RRW**
LDP	1.00	0.63	0.54	0.48	0.47	0.45	0.10	0.13
RDP	0.63	1.00	0.43	0.68	0.38	0.59	0.05	0.07
LRD	0.54	0.43	1.00	0.40	0.92	0.36	0.48	0.06
RRD	0.48	0.68	0.40	1.00	0.34	0.95	-0.03	0.44
LRA	0.47	0.38	0.92	0.34	1.00	0.29	0.66	0.03
RRA	0.45	0.59	0.36	0.95	0.29	1.00	-0.01	0.62
LRW	0.10	0.05	0.48	-0.03	0.66	-0.01	1.00	0.05
RRW	0.13	0.07	0.06	0.44	0.03	0.62	0.05	1.00

4.5.5.2 Rut Type and Rut Attributes

According to Simpson's definition introduced in Chapter 2, there are three types of rut (Figure 2.1): the one dimensional surface depression, the subgrade rut, and the lateral movement in surface layer. To determine the rut type is significant to pavement engineers. The first type rut is

mostly caused by compression of asphalt surface, the subgrade rut might imply problems of underlying layers, and the lateral movement is likely to be the failure of mixture materials. Research indicates it is possible to distinguish the types of rut through investigating the rut measures (1, 10).

As shown in the definitions of the three types of rut in Section 2.1.2 (Figure 2.2), based on the shape of the ruts, it is recognized the Type 1 and Type 2 ruts are more regular and the Type 3 rut is more irregular. For the Type 1 rut, the deformation should be principally caused by the downward depression of the pavement surface. It is evident in this case that the pavement deformation measures should have a relatively high correlation with the rut depth and rut width measures. In contrast, the deformation measures for Type 3 rut should have less correlation with the rut depth and rut width measures. Therefore, it is assumed that the larger correlation between deformation measures and rut depth and rut width measures is, the more possible the rut is the Type 1 rut or Type 2 rut, and vice versa.

From the Table 4.6, the correlations between rut depth measures and deformation measures are 0.54 and 0.68 for left and right wheel-path, respectively. The correlations between width measures and deformation measures are 0.1 and 0.07 for left and right wheel-path, respectively. Apparently, rut width has little contribution to deformation for both wheel-paths. The rut depth measures have moderate correlations with deformation measures, 0.54 and 0.68 for left and right wheel-paths, respectively. Therefore, it can be inferred that both wheel-paths are only moderately regular, which should be considered Type 3 rut rather than Type 1 rut. Furthermore, the right wheel-path is more regular than the left wheel-path as it has larger correlation between RRD and RDP, which means the rut on the right wheel-path is more prone to be Type 1 or Type 2 rut than left wheel-path. This inference is verified by the conclusions from Section 4.5.4 as well as statistics from the new data set with non-rut profiles removed (Table 4.5):

the left wheel-path has a larger mean and median deformation measure than that of the right wheel-path. However, the right wheel-path has more quantities in all rut measures than left wheel-path in all other attributes such as rut depth, rut width, and rut cross-sectional area. However, recalling the definition of the classification of the rut, the Type 1 rut should be at low or moderate severe level in terms of rut depth. Therefore, it is highly possible that the deformation on the right wheel-path could belong to Type 2, the subgrade rut.

4.5.5.3 The Ratio of Rut Depth to Rut Width

The mechanistic cause of various rut performances between left and right wheel-path is difficult to be determined solely based on parameter values. However, it is helpful to develop an indicator to estimate the type of rut. The ratio of rut depth to rut width (DTWR) is defined as Equation 4.19 in this study. This DTWR is only meaningful when the rut exists. The unit of rut depth and width is the same. The physical significance of the DTWR is that if the rut width does not grow with the increase of rut depth, in which case the DTWR is larger under the same amount of rut depth or width, the surface asphalt materials are likely to be compressed downwardly and the more possibly the rut is more regular. On the other hand, if the rut width is expanding with the increase of rut depth, then it is likely that the asphalt surface is distorted with uplifts besides of rut depression.

$$DTWR = \frac{Rut\ Depth}{Rut\ Width} \times 100 \tag{4.19}$$

From the profile data sets, it is found that the mean DTWR of the left wheel-path is 1.34 and the right wheel-path is 1.70. The median is 1.24 and 1.58, respectively. The histograms of DTWR for both wheel-paths are shown in Figure 4.7. It is seen both DTWR are slightly right skewed. The DTWR of the left wheel-path is less than that of the right wheel-path. Based on the physical significance of DTWR and the above drawn conclusions, it is reasonable to believe that

the larger DTWR is the more possible the rut is a Type 1. For example, in the example given in Section 3.4.4, the DTWRs for left wheel-path and right wheel-path are 1.14 and 1.99, respectively. As shown in Figure 3.11, the left wheel-path has a significant uplift on the left side of wheel-path whereas the right wheel-path is more regular (majorly downward depression) with compare to left wheel-path. The same observations are seen in many profiles.

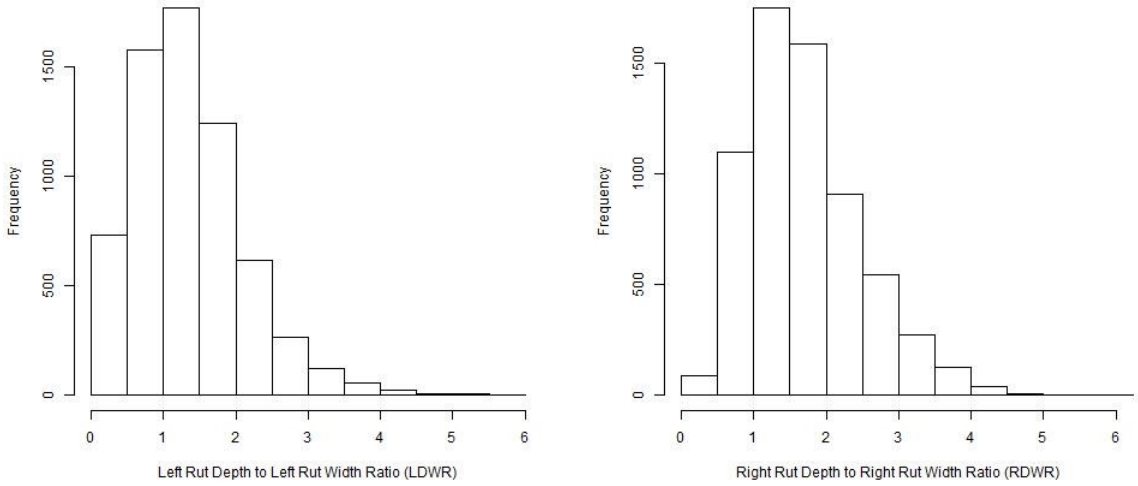

Figure 4.7 Histograms for Left and Right DTWR

4.5.5.4 Summary

The rut shape is analyzed based on the sample data set. The following conclusions are drawn:

- The performances of left and right wheel-paths are significantly different from each other.
- Both wheel-paths are moderately irregular; however the left wheel-path is prone to show Type 3 rut than the right wheel-path. The right wheel-path rut is prone to be Type 2, subgrade rut.

- The ratio of rut depth to rut width (DTWR0 can be a preliminary indicator for predicting the type of the rut; however, it is empirical in nature and needs further investigation. In this study, the left wheel-path has a smaller DTWR than the right wheel-path.

4.6 Comparison of Cross Slopes

Cross slope is an important characteristic of pavement. In literature review, two methodologies are widely used to calculate the present cross slope from pavement transverse profile. PP69-10 presents a different methodology for cross slope calculation. The relations among the three types of cross slope calculation methods are examined.

The computation process of PP69-10 method for cross slope is detailed in Section 3.4.4. To keep the data comparable, minor modifications are applied to the two traditional methods without impacting their applications.

- Regression line method: First, a least square regression line fits all the data points within the lane limit on the transverse profile. Second, the cross slope is the slope of regression line times -100.
- Edge-point method: First, the two edge points of the lane on the transverse profile are identified. Second, use the elevation of the left point to minus the elevation of right point. Third, the cross slope is the difference divided by the lane width times 100.

The correlation matrix for the results from three types of methods is presented in Table 4.7. Strong correlations are obtained among these measures. The largest correlation coefficient is between regression line method and PP69-10 method, which suggests that cross slope measures from these two methods can be converted in a robust manner. A 0.88 correlation with PP69-10 cross slope implies for a majority of the cases the cross slope can be determined with the two edge points.

Table 4.7 Correlation Matrix of Three Types of Cross Slope Calculations

	PP 69-10	Regression Line	Edge-Point
PP 69-10	1.00	0.97	0.88
Regression Line	0.97	1.00	0.93
Edge-Point	0.88	0.93	1.00

4.7 Conclusions and Recommendations

4.7.1 Conclusions

With a large data set of transverse profiles, the relationships among different parameters for permanent deformation are studied in this chapter. Some noticeable conclusions are found:

First, through the comparison of traditional and new PP69-10 measures, the rut depth measures and cross slope measures are found to have strong correlations with the existing measures. Especially, the relationship between the straight edge and PP69-10 rut depth measures not only validates the reliability of PP69-10, but also provides a bridge for agencies linking the traditional measures to promising new measures.

Second, it is found that rut cross-sectional area measures have strong correlation with rut depth measures and can be satisfactorily approximated by rut depth measures. This finding is significant to pavement engineers in terms of estimating the rut volume with current rut depth measures.

Third, a geometric model is established to determine the abnormal values of the deformation parameters. A profile produces permillage deformation value greater than 10 is recognized as an abnormal profile. The causes of the abnormal values are outlined.

Fourth, it is meaningful through the statistics and correlation analysis of the derived data set to understand the characteristics of pavement performance. The left rut depth, width, and

cross-sectional area are significantly less than those of the right wheel-path. Inferences are drawn: both wheel-paths are moderately irregular; however, the left side is more irregular than right side. Left wheel-path has less rut depth than right wheel-path under the same amount of rut width. The ratio of rut depth to rut width (DTWR) is proposed in the study as a preliminary indicator for predicting the type of the rut. These inferences are made from data collected from the network level.

4.7.2 Recommendations

Three major restrictions of data availability limit the scope of this research.

First is the pavement trench data, which can be used to measure permanent deformation occurred on underlying layers. It will be very significant to explore the interaction between rut measures from trenches and newly derived rut parameters from PP69-10.

The second is the lack of accurate historical data sets for comparison. How does the change of pavement performance with traffic loadings and environmental factors affect the increase of each parameter is worth examining. In addition, the research on impact of water entrapment on pavement structural performance has significant values to pavement modeling.

Third, the original design scheme is a necessity for the study of cross slope. Change of measured cross slope is an important indication for pavement deterioration. More importantly, the change of present cross slope at horizontal curves vitally affects traffic safety. With these data, the evaluation for cross slope is more meaningful and practical.

CHAPTER 5 A COMPREHENSIVE SYSTEM FOR RUT EVALUATION

5.1 Problems and Objectives

Since the AASHO Road Test in the late 1950s and early 1960s, the rut depth has been the sole technical parameter collected and recorded by agencies for characterizing pavement permanent deformation. Over the years, agencies and researchers have realized that only rut depth is insufficient to describe the characteristics of pavement permanent deformation (10, 35).

As introduced in the previous chapters, one of the most valuable contributions of PP69-10 is the proposal of multiple rut technical parameters. However, how to actually apply these parameters in practices is an unknown. As a matter of fact, some of the proposed parameters in PP69-10 have been introduced by other organizations or parties but never widely applied in practice. Based on literature review and the author's experience, various reasons that have hindered the widespread of multiple parameters for rut evaluation are summarized (7, 13, 28, 33, and 35):

- Premature data collection technologies are unable to collect pavement transverse profiles with high resolution. As a result, rut measures other than rut depth are difficult if not impossible to be accurately derived.

  For the measurement of rut depth, there are a few widely accepted and adopted protocols which specify explicit methodologies. For example, the straightedge method in the LTPP

program is the predominant method for rut depth measurement (2). On the other hand, there is not any national standard that explicitly defines other measures. Only some concepts or terminologies without standardized implementation procedures would not drive the promotion of applications.

- The agencies are accustomed with the practice of rut depth being the sole representation of pavement rut condition. They tend to insist that performance of transverse profiles should be treated as an integrated part but not a set of isolated parameters. Therefore, the management is to some extent reluctant to introduce more measurement items to the management system.
- Use of multiple parameters poses difficulties for agencies to prioritize maintenance and rehabilitation projects. In some agencies, rut condition which is represented by average rut depth, a single number, is a trigger for prioritization decisions or funding allocations. If multiple parameters are introduced for the same distress, agencies will have a dilemma in balancing the parameters and rating the pavement performance. Multiple parameters also cause complications in information communication.

At present, the first two concerns are mostly non-existent because of the recent developments: advance of data collection technology and updates of standard documentations. The latter two concerns are focused in the study because it is the management who applies single or multiple parameters. In other words, a methodology should be tailored to allow the management to keep their customs of using a single parameter and apply the multiple attributes at the same time. In the wake of 3D Ultra and the release of AASHTO PP69-10 and PP70-10, a comprehensive evaluation system for pavement permanent deformation is proposed in this chapter to resolve this management concern.

The principal objective of constructing such a comprehensive system is to evaluate all parameters derived from PP69-10 from a systematic process. Some specific objectives of this comprehensive evaluation for pavement permanent deformation include:

- Comprehensive. PP69-10 provides three aspects of technical parameters to represent the deformation condition, rut attributes, and water entrapment condition. Exclusion of any parameter in these three categories leads to loss of information. Therefore, all parameters of the three aspects must be included in the new evaluation system.
- Hierarchical. A number of parameters could be useful to project-level analysis. However, it would be difficult to be used in overall pavement rating for trade-off analyses or prioritizations. This system needs to have multiple layers so that different levels of stakeholders can access useful information at their own interest.
- Standardized. This system needs to be a standardized index system but not a category system. A category system produces many inaccuracies. Simple and straightforward standardized scales will facilitate and benefit the rut condition characterization. With this index system, pavement permanent deformation can be evaluated as a standardized numerical integration so that the management does not need to review the complicated performance parameters.

5.2 Terminologies

In this chapter, some terminologies regarding a comprehensive evaluation are presented. The following interpretations are developed based on literature review and the Merriam-Webster Dictionary.

- Attribute: It is an inherent characteristic of an object. In this research, the technical parameters such as deformation permillage, rut depth, and water entrapment depth are all attributes of pavement permanent deformation.

- Alternative: It means a selection from some mutually exclusive possibilities, or something can be chosen instead. In a comprehensive evaluation system, different alternatives refer to different combinations of the evaluation attributes that yield different preferences to stakeholders. For example, five pavement sections to be evaluated are the five alternatives. Criteria such as rut depth and rut width are the attributes to evaluate the alternatives.
- Hierarchy: It is a series of graded or ranked groups in a system.
- Score: It is a number that expresses quality of an attribute in this research. A standard score can be used for comparison between different attributes. In a hierarchical system, the aggregated values of objects or criteria at higher layers are also called scores.
- Weight: The relative importance of an attribute or an objective in a system. Weight reflects stakeholders' preferences over a set of attributes or objectives. The array of weights for multiple variables is called weight vector.

5.3 Overall Methodology

Based on the defined objectives, Comprehensive Evaluation (CE) methodologies are employed to develop this system. CE is an interdisciplinary research area which is relevant to psychology, statistics, management science, and systems engineering (43, 44). The objective of CE is to use systematic and methodical approaches to assess multiple decision criteria. A typical flowchart to deal with CE problems is shown in Figure 5.1 (45). The results of CE can be used for different purposes such as ranking, classification, and prioritization of the alternatives.

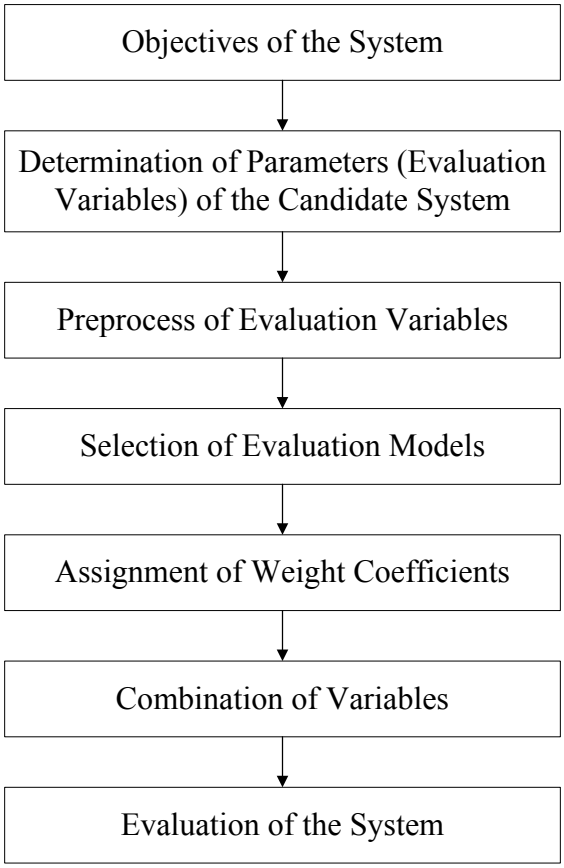

Figure 5.1 Typical Flowchart of Comprehensive Evaluation Problem

(Modified from Li and Yun (45))

To implement the objectives, this research is split into three phases, the procedures of which are presented in Figure 5.2. First, the twelve rut parameters are derived according to PP69-10. The statistics, distribution, and the interrelationship of the attributes are analyzed. This phase is accomplished in Chapter 3 and Chapter 4. Second, utility-theory based standard scoring functions are elicited for all of these attributes. Experts' opinions are collected to map all attributes to a dimensionless standardized scale. In the third phase, under the general framework of Analytical Hierarchy Process (AHP), a four level hierarchical structure for rut evaluation is established. Factor Analysis (FA) is employed to group bottom level attributes. The Principal Component Analysis (PCA) is applied with the sample data set to obtain objective weight for the

bottom level attributes and pairwise comparison is conducted to obtain subjective weight for all hierarchies. The specific methodologies used and their literature reviews in each step are introduced in their corresponding sections, respectively.

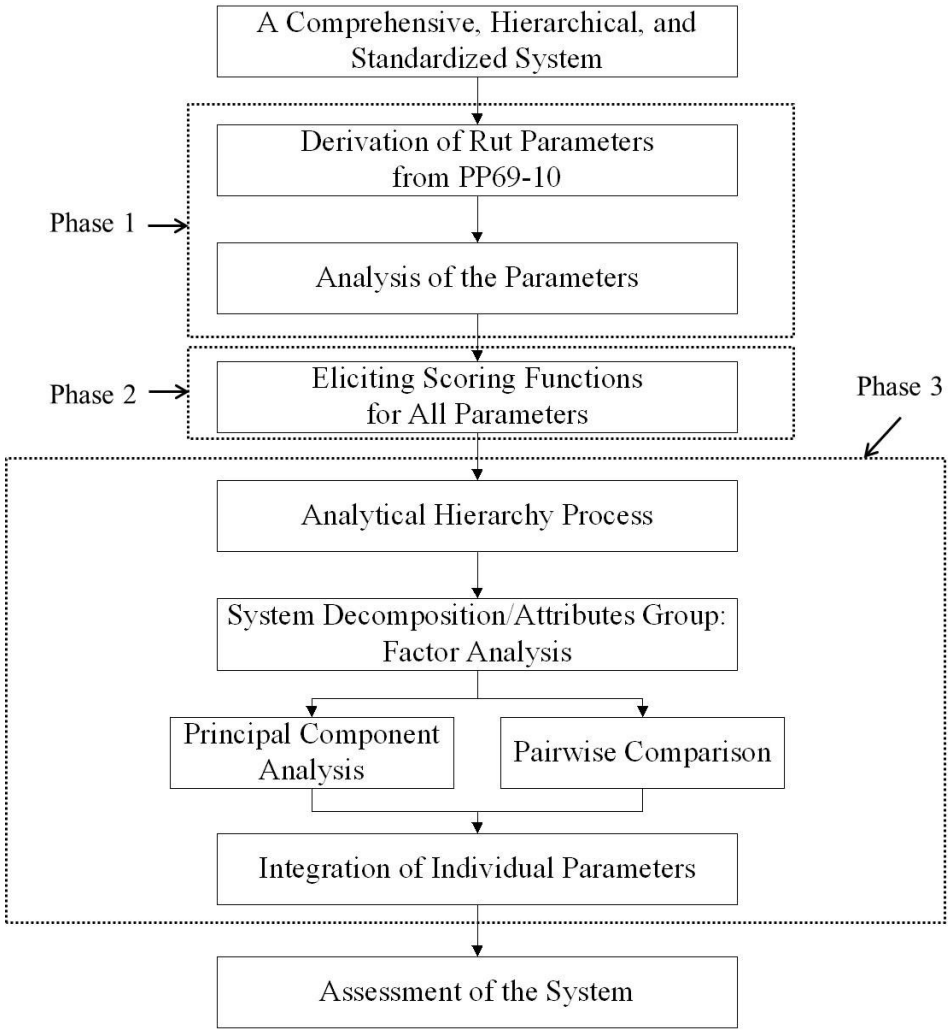

Figure 5.2 Flowchart of Constructing the Comprehensive Rut Evaluation System

5.4 Eliciting Single Attribute Functions

5.4.1 Overview

The Phase 1 of the construction this comprehensive system achieves satisfactory results. Among the thirteen parameters derived from PP69-10, Cross Slope (CS) is excluded from this system

because of lack of historical data. The remaining twelve technical parameters are selected for this comprehensive evaluation process:

- Total Deformation Permillage (TDP)
- Left Deformation Permillage (LDP)
- Right Deformation Permillage (RDP)
- Left Rut Depth (LRD)
- Right Rut Depth (RRD)
- Left Rut Width (LRW)
- Right Rut Width (RRW)
- Left Rut Cross Sectional Area (LRA)
- Right Rut Cross Sectional Area (RRA)
- Total Number of Water Entrapment Points (TNW)
- Total Water Entrapment Depth (TWD)
- Total Water Entrapment Width (TWW)

Since the above selected measures appear to be in various scales and dimensions, one of the objectives of Phase 2 is to enable all attributes physically and mathematically comparable and combinable (43, 46, and 47). First, a brief literature review is conducted to compare the techniques for data normalization. The utility theory based scoring functions are selected to map the original data to a standardized range. The shapes of the scoring functions are determined by interviewing a group of expert raters.

5.4.2 Data Standardization Techniques

Data standardization is a process to normalize a set of variables with different units into a same scale so that the analysts can better understand and compare the different variables (41).

5.4.2.1 Basic Techniques

There are a host of methodologies to normalize a data set with statistical principles. Traditionally three of them are widely used (41, 48, and 49):

Range based scaling: the candidate variables v are transformed to another new set of variables v' with Equation 5.1. This method does not require equality in means, variances, and ranges of the original. However, similar ranges between variables are preferred.

$$v' = \frac{v}{\max v - \min v} \tag{5.1}$$

0-1 scaling: the candidate variables v are transformed to another new set of variables v' with Equation 5.2. This method is applicable when the candidate variables have different means and standard deviations but equal ranges.

$$v' = \frac{v - min\, v}{\max v - \min v} \tag{5.2}$$

z-score: the candidate variables v are transformed to another new set of variables v' with Equation 5.3, where $\bar{v}$ and σ are the mean and standard deviation of the population, respectively. With applying this method, all new variables will have equal means of 0 and standard deviations of 1.

$$v' = \frac{v - \bar{v}}{\sigma} \tag{5.3}$$

The advantages of these data standardization techniques are objective and simple. However, their weaknesses are evident. First, these standardizations are subject to the sample data set per se. The population of the data set will affect the results. Second, these methodologies lack physical significance. Therefore, these techniques are mostly applied in the initial step of computing data processing such as Neural Networks (41).

5.4.2.2 Utility Theory Based Techniques

Another prevailing data standardization technique is the utility theory based method. Utility theory originates from economics two centuries ago, where researchers characterize the preferences of customers over some set of goods and services (51). The classic utility theory is utilized to compare the preference between pairs of alternatives (51). According to customers' preferences, utility functions are mathematically formulized to support decisions makers.

Currently, a few commonly used data classification or analysis methods are derivatives from utility theory. Standardized scoring function, gray theory based whitenization process, and fuzzy set functions are all essentially developed on the basis of utility theory (43, 47). Some of these applications involve uncertainties, such as fuzzy set model. The others directly quantify customers' preference, such as standard scoring functions. These methodologies are extensively applied in psychology and management science as well as in the area of pavement management. Zhang et al. employed fuzzy set model to establish membership function for different aspects of pavement measures such as roughness and distresses (52). Li elicited whitenization weight functions for different distresses in flexible pavements (53). In addition, the classifications of low, moderate and severe levels in LTPP distress guide and the MEPDG are also based on utility theory (9, 13). The common point of the methodologies is that all their forms attempt to quantify the degree of change of the customers' preference, which is marginal utility. This marginal utility is always reflected in the shapes of the utility functions.

A standard scoring function, sometimes called value function, is a mathematical mapping between the candidate attributes to a standardized range of values common to all attributes (47, 54). Ideally, sufficient evaluation data are desired to precisely portray the preferences; however, studies imply that if the general shape of scoring functions were predetermined, a handful of so called "shape parameters" would be the necessity to reach a satisfactory mapping (47). All

scoring functions suggest limit the output values to a 0-to-1scale for the convenience of further analysis (43, 47, 50, and 54). The domain of the function is the actual measures from the field and codomain, which is the output values of the function, is the score of the attribute.

Many instances and models of predefined scoring functions are reviewed (43, 47, 50, and 54). The standard value functions proposed by Kirkwood consist of four Returns to Scale (RTS) shapes, which are all in exponential form (47, 54). Wymore's scoring functions include twelve families in which the exponential term is determined with lower threshold, baseline value of the measure and other parameters (50). In this study, two models of standard scoring function are referenced: the Lamar's model and Su's model (43, 55).

A logistic min-additive model is introduced by Lamar for identifying preferences between two selections. The prototype of this model is shown in Equation 5.4. This equation needs to be examined associated with Figure 5.3. In Figure 5.3, the left end and right "infinite end" of the x axis represent the left and right selections, respectively. In Equation 5.4, the $w(x)$ is the strength or the probability that the decision makers choose the right selection and x is the decision makers' preference. α is a "measure of location" and β is a "measure of spread". As shown in Figure 5.3, the α and β are two coefficients determined by two additional parameters m and n. According to Lamar, m is the point below which the decision makers "strongly prefer" the left selection and n is the point beyond which the decision makers "strongly prefer" the right selection; k is the coefficient determined by probability of the selection when the preference x is equal to m or n. In the example of Lamar's model, the $k = -4$ means when $x = m$, there is an 88% chance that the decision makers will prefer the left selection.

$$w(x) = \frac{1}{1+\exp(k(\frac{x-\alpha}{\beta}))} \tag{5.4}$$

where $\alpha = \frac{1}{2}(m+n)$;

$\beta = n - m.$

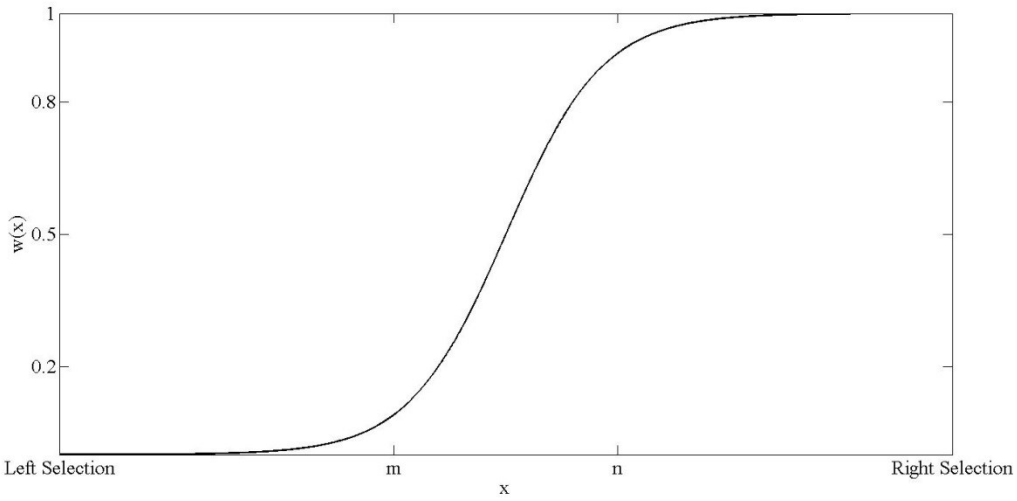

Figure 5.3 Lamar's Logistic Function for Determining Preferences over Two Selections (55)

Su presented a series of scoring functions for data normalization (43). The concave up exponential scoring function is presented in Equation 5.5 and Figure 5.4. $f(x)$ is the utility score of the candidate variables which the larger the attribute value is the smaller the standardized score is; when $x \leq m$ the score is c and when $x > m$ the score is determined by coefficients a and b; a and b are determined by two points on the exponential curve with one point is the (m, c) and another point (n, p) at which the score p of the variable is predetermined $(n > m)$. It can be seen that if the value of the variable exceeds m, the score drops abruptly with the increase of value.

$$f(x) = \begin{cases} c, & 0 \leq x \leq m \\ 1 - \exp(ax + b), & x > m \end{cases} \tag{5.5}$$

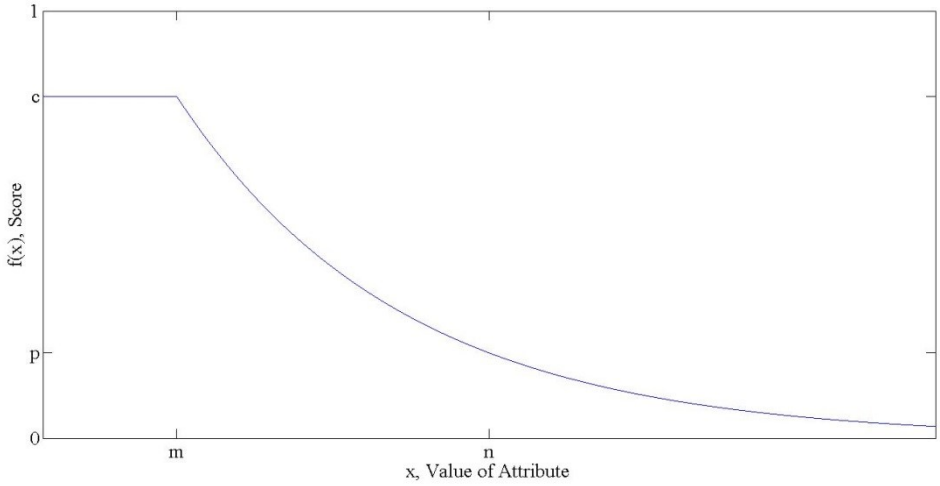

Figure 5.4 An Example of Su's Exponential Function (43)

5.4.3 Selection of Scoring Function

Due to the data distribution and variation and nature of pavement deterioration, the normal data standardization techniques are improper for this research. The utility theory based standard scoring functions are adopted in this research (43, 47, and 50). By applying this methodology, two purposes are served:

- The original data can be converted to dimensionless data that allow comparison and combination of different attributes.
- The original data are mapped to a meaningful scale, which reflects the preferences of pavement engineers. The essence of this process is the evaluation of each single rut attribute.

5.4.3.1 Assumptions

Determining the prototype of the scoring functions is critical as the shape of the curve reflects the general pattern of utility change (47). Due to the inexperience of expert raters to the new attributes, the principle for determining the predefined scoring functions is to select reasonable

curves which require providing minimal judgment information. In order to simplify the complexity of the survey, the scoring functions that can be determined by two data points are selected for this research.

In this study, the predefined scoring function is developed based on a five-grade categorization: “very good”, “good”, “fair”, “poor”, and “very poor”. Two threshold values (m and n) are obtained from the survey to map the five-grade system. The adequate threshold (m) distinguishes “very good” condition from “good”; the inadequate threshold (n) stands between “poor” condition and “very poor”. These two thresholds are used to determine the shape parameter of the scoring functions. In the predefined functions, the score of an attribute is defined as a 0-to-1 scale with 1 being the perfect condition, and 0 being the totally unacceptable.

5.4.3.2 Functions for Rut and Deformation Attributes

A sigmoid curve is assumed to fit the shape of pavement deformation and rut related attributes because their marginal utility decreases slowly at the initial stage but rapidly descends after reaching a certain point. This assumption conforms to pavement deterioration curves for these attributes (2, 7, and 56). Lamer’s logistic min-additive model is modified to serve this case (55). Two modifications are made to Equation 5.4, the Lamer’s model:

- The Lamer’s model is a monotone increasing function, which does not meet the reality of pavement deterioration. Therefore, the logistic function is modified to a monotone decreasing function by using 1 minus Equation 5.4.
- In the modified logistic equation, as shown in Figure 5.5, when x increases y asymptotically approaches 0 but never equals to 1. This phenomenon fits the infinite increasing property of the attributes; however, when x approaches 0, the scoring function asymptotically approaches 1 but never equals to 1 even when x is 0. This is undesirable

for a scoring function. Therefore, A linear function (Equation 5.6a) is considered for the interval of $[0, m]$.

As a result, a piece-wise function (Equation 5.6 and Figure 5.5) is defined for rut and deformation related attributes. In this standard scoring function, $f(x)$ is considered the score of the attributes and x is recognized as pavement engineers' judgment on the condition of the pavement. According to the previous "five grade" assumption, m and n are corresponded to a score of 0.8 and 0.2, respectively.

$$f(x) = \begin{cases} \frac{-0.2}{m}x + 1, & 0 \le x \le m \quad (a) \\ 1 - \frac{1}{1+\exp\left(k\left(\frac{x-\alpha}{\beta}\right)\right)}, & x > m \quad (b) \end{cases} \tag{5.6}$$

where $\alpha = \frac{1}{2}(m+n)$;

$\beta = n - m$;

$k = -2ln4$.

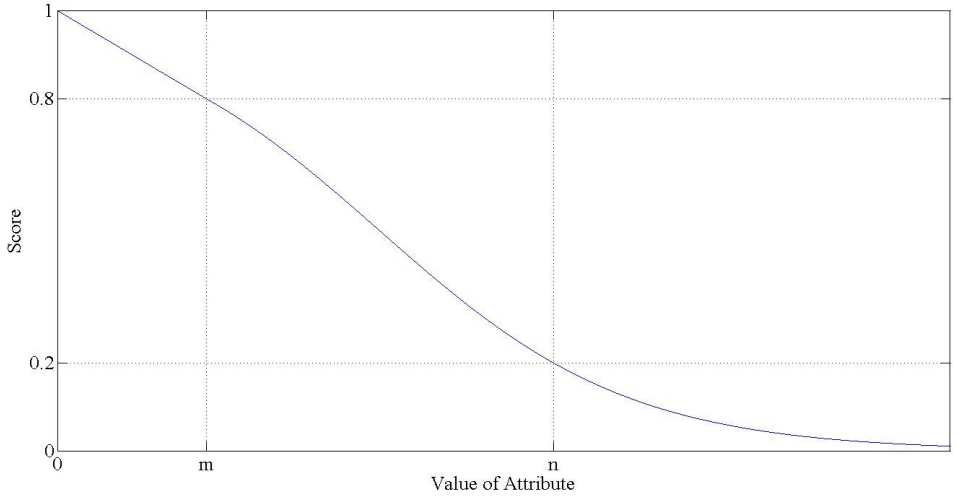

Figure 5.5 Standard Functions for Rut and Deformation Related Attributes

5.4.3.3 Functions for Water Related Attributes

The characteristics of the water related attributes are different from rut and deformations; therefore, another set of predefined functions is adopted. The Su's concave exponential function is modified for fitting water entrapment related attributes TWD and TWW. The assumption is that if the water related attributes no longer belong to the "very good" condition, their expected scores will drop abruptly with the increase of the attributes (*7, 15*). One modification is applied to Su's model: a linear function (Equation 5.7a) is employed to instead the constant score c in Equation 5.5. A piecewise function is generated to represent the TWD and TWW. Likewise, m and n are corresponded to a score of 0.8 and 0.2, respectively.

$$f(x) = \begin{cases} \frac{-0.2}{m}x + 1, & 0 \le x \le m \quad (a) \\ 1 - \exp(ax + b), & x > m \quad (b) \end{cases} \tag{5.7}$$

where $a = \frac{ln(0.25)}{m-n}$;

$b = ln0.2 - \frac{ln(0.25)}{m-n}m.$

5.4.3.4 Summary

All the predefined scoring functions are differentiable in their entire domains, where their first order derivatives are less than zero. All coefficients in Equation 5.6 and Equation 5.7 are flexible to be adjusted as per change of preferences or basic score scales. Considering TNW is a discrete measure, direct mapping is applied instead of eliciting a scoring function.

5.4.4 Subjective Survey

Subjective survey is taken with ten pavement professionals from Oklahoma State University and three from other agencies or institutes. Per the design of the scoring functions, only the adequate and inadequate thresholds (m and n) are obtained from the survey (43, 47, and 50). Unlike the

use of traditional rut depth that engineers have years of experiences and knowledge regarding its inherent characteristics, most of the twelve technical parameters in this survey, which are derived from PP 69-10, are new to pavement engineers with no historical data ever collected, nor any field survey taken before this research (28). Statistical summary of the attributes in Figure 4.4 and Table 4.3 are provided to raters for reference. Results are discussed with the survey participants until consensus is reached and summarized in Table 5.1. The survey questionnaire is attached in Appendix D.

Table 5.1 Results of the Subjective Survey

No.	Attribute	Adequate Threshold (m)	Inadequate Threshold (n)
1	TDP	1.50	5.00
2	LDP	1.50	5.00
3	RDP	1.50	5.00
4	LRD (mm)	5.00	20.00
5	RRD (mm)	5.00	20.00
6	LRW (mm)	500.00	1500.00
7	RRW (mm)	500.00	1500.00
8	LRA (mm^2)	4000.00	25000.00
9	RRA (mm^2)	4000.00	25000.00
10	TNW	0	4
11	TWD (mm)	5.00	40.00
12	TWW (mm)	450.00	1500.00

5.4.5 Single Attribute Evaluation Results

The threshold values m and n from the subjective survey are substituted into the predefined equations to calculate shape parameters. In the AASHO Road Test, a 0-to-5 score, the Present Serviceability Index (PSI), was developed to describe the overall condition of the pavement. This tradition is widely accepted by pavement engineers over the years. Therefore, the single attribute scores ranging from 0-to-1 are multiplied by 5 to have "a scale of 0-to-5 conforming to PSI convention". The 0-to-5 scale is established for all twelve attributes. The piece-wise curves for all

attributes are shown in Figure 5.6 and scoring functions are listed as Equation 5.8-5.13. Since attributes of left and right sides of pavement lane have the same numerical definition, only one function for each pair is elicited.

For TNW, when the number of water entrapment spots is greater than four, a score of 0 is assigned. When the number of water entrapment increases from 0-to-4, the score decreases from 5-to-1. For example, if there are 2 water entrapment spots on a profile, the score is set to 3.

For TDP, LDP, and RDP:

$$f(x) = \begin{cases} -0.665x + 5, & 0 \le x \le 1.5 \quad (a) \\ 5 - \frac{5}{1+exp(-0.792x+2.575)}, & x > 1.5 \quad (b) \end{cases} \tag{5.8}$$

For LRD and RRD:

$$f(x) = \begin{cases} -0.2x + 5, & 0 \le x \le 5 \quad (a) \\ 5 - \frac{5}{1+exp(-0.185x+2.31)}, & x > 5 \quad (b) \end{cases} \tag{5.9}$$

For LRW and RRW:

$$f(x) = \begin{cases} -2 * 10^{-3}x + 5, & 0 \le x \le 500 \quad (a) \\ 5 - \frac{5}{1+exp(-2.773*10^{-3}x+2.773)}, & x > 500 \quad (b) \end{cases} \tag{5.10}$$

For LRA and RRA:

$$f(x) = \begin{cases} -2.5 * 10^{-4}x + 5, & 0 \le x \le 4000 \quad (a) \\ 5 - \frac{5}{1+exp(-1.32*10^{-4}x+1.914)}, & x > 4000 \quad (b) \end{cases} \tag{5.11}$$

For TWD:

$$f(x) = \begin{cases} -0.2x + 5, & 0 \le x \le 5 \quad (a) \\ 5 - 5 * \exp(0.0396x - 1.807), & x > 5 \quad (b) \end{cases} \tag{5.12}$$

For TWW:

$$f(x) = \begin{cases} -2.22 * 10^{-3}x + 5, & 0 \leq x \leq 450 \quad (a) \\ 5 - 5 * \exp(1.32 * 10^{-3}x - 2.204), & x > 450 \quad (b) \end{cases} \tag{5.13}$$

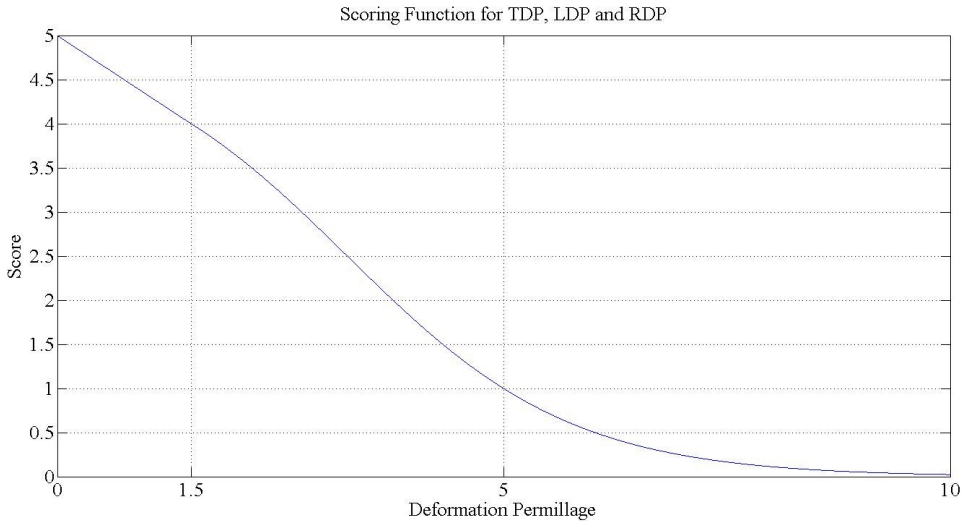

a. Deformation Scoring Function Curve

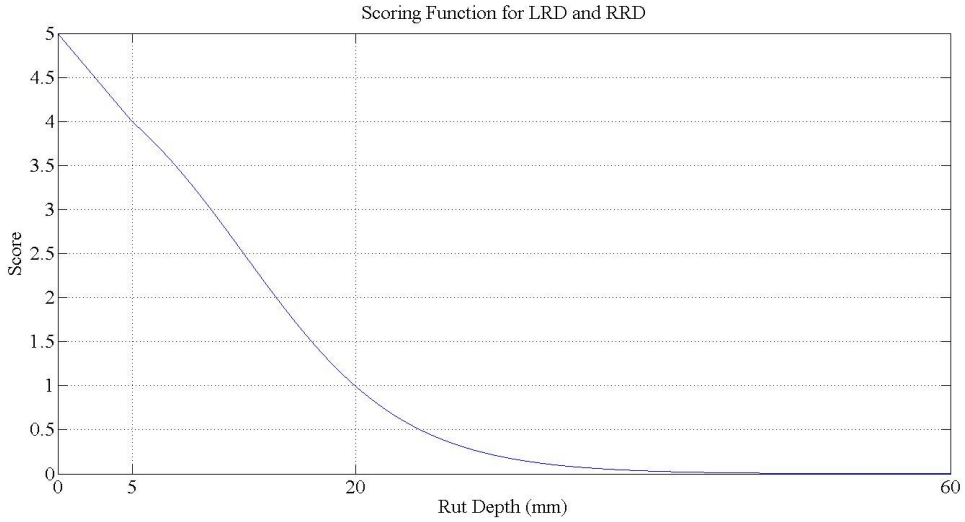

b. Rut Depth Scoring Function Curve

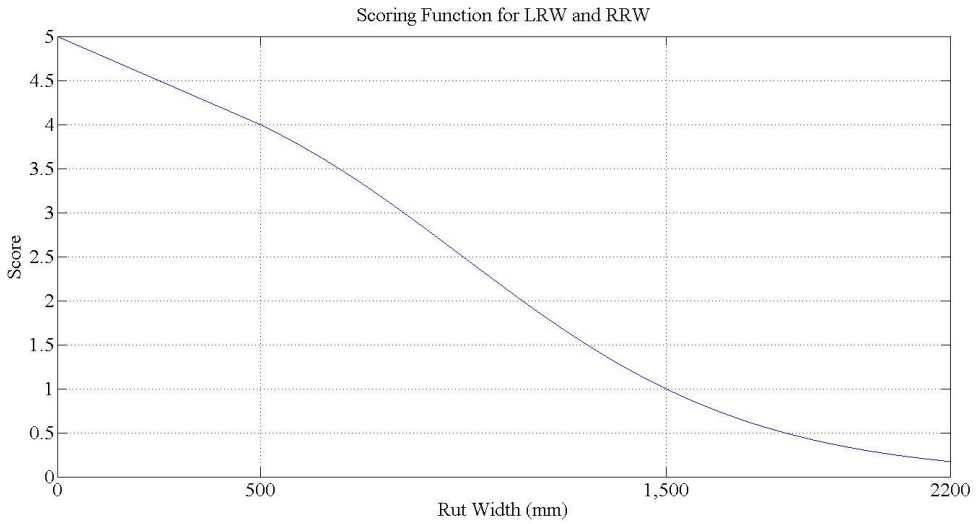

c. Rut Width Scoring Function Curve

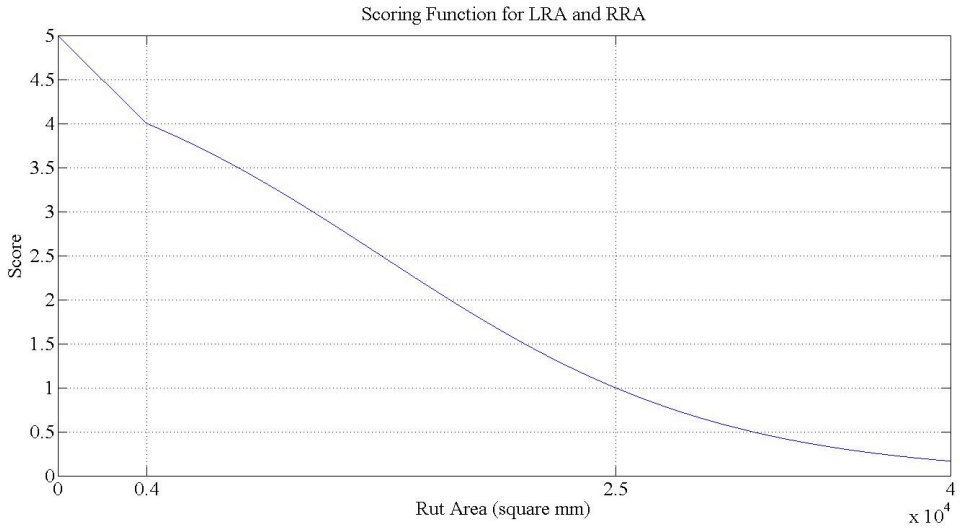

d. Rut Cross-Sectional Area Scoring Function Curve

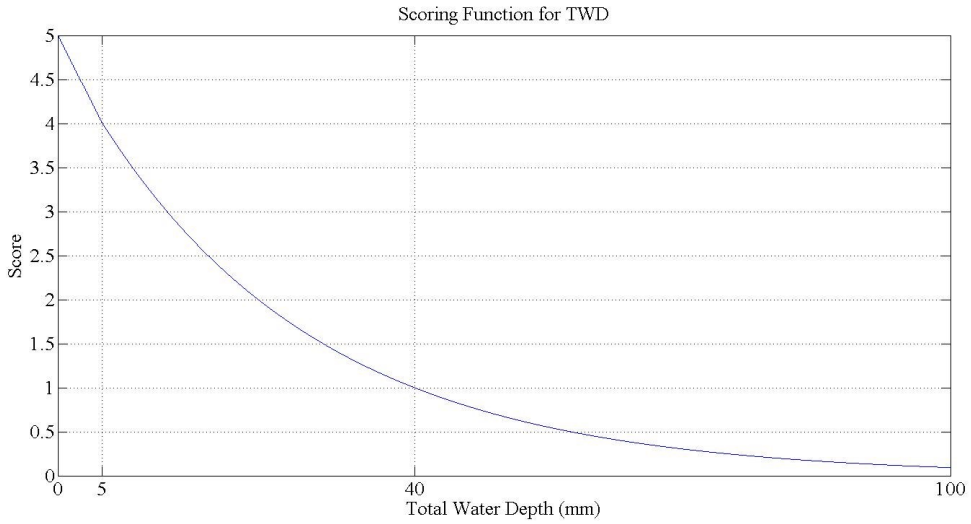

e. Total Water Depth Scoring Function Curve

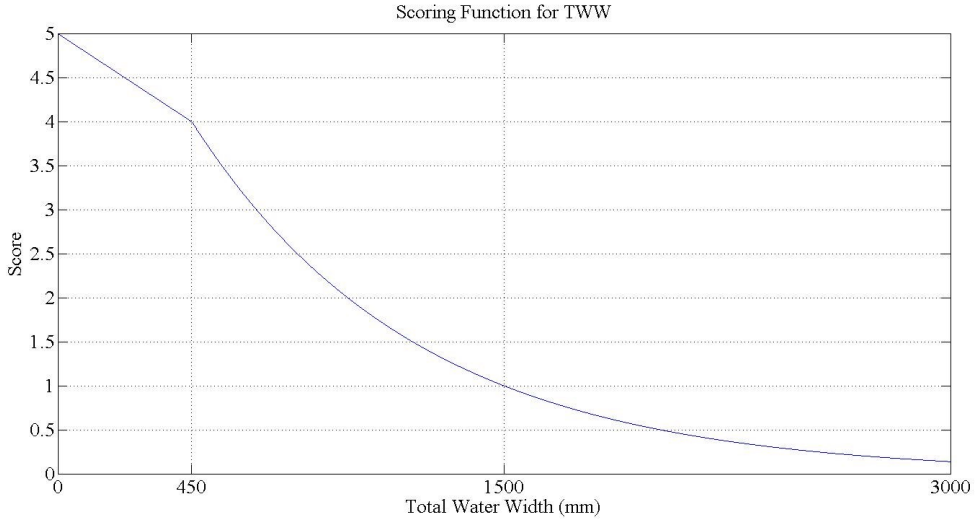

f. Total Water Width Scoring Function Curve

Figure 5.6 Scoring Function Curves for Attributes

5.5 Comprehensive Evaluation of Permanent Deformation

5.5.1 Overview

As a three-phase study, the first two phases involve the assessment of individual attributes. The principal task for the third phase is to establish a framework of comprehensive evaluation of these standardized attributes. Three core components in constructing this system are creating hierarchical structure, determining data combination technique, and assigning weights for evaluated individual attributes.

A number of methodologies are utilized in this CE process. Under the general framework of Analytical Hierarchy Process (AHP), the analytical thinking for system decomposition and the Factor Analysis (FA) are used for system structuring. The Principal Component Analysis (PCA) and the pairwise comparison technique which is a key contribution of AHP are attempted to obtain weight coefficients for all parameters. The linear data combination technique is utilized to integrate multiple attributes. The implementations of these methodologies are discussed in detail after an introduction to these methodologies and brief literature reviews.

5.5.2 Methodologies for Comprehensive Evaluation

5.5.2.1 System Structuring Methodologies

In a candidate system to be evaluated, there are initially two elements. One is the goal or objective of the system and the other one is a number of attributes to implement the goal. This is called a two-level system. Decision makers use their expertise and empirical thinking to assess the contributions of the attributes to the goal. With these assessments, the alternatives can be evaluated. However, research indicates examining more than seven attributes at a time makes the decision makers less pleasant (47). A hierarchical structure is preferred to be adopted in this case.

Therefore, for those systems contain many candidate attributes, the first step of comprehensive evaluation is to establish a hierarchical structure.

According to Kirkwood (54) and Saaty (58), a small number of hierarchies are beneficial for information communication and analysis. In practice, a system is usually comprised of a top layer, a bottom layer and a few intermediate layers (57, 58). The top layer is the overall evaluation objective of the system and the bottom layer consists of the attributes to be evaluated. The intermediate layers are generally set up based on specific purposes. Typically, there are two types of methods to construct the intermediate hierarchies: the top-down method and the bottom-up method (57).

The top-down method is also named objectives-driven method. It is used when the objective is determined but the alternatives are unclear, usually at the beginning of the evaluation process. With this method, the overall objective of system is decomposed into a few subsystems with different sub-goals. Empirical strategies and human experiences are the most valuable resources for top-down partitioning. The Analytical Hierarchy Process (AHP) provides an insight to structure top-down system division (58). In AHP, it is advised the overall objective can be first divided to a few sub-objectives with which the evaluation process can be more understandable and goals are more explicit and straightforward.

The bottom-up method is also named alternatives-driven method. It is usually used when the properties of alternatives are known. Based on the intrinsic properties and differences of the alternatives, the evaluation attributes are grouped. Mathematically, the Factor Analysis (FA) is an ideal tool for grouping bottom-level attributes (41, 43, and 49). The advantage of FA is to reveal the underlying relations of the attributes which are unobservable in the original form by performing a series of linear transformations (49). The grouped attributes are used to form higher levels of measures.

5.5.2.2 Techniques for Combining Attributes

In a comprehensive evaluation system, the scores of the attributes are only assigned for the bottom-level attributes (47). The scores of the evaluation objects at higher layers are derived by combining the lower level scores with their assigned weights. To keep the score consistency between multiple layers, standard data combination techniques are developed (47). Suppose there are n attributes to be combined, each attribute has a score x and is assigned a weight w. The attributes can be combined with the following commonly used methods (47):

Linear combination: As shown in Equation 5.14, it is the linear combination of multiple attributes and the coefficients are their respective weights. Usually, the sum of all weights is normalized to 1 so that the scale of the score does not change with data combination. Linear combination is the most straightforward and common method for combining attributes. The most representative application is the calculation of grade-point average (GPA) system for students.

$$f = \sum_{i=1}^{n} w_i x_i \tag{5.14}$$

where n is the total number of attributes;

w_i is the weight of the ith attribute;

x_i is the output of the scoring function of the ith attribute;

$\sum_{i=1}^{n} w_i = 1$.

Product combination: As shown in Equation 5.15, being different from the linear combination, it is the product combination of the attributes and weights. The output of this product combination is largely affected by the attributes with extreme weights or scores. It is often used for mission critical functions.

$$f = \prod_{i=1}^{n} w_i x_i \tag{5.15}$$

where n is the total number of attributes;

w_i is the weight of the ith attribute;

x_i is the output of the scoring function of the ith attribute.

Exponential combination: The original exponential combination model includes two functions, one for increase of preference and the other for decrease of preference. The former one is shown as an example in Equation 5.16. A constant scaling factor k is introduced in this model to adjust the output range. This model is effective when uncertainty is incorporated in the system.

$$f = 1 - e^{-\sum_{i=1}^{n} k w_i x_i} \tag{5.16}$$

where n is the total number of attributes;

w_i is the weight of the ith attribute and $0 \leqslant w_i \leqslant 1$;

x_i is the output of the scoring function of the ith attribute;

k is the scaling factor.

In addition to these listed methods, some other methods such as sum minus product combination and compromise combination are developed by systems engineers (47). Generally, different methods are applicable to different situations. However, the more complicated the model is, the more professional experiences and adaptive tunes are needed to control the reliability.

5.5.2.3 Principal Component Analysis

Principal Component Analysis (PCA) is a well-known and widely used statistical tool for multi-variable data analysis. The objective of PCA is to reduce the dimensionality of data while retaining as much variation as possible (59). Two most noticeable features of PCA are:

- PCA transfers the original data to a set of uncorrelated vectors;
- The first a few vectors, also known as principal components (PCs), can be used to explain most of the variations of the data.

There are two methodologies to generate the PCs, which are the covariance method and the correlation coefficient method. The derivation of the PCA is defined as follows (41, 49, and 57):

Suppose data set M contains k vectors (variables) Y_i where $i = 1, \dots, k$ ($k \geq 2$). The Y_i are usually interrelated and each Y_i should have a number of observations. R is the covariance matrix or correlation matrix of M (If R is the covariance matrix, the method is the covariance method, and vice versa). By applying an orthogonal transformation to R, a new set of uncorrelated vectors which are the eigenvectors C_j of R are obtained. If the corresponding eigenvalues l_j are following a descending order, the eigenvector corresponding to the largest eigenvalue explains the largest amount of the variance and is defined the first principal component (PC_1). The eigenvector which corresponds to the second largest eigenvalue is the second PC (PC_2). PC_2 explains the largest amount of variance among all the components uncorrelated with PC_1. Likewise, PC_3 to PC_k can be derived. Since the covariance method is affected by the magnitude of different variables, the correlation coefficient method is primarily exercised in many practices.

Mathematically, as shown in Equation 5.17, the original vectors (Y_i) are linear combinations of PCs (C_j); the a_{ij} are the loadings or namely the coefficients of the jth PC.

$$Y_i = \sum_{j=1}^{k} a_{ij} C_j \tag{5.17}$$

The essence of PCA is to perform linear transformation to the original data set and obtain new data set at a coordinate system where the principal variances are carried. As intuitively

illustrated in Figure 5.7, the original coordinates of the data are (x1, x2), where the variances on both axes are significant. By conducting PCA, the coordinates are shifted to (y1, y2) where the majority of variance of the data set can be explained on the new axis y1 and the variance on y2 is significantly diminished. In this example, the data dimension is reduced to 1 from 2 with applying PCA.

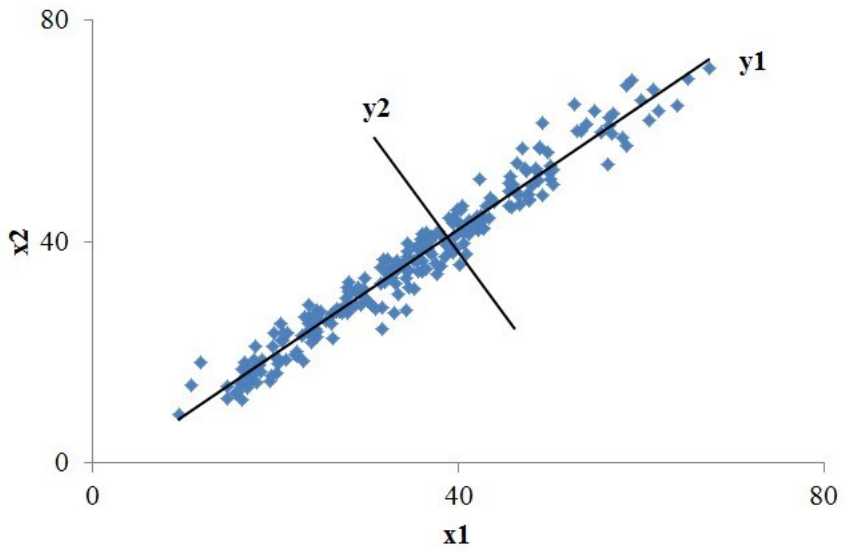

Figure 5.7 Illustration of PCA

Usually, if a large portion of (e.g. 85%) the cumulative variance of the original data set can be explained by the first few PCs, the original data set can be represented by the first few PCs so that the dimension of the data is reduced to the number of these PCs.

When the PCA is used in comprehensive evaluation, the cumulative variance on the PCs is first examined. Some researchers believe that all PCs within 85% cumulative variations should be used for comprehensive evaluation with their loadings being the relative weights. However, this method is disputed because of the positive and negative weights are unexplainable in comprehensive evaluation. Currently, the main stream believes that if the first few PCs retained a

significant amount of total variation, the loadings on the first PC (a_{i1}) would be considered as the relative weights of original variables (Y_i) for data combination. Otherwise, the data set is claimed improper for applying PCA based comprehensive evaluation. The physical significance of the weight vectors from PCA is the ability of the original variable to carry variances.

PCA is widely adopted for comprehensive evaluation in many areas such as environmental quality assessment and city development evaluation. One study is seen in the field of pavement management engineering utilizing this methodology to evaluate noise-levels of pavement (60).

5.5.2.4 Factor Analysis

Factor Analysis (FA) is an extended application of PCA. The basic mechanism of FA is similar to PCA, which is to reduce data dimension by applying orthogonal transformations. However, FA explicitly aims to reduce the original k variables to m groups of hypothetical variables, which are called factors. The derivation of factors can be calculated with the procedures calculating PCA and likewise, m factors are uncorrelated with each other. The difference of FA from PCA is that the number of factors m needs to be predefined. Usually, this number of factors can be objectively determined (i.e. the number of PCs that carry more than 85% cumulative variance) or subjectively determined (i.e. based on the needs or actual situations). From the m derived factors, the patterns of loadings (a_{ij}) are used to determine the hypothetical variables, which are called common factors.

However, the underlying relations of the loadings are often directly unobservable from the factors that obtained by PCA method. An important technique called Factor Rotation (FR) is introduced to find out the common factors. The most commonly used FR is the "Varimax Rotation (VR)" method. The principle of VR is to transform as many factor loadings as possible to either "near zero" or "far from zero (close to -1 or 1)". With applying VR, the original

variables that correspond to the a few largest loadings (absolute value) of each factor are obvious to be identified. Since these underlying variables always have some intrinsic or natural similarities, they can be grouped and named based on their common characteristics (41, 59). For each factor, there should be a group of common variables; then each group represents a common factor of the variables. By applying these transformations, the original k variables are reduced to m common factors.

Like PCA, FA is extensively used in social sciences and multiple engineering disciplines such as agriculture and biology. However, rare sources are found for pavement evaluation.

5.5.2.5 Analytical Hierarchy Process

Analytical Hierarchy Process (AHP) is a structured technique to assist decision making in complex systems. Since introduced by Saaty in the 1970s, AHP has two unique contributions to systems engineering: first, it outlines the analytical thinking process for complex and fuzzy system and introduces an objective-orientated hierarchical structure for comprehensive evaluation problems; and second, it proposes a methodology called pairwise comparison to quantitatively evaluate multiple attributes. The first system structuring problem is discussed in Section 5.5.2.1. The second pairwise comparison technique is introduced as follows:

When facing a number of candidate attributes, it is often difficult for decision makers to directly assign relative weights for every attribute in a robust manner. To avert this risk, pairwise comparison is introduced in AHP (58). Generally speaking, pairwise comparison is a method to assist decision makers to formulize their empirical knowledge and judgment into a weight vector so that the evaluation over a number of candidate attributes is more reliable.

Suppose there are n attributes x_i $(i = 1, 2, \dots, n)$ to be evaluated. The goal of comparison is to identify the relative importance of x_i to x_j in terms of their goal, which is the superior level

objective or sub-objective. The decision maker assigns the relative importance of x_i to x_j as per the principle given in Table 5.2 provided by Saaty (58). This importance of x_i to x_j is recorded as a_{ij}. To evaluate n attributes, $n(n-1)/2$ comparisons are needed for decision makers. Then the importance matrix A is then defined in Equation 5.18.

$$A = \begin{pmatrix} 1 & a_{1,2} & \cdots & a_{1,n} \\ a_{2,1} & 1 & \cdots & a_{2,n} \\ \vdots & \vdots & \ddots & \vdots \\ a_{n,1} & a_{n,2} & \cdots & 1 \end{pmatrix}_{n \times n} \tag{5.18}$$

Table 5.2 Scales System for Pairwise Comparison (58)

Numerical Scale	**Degree of Preference**
9	Extremely Preferred
7	Very Strongly Preferred
5	Strongly Preferred
3	Moderately Preferred
1	Equally Preferred
1/3	Moderately Less Preferred
1/5	Strongly Less Preferred
1/7	Very Strongly Less Preferred
1/9	Extremely Less Preferred

Note: 2, 4, 6, 8 are used to represent the intermediate preferences between two adjacent numbers and so are 1/2, 1/4, 1/6, 1/8.

After the importance matrix A is obtained, the Equation 5.19 is used to find the weights vector of the attributes.

$$A\bar{W} = \lambda\bar{W} \tag{5.19}$$

where A is the importance matrix;

$\bar{W}$ is the weight vector of the attributes;

λ is the eigenvalues of A.

Since it is possible that the decision maker assigns inconsistent or conflicting values in different comparisons (e.g. the decision maker assigns $a_{ij} > a_{jk}$ and $a_{jk} > a_{kl}$ but also $a_{kl} > a_{ij}$), the next step is the consistency check of the results. The Consistency Ratio (CR) is defined by Saaty as in Equation 5.20 and 5.21. The general acceptable level is that CR being less than 0.1. Otherwise the pairwise comparison is invalid because of significant inconsistency. The above process is iterated among all candidate attributes and objectives at each level except the top level. The verified weight vectors are used to combine the attributes.

$$CR = \frac{\mathrm{CI}}{RI} \tag{5.20}$$

$$CI = \frac{\lambda_{max} - \mathrm{n}}{n-1} \tag{5.21}$$

where λ_{max} is the maximum eigenvalue of A;

n is number of evaluation attributes;

RI is the random index given by Saaty (Table 5.3) (58).

Table 5.3 List of RI Values (58)

n	1	2	3	4	5	6	7	8	9
RI	0	0	0.58	0.9	1.12	1.24	1.32	1.41	1.45

AHP has been extensively used in infrastructure asset management as well as pavement condition evaluation (61, 62). Xiao adopted it to identify priorities in terms of risk prevention in pavement design (63).

5.5.3 Construction of Evaluation System

5.5.3.1 Structuring the System

The overall objective of this system is to establish a single index system that is able to rationally represent all attributes of pavement permanent deformation. According to AHP, a top-down objective decomposition is first performed to the system. Based on the major objectives of pavement evaluation process and the definition of the candidate attributes, three functional objectives are determined for this system: pavement safety, ride quality, and structural health. As it is difficult to directly judge the contribution of each parameter to these three sub-objectives, an intercrossing structure is used to aggregate the attributes, as shown in Figure 5.8.

However, it would be too many if each sub-objective directly corresponds to twelve parameters. The bottom-up system structuring technique is considered to categorize the twelve parameters into a few groups. Factor Analysis (FA) is applied to identify the underlying variables to be grouped.

The standardized attributes of the 8,829 transverse profiles from Chapter 4 (8,960 profiles after abnormal profiles removal) are used to conduct the FA. The *r project* is utilized to conduct FA calculations (42). The first three factors are examined after applying the Varimax Rotation (VR), where results are shown in Table 5.4. It is seen that TDP, LDP, and RDP all carry more than 0.8 loadings in Factor 1. Similarly, high loadings observed in Factor 2 are LRD, LRA, and LRW and Factor 3 are RRD, RRA, and RRW. The three factors carry about 68% of the variance. The physical interpretation of these three underlying factors is quite straightforward. It is obviously that deformation condition, left rut condition, and right rut condition should be considered three common factors and categorized into three groups. However, the three remaining variables, TNW, TWD and TWW are not found carrying significantly high loadings. Considering their physical significance of the three variables, they are empirically categorized

into the fourth group. Thus, the four evaluation objects for intermediate level are determined. The structure of the system is shown in Figure 5.8.

Table 5.4 Factor Analysis Results

Loadings	**Factor1**	**Factor2**	**Factor3**
Total Deformation Permillage	0.964	0.225	0.123
Left Deformation Permillage	0.840	0.297	0.102
Right Deformation Permillage	0.871	0.173	0.206
Left Rut Depth	0.342	0.870	0.115
Right Rut Depth	0.354	0.109	0.802
Left Rut Cross-Sectional Area	0.311	0.945	
Right Rut Cross-Sectional Area	0.325	0.120	0.935
Left Rut Width	0.101	0.842	
Right Rut Width	-0.103		0.781
Total Number of Water Entrapment Points	0.264	0.149	
Total Water Entrapment Depth	0.332	0.263	0.358
Total Water Entrapment Width	0.188	0.237	0.114
Proportion Var	0.256	0.225	0.197
Cumulative Var	0.256	0.481	0.678

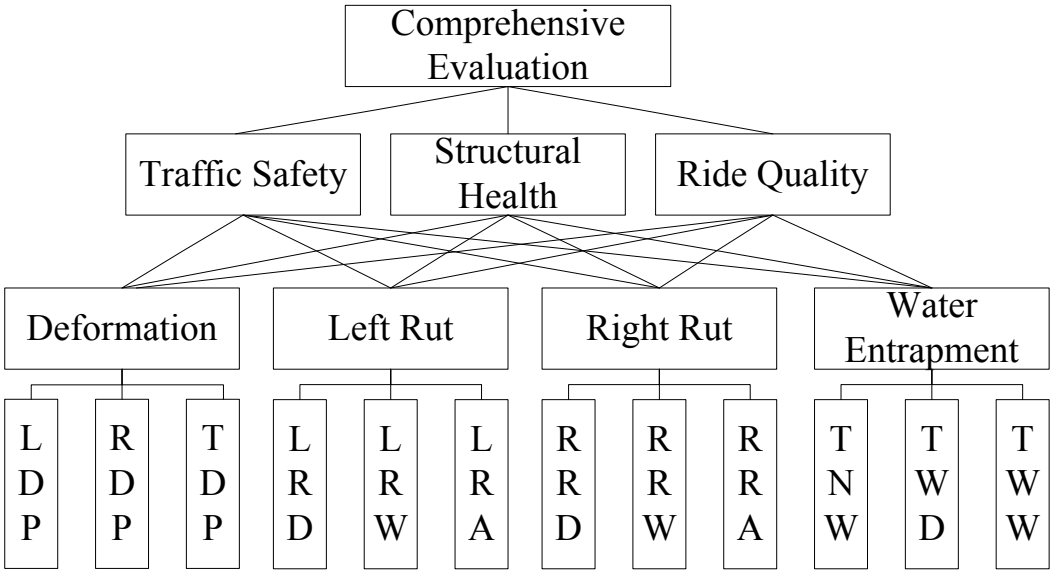

Figure 5.8 Structure of the Comprehensive Evaluation System

5.5.3.2 Acquisition of Weight Vectors

Based on the literature review of relevant studies and the physical significance of the attributes, a linear combination of the attribute is applied to this comprehensive evaluation system. The data combination follows the Equation 5.14. The determination of the weight coefficients is explored in two approaches: the PCA based evaluation and AHP pairwise comparison.

PCA is only able to be conducted for the bottom level evaluation. Therefore, independent PCA is conducted for the four groups of measures, respectively. Each PCA analyzes the three attributes produced with the 8,829 profiles. The *r project* is utilized to calculate the PCs and their loadings (42). The coefficient matrix is used for calculation in this study. The outputs of *r project* are summarized in Table 5.5. It can be seen that all of the first PC carry more than 80% of the total variance except the water attributes, which only carries 54% of total variance. For consistency, all the absolute values of the loadings on the first PC are used to derive the relative weight of the bottom level parameters. The weight vectors are normalized to a sum of "1" as per requirement of linear data combination, as shown in Table 5.6.

As an objective weight assignment process, the PCA method does not consider the actual importance of the attributes from perspectives of stakeholders but rather the ability of carrying variance. To consider pavement engineers' assessment, the AHP pairwise comparison is applied to (1) assign weights for all hierarchies and (2) compare with the PCA results.

Table 5.5 Results of PCA Analysis for Bottom-Level Attributes

PCA No.	Group	Loadings	PC1	PC2	PC3
1	Deformation	Total Deformation Permillage	-0.609		0.793
		Left Deformation Permillage	-0.559	-0.719	-0.142
		Right Deformation Permillage	-0.563	0.694	-0.448
		Proportion Var	0.886	0.106	0.008
		Cumulative Var	0.886	0.992	1.000
2	Left Rut	Left Rut Depth	0.580	-0.543	0.607
		Left Rut Width	0.598	-0.222	-0.770
		Left Rut Cross-Sectional Area	0.553	0.810	0.196
		Proportion Var	0.891	0.092	0.017
		Cumulative Var	0.891	0.983	1.000
3	Right Rut	Right Rut Depth	0.581	-0.554	0.596
		Right Rut Width	0.624	-0.166	-0.764
		Right Rut Cross-Sectional Area	0.552	0.816	0.250
		Proportion Var	0.800	0.171	0.029
		Cumulative Var	0.800	0.971	1.000
4	Water	Total Number of Water Entrapment Points	-0.461	0.801	-0.382
		Total Water Entrapment Depth	-0.569	-0.597	-0.565
		Total Water Entrapment Width	-0.681		0.731
		Proportion Var	0.540	0.306	0.154
		Cumulative Var	0.540	0.846	1.000

Table 5.6 Weight Coefficients for Bottom Level Derived from PCA

No.	Group	Attribute	Weight
1	Deformation	Total Deformation Permillage	0.35
		Left Deformation Permillage	0.32
		Right Deformation Permillage	0.33
		Sum	1.00
2	Left Rut	Left Rut Depth	0.34
		Left Rut Width	0.35
		Left Rut Cross-Sectional Area	0.32
		Sum	1.00
3	Right Rut	Right Rut Depth	0.33
		Right Rut Width	0.36
		Right Rut Cross-Sectional Area	0.31
		Sum	1.00
4	Water	Total Number of Water Entrapment Points	0.27
		Total Water Entrapment Depth	0.33
		Total Water Entrapment Width	0.40
		Sum	1.00

The same group of survey participants for the development scoring function is invited to conduct pairwise comparisons for the attributes for each level. The survey questionnaire is attached in Appendix E. Thirteen groups of importance matrices are obtained from the survey and their weight vectors are calculated separately. The Consistency Ratio (CR), which is an indicator to assess the consistency of evaluation, is less than 0.1 based on each rater's importance matrix, which is acceptable according to Saaty (58). The weight vectors from different raters are directly averaged to obtain the final weight vectors. The weights derived for the bottom level comparison are summarized in Table 5.7. The weights derived for the intermediate level and sub-objective level are presented in Table 5.8 and Table 5.9, respectively.

Table 5.7 Weight Coefficients for Bottom Level Derived from Pairwise Comparison

No.	Group	Attribute	Weight
1	Deformation	Total Deformation Permillage	0.55
		Left Deformation Permillage	0.21
		Right Deformation Permillage	0.24
		Sum	1.00
2	Left Rut	Left Rut Depth	0.46
		Left Rut Width	0.19
		Left Rut Cross-Sectional Area	0.35
		Sum	1.00
3	Right Rut	Right Rut Depth	0.46
		Right Rut Width	0.19
		Right Rut Cross-Sectional Area	0.35
		Sum	1.00
4	Water	Total Number of Water Entrapment Points	0.26
		Total Water Entrapment Depth	0.35
		Total Water Entrapment Width	0.39
		Sum	1.00

Table 5.8 Weight Coefficients for Intermediate Level from Pairwise Comparison

No.	Sub-Objective	Attribute	Weight
1	Traffic Safety	Deformation	0.19
		Left Rut	0.15
		Right Rut	0.24
		Water Entrap	0.43
		Sum	1.00
2	Structural Health	Deformation	0.31
		Left Rut	0.16
		Right Rut	0.21
		Water Entrap	0.31
		Sum	1.00
3	Ride Quality	Deformation	0.34
		Left Rut	0.15
		Right Rut	0.25
		Water Entrap	0.26
		Sum	1.00

Table 5.9 Weight Coefficients for Sub-objective Level from Pairwise Comparison

No.	Sub-Objective	Weight
1	Traffic Safety	0.69
2	Structural Health	0.15
3	Ride Quality	0.16
	Sum	1.00

It can be seen that there are some differences between the evaluation results derived from PCA and AHP methods. Numerically, the differences between the weights from PCA are smaller than those from AHP pairwise comparison. For example, the rut width measures have a little more weights than the rut depth measures based on PCA but have much less weights than rut depth measures in AHP results. This is reasonable since the principle of PCA is to retain the variance of the information but AHP is to reflect engineers' judgment. However, surprisingly, the

AHP and PCA produce very close weights for water entrapment attributes, which is assumed a coincidence. To retain the advantages of AHP and PCA, the average values of both methods are used as weight vectors for the aggregation of the bottom level attributes.

In addition, it can be seen from Table 5.9 that the traffic safety is weighted significantly higher than the other two sub-objectives with pairwise comparison. In Table 5.8, water related attributes weight higher than other three groups of attributes for the sub-objective traffic safety. These results reflect the pavement engineers' concern on water entrapment on the pavement.

With different levels of weight vectors, the coefficients from the bottom level attributes to the overall objective as well as each sub-objective are calculated and summarized in Table 5.10.

Table 5.10 Weights of Attributes under All Objectives

Attribute	Comprehensive Evaluation	Traffic Safety Only	Structural Health Only	Ride Quality Only
Total Deformation Permillage	0.11	0.09	0.14	0.15
Left Deformation Permillage	0.06	0.05	0.08	0.09
Right Deformation Permillage	0.07	0.05	0.09	0.10
Left Rut Depth	0.06	0.06	0.07	0.06
Left Rut Width	0.04	0.04	0.04	0.04
Left Rut Cross-Sectional Area	0.05	0.05	0.05	0.05
Right Rut Depth	0.09	0.09	0.08	0.10
Right Rut Width	0.06	0.06	0.06	0.07
Right Rut Cross-Sectional Area	0.08	0.08	0.07	0.08
Total Number of Water	0.10	0.11	0.08	0.07
Total Water Entrapment Depth	0.13	0.15	0.11	0.09
Total Water Entrapment Width	0.15	0.17	0.12	0.10
Total Weight	1.00	1.00	1.00	1.00

5.5.3.3 Summary

From the results of the above coefficients, the agencies are able to evaluate the permanent deformation from different perspectives. One single index can be used to comprehensively represent the permanent deformation, which can be applied in lieu of average rut depth in current Pavement Management Systems (PMS).

5.5.4 Case Study

Based on the survey results, it is apparent that safety is the first consideration where water involved attributes play a significant role in the proposed new evaluation system. A case study is performed to compare the traditional rut depth based evaluation practice with the proposed evaluation system at different levels. Five profiles are randomly selected from US Highway 65 North Bound (US 65 N) and US Highway 70 East Bound (US 70 E), respectively. The attributes of the profiles and their single attributes scores are listed in Table 5.11. The ranking based on five criteria, which are the traditional averaged rut depth, comprehensive index, traffic safety, structural health, and ride quality, are listed in Table 5.12.

It is seen that the traditional average rut depth ranking has significantly different sequences to all other rankings. Pavements with higher rut depth values may have better overall performance than those with lower rut depth values and vice versa. This comparison result demonstrates that only rut depth cannot represent the whole picture of pavement permanent deformation. The rankings between the comprehensive objective and three sub-objectives are slightly different, which provides stakeholders different information.

Table 5.11 Performance of Single Attribute of Sample Profiles

Sample Number		1		2		3		4		5	
		Measure	**Score**	**Measure**	**Score**	**Measure**	**Score**	**Measure**	**Score**	**Measure**	**Score**
Single Attribute Performance	Cross Slope	1.40	/	-1.83	/	0.83	/	0.65	/	1.19	/
	Total Deformation Permillage	2.91	2.79	4.29	1.63	3.01	2.70	2.31	3.31	4.37	1.57
	Left Deformation Permillage	3.35	2.42	2.67	2.99	2.53	3.12	2.77	2.91	5.14	1.02
	Right Deformation Permillage	2.06	3.56	5.40	0.87	2.67	3.00	1.72	4.01	3.59	2.21
	Left Rut Depth (mm)	12.11	2.58	14.57	2.09	18.23	1.40	28.77	0.26	17.16	1.59
	Left Rut Width (mm)	946.00	2.78	989.00	2.67	1301.00	1.82	1489.00	1.36	1605.00	1.11
	Left Rut cross-sectional area (square mm)	9322.89	3.24	12225.58	2.82	15051.44	2.42	22761.42	1.37	14972.53	2.43
	Right Rut Depth (mm)	33.41	0.11	62.20	0.00	17.36	1.56	19.96	1.12	9.51	3.10
	Right Rut Width (mm)	1698.00	0.92	1673.00	0.97	1530.00	1.27	1588.00	1.14	1188.00	2.12
	Right Rut cross-sectional area (square mm)	36031.32	0.31	52742.71	0.03	18302.15	1.96	17520.37	2.07	5904.79	3.85
	Total Number of Water Points	3.00	2.00	1.00	4.00	1.00	4.00	2.00	3.00	2.00	3.00
	Total Water Depth (mm)	30.76	1.44	45.53	0.80	39.07	1.04	29.34	1.53	6.70	3.74
	Total Water Width (mm)	1707.00	0.76	941.00	2.09	1437.00	1.09	1015.00	1.90	605.00	3.26

Sample Number		6		7		8		9		10	
		Measure	**Score**	**Measure**	**Score**	**Measure**	**Score**	**Measure**	**Score**	**Measure**	**Score**
Single Attribute Performance	Cross Slope	-1.15	/	0.05	/	1.87	/	0.21	/	0.11	/
	Total Deformation Permillage	2.71	2.96	2.45	3.19	9.91	0.02	4.55	1.43	3.31	2.45
	Left Deformation Permillage	2.33	3.30	1.87	3.78	8.48	0.08	5.30	0.93	3.18	2.56
	Right Deformation Permillage	2.08	3.53	2.83	2.86	11.32	0.01	3.43	2.35	2.54	3.11
	Left Rut Depth (mm)	10.58	2.88	1.88	4.62	8.82	3.24	20.15	1.09	3.62	4.28
	Left Rut Width (mm)	1077.00	2.43	1161.00	2.20	76.00	4.85	1220.00	2.04	830.00	3.10
	Left Rut cross-sectional area (square mm)	7909.87	3.46	5033.16	4.11	661.42	4.83	13945.60	2.58	2367.14	4.41
	Right Rut Depth (mm)	25.90	0.44	23.37	0.68	22.52	0.77	29.91	0.21	21.89	0.85
	Right Rut Width (mm)	1297.00	1.84	1392.00	1.59	1067.00	2.45	1446.00	1.46	1479.00	1.38
	Right Rut cross-sectional area (square mm)	15453.00	2.36	20091.32	1.72	16439.31	2.22	20862.12	1.61	22638.74	1.39
	Total Number of Water Points	1.00	4.00	1.00	4.00	1.00	4.00	2.00	3.00	1.00	4.00
	Total Water Depth (mm)	39.91	1.00	33.63	1.29	5.33	3.95	35.12	1.21	41.36	0.95
	Total Water Width (mm)	985.00	1.97	982.00	1.98	735.00	2.75	1579.00	0.90	1299.00	1.30

Table 5.12 Ranking of Sample Profiles

Sample Number	Evaluation Method									
	Average Rut Depth		Comprehensive		Traffic Safety		Structural Health		Ride Quality	
	Value(mm)	Rank	Score	Rank	Score	Rank	Score	Rank	Score	Rank
1	22.76	7	1.70	8	1.63	9	1.87	8	1.86	8
2	38.38	10	1.67	9	1.68	8	1.69	9	1.61	9
3	17.79	5	2.03	6	1.99	7	2.12	7	2.15	6
4	24.37	8	2.06	7	2.00	6	2.16	5	2.20	5
5	13.34	3	2.64	1	2.72	1	2.48	2	2.45	3
6	18.24	6	2.36	3	2.32	4	2.47	3	2.47	2
7	12.63	1	2.49	2	2.45	3	2.62	1	2.59	1
8	15.67	4	2.37	4	2.51	2	2.14	6	1.97	7
9	25.03	9	1.47	10	1.47	10	1.49	10	1.47	10
10	12.75	2	2.22	5	2.18	5	2.33	4	2.30	4

5.6 Summary

5.6.1 Concluding Remarks

A comprehensive evaluation system for pavement permanent deformation is constructed in this chapter. The major characteristics of this system include:

- Scoring function for each technical parameter is elicited. All of the parameters can be evaluated with a standardized score.
- A hierarchical system is established. Pavement permanent deformation can be evaluated under a comprehensive goal or multiple sub-objectives.
- A standard index system is constructed. Pavement permanent deformation can be assessed in a “0-5 scale PSI convention”.
- Both subjectivity and objectivity are considered and balanced in deriving shape parameters for scoring functions and weight coefficients for data combination.

- Flexible structure of the evaluation process leaves spaces for future improvement or adjustment.

This study provides a rationale for utilizing multiple parameters in rut measurement. It is anticipated that the proposal of this comprehensive evaluation system poses an opportunity to reconstruct the landscape of measurement of pavement permanent deformation. The final product of this research the single comprehensive evaluation index for permanent deformation is able to supersede the practice of average rut depth evaluation. With this multi-level index system, information can be delivered to different stakeholders as per their distinctive demand and interests.

5.6.2 Limitations and Recommendations

This is a pilot study for comprehensive rut evaluation. Further research is recommended for studying on how to use these indices for agency decision making in a practical setting.

Furthermore, a larger number of surveys are preferred to build the knowledge base in the future. Also, this evaluation is developed based on data from pavement transverse profiles on national highway systems (NHS). Data from other pavement classifications are desired to validate this comprehensive evaluation process.

CHAPTER 6 ERROR REDUCTION IN PP69-10 BASED RUT MEASUREMENT

6.1 Introduction

According to PP69-10, the identification of the wheel-path is the foundation of the rut attributes derivation process since the scanning algorithms are designed based on the location of wheel-paths and the five spots. In practice, the wheel-path location on the collected transverse profiles is associated with the location of lane with lane markings as references (5). In addition, as required in PP70-10 a collected transverse profile must be wider than the actual lane occupation because of the traffic wandering (6). Therefore, lane identification and extraction is an important and indispensable step in transverse profile analysis.

In practice, three problems as shown below may cause inaccurate lane identification:

- The transverse measurement width is fixed for most automated systems. However, as shown in Figure 6.1, vehicle wandering may change lane position from time to time. It is inaccurate to apply one fixed measure of lane location to transverse profiles collected at different locations. This impact can be adequately controlled in project-level surveys but may be significant in network-level surveys.
- In the current practice, rut data collection systems are generally not able to accurately detect lane markings on consistent basis (29, 32).

- Even the systems with the capability to automatically detect lane markings through visual images, the measurement may not be accurate since lane markings are frequently not present in many collected images due to the broken lane markings (64). In addition, deteriorated lane marking may not be well captured and results in inaccurate identification of lane locations.

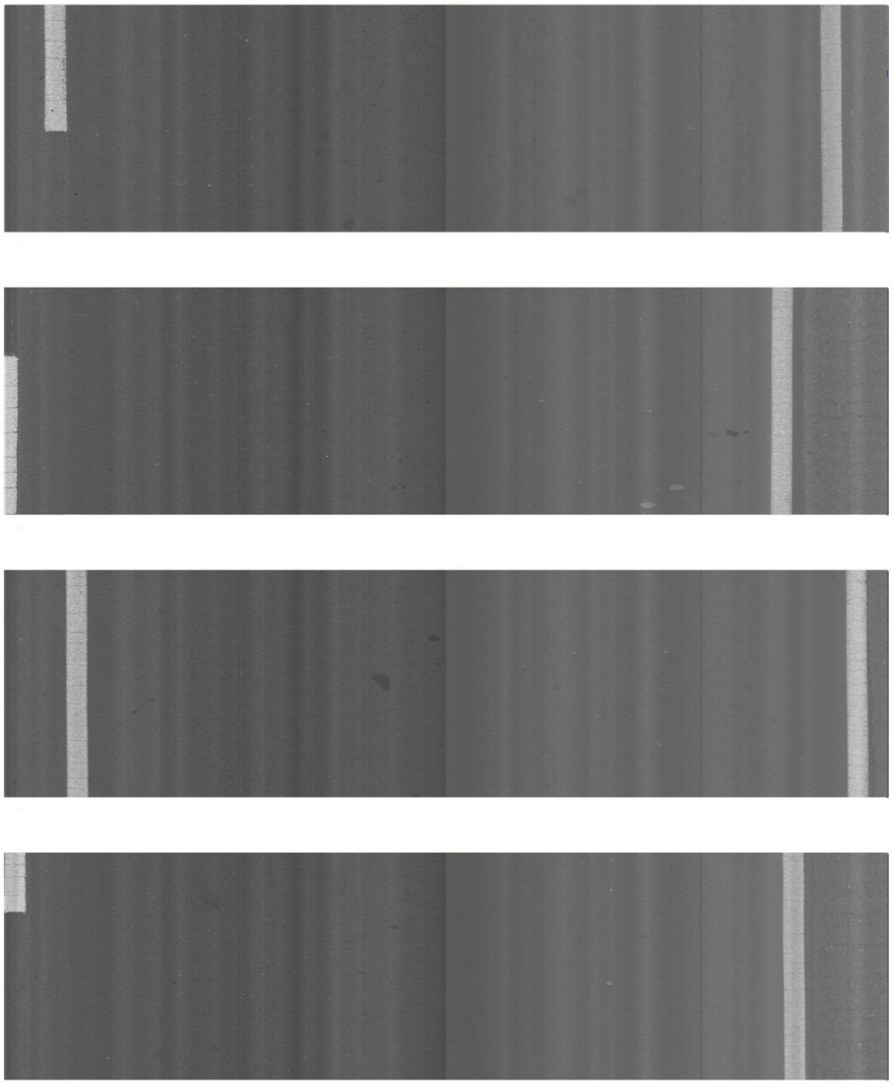

Figure 6.1 Lane Positions with Vehicle Wandering

Since the 3D Ultra system provides both 2D and 3D images for transverse profile analysis, data sets from transverse profiles and associated pavement surface images allow the engineers to examine the actual impact of inaccurate lane detection on the accuracy of the attributes. In this chapter a two-step procedure is adopted to investigate the impact of the lane position measurement on accuracy of rut measurement and present a solution to minimize the impact:

- Eight hypothetical scenarios of artificial lane offsets are analyzed to statistically identify the impact due to inaccurate lane measurement.
- This study develops a methodology to minimize the effect of inaccurate lane measurement on rut measurement.

For the first study, the statistical tool of hypothesis test introduced in Chapter 4 is used. For the second study, three machine learning techniques are used to develop the self-adaptive models.

6.2 Impact of Lane Measurement on Accuracy of Rut Measurement

It is found in Chapter 3 that many abnormal values in deformation measures are observed through fully automated data processing. It is believed that the majority of these values are produced with inaccurate lane marking position identification. As lane marking positions are used as reference to compute left and right wheel-path ruts, the potential errors are apparent.

In this study, experiments are designed to test the impact of simulating lane wandering with lane offsets on the seven attributes proposed by PP69-10. The seven attributes are:

- Cross Slope (CS)
- Total Deformation Permillage (TDP)
- Left Rut Depth (LRD)

- Right Rut Depth (RRD)
- Left Rut Cross-Sectional Area (LRA)
- Right Rut Cross-Sectional Area (RRA)
- Total Water Entrapment Depth (TWD)

Among these seven attributes, LRD, RRD, LRA, and RRA highly rely on the wheel-path locations. All parameters are subject to being affected by inaccurate lane measurement.

6.2.1 Data Acquisition

The transverse profiles used for this study are selected from the first 60 km (38 miles) of the US Highway 65 North Bound (US 65 N). As a result, the first 2,916 transverse profiles in the study of Chapter 4 are selected for this research. In the analyzed sections, the width of the pavement ranges from 3,234 mm (10.61 ft) to 3,653 mm (11.98 ft) with an average of 3,511 mm (11.52 ft). The standard deviation of the pavement width is 70.37 mm (2.8 in.). The distribution of the pavement width for these selected profiles is shown in Figure 6.2. The semi-automated measured average left margin (LM) and right margin (RM) are 245 mm and 339 mm, respectively. Their standard deviations are 100 mm and 107 mm, respectively.

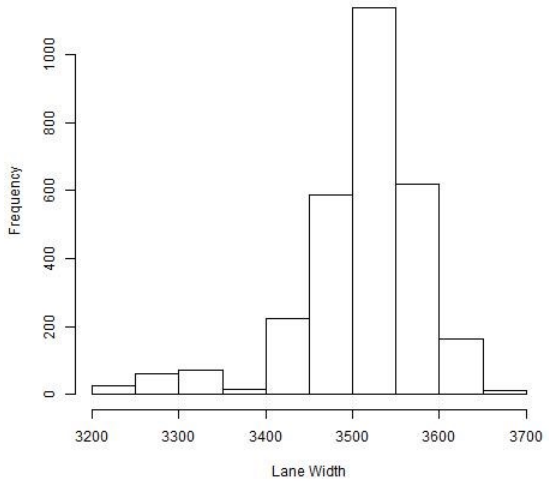

Figure 6.2 Distribution of Pavement Width for the Study Section

As shown in Figure 6.3, the studied pavement section is a divided highway with median and shoulder. The detected lane is the right lane. The shoulder width is not measured. Based on visual detection, the shoulder is more than half lane wide.

Figure 6.3 Road Configuration at the Studied Section

(Image taken by PaveVision3D Ultra on March 7th 2013, on US 65 North Bound near Lake Village, AR)

6.2.2 Inaccurate Lane Identification Scenarios

Based on the wheel-path definitions in PP69-10 (*5*), eight hypothetical scenarios are proposed to simulate inaccurate lane identification. The lane location is shifted to either left or right side of the pavement surface at 20 mm, 50 mm, 100 mm, and 150 mm offsets, respectively. The actual lane positions are obtained from semi-automated measurements (Section 3.4.3) are used as the base scenario.

The configurations of all the eight scenarios are summarized in Table 6.1. Figure 6.4 illustrates the lane and wheel-path location for base scenario (Top two graphs) and scenarios L150 (Third graph) and R150 (The bottom graph). Note that if the shifted profile exceeds the edge of the image, the LM and RM are set to 0.

Table 6.1 Scenarios to Simulate Vehicle Wandering

Scenario	Description	Acronym
1	Base	Base
2	Left Offset 20 mm	L20
3	Right Offset 20 mm	R20
4	Left Offset 50 mm	L50
5	Right Offset 50 mm	R50
6	Left Offset 100 mm	L100
7	Right Offset 100 mm	R100
8	Left Offset 150 mm	L150
9	Right Offset 150 mm	R150

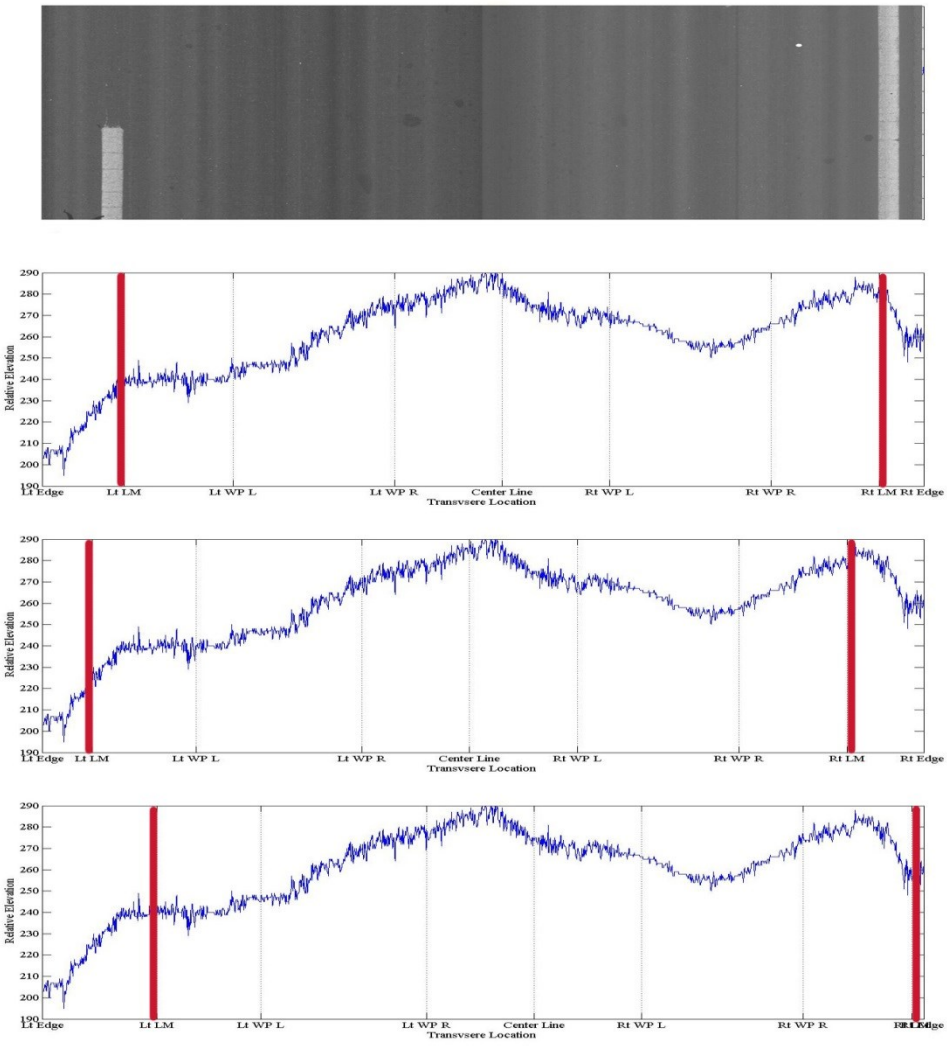

Figure 6.4 Illustration of Hypothetical Lane Offset Scenarios

The attributes of the nine scenarios are derived with the measured or adjusted LM and RM. According to the definition given in Section 3.5.2, a deformation permillage larger than 10 is an abnormal value. In this data derivation, no abnormal values are observed in base scenario but some are observed in the hypothetical scenarios. The profiles with abnormal values are removed for the calculation of the mean values. In total 193 profiles (6.7%) are removed from the 2,916 profiles and 2,723 profiles remain. The mean values of seven attributes for the nine scenarios are plotted in Figure 6.5.

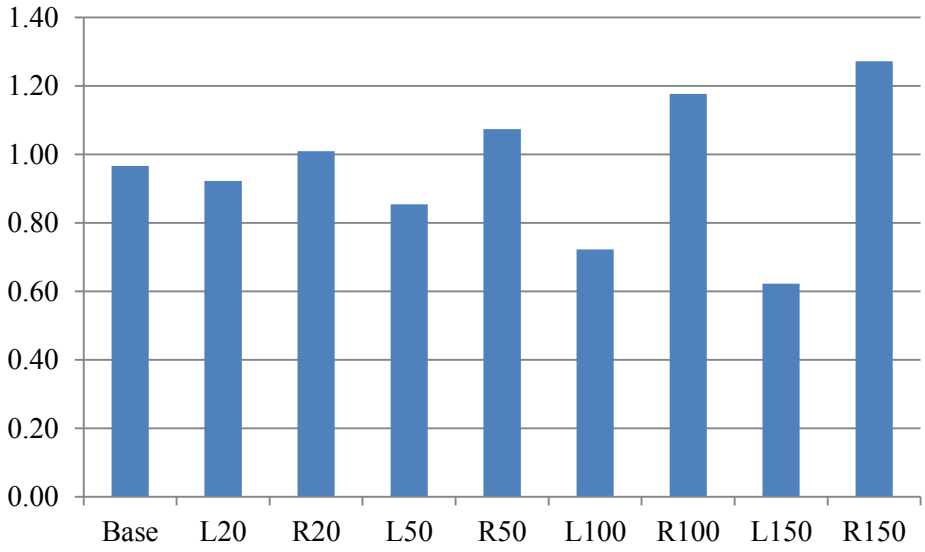

a. Mean Value of Cross Slope

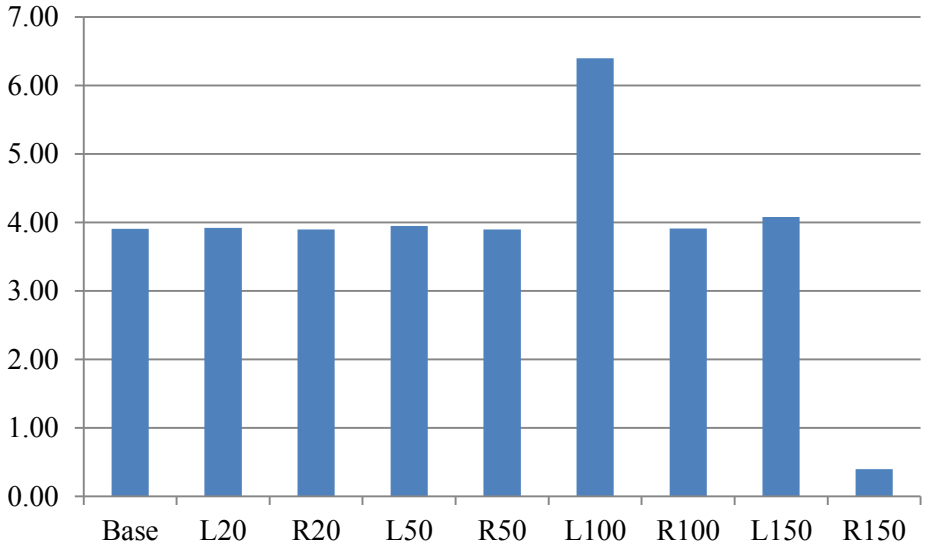

b. Mean Value of Total Deformation Permillage

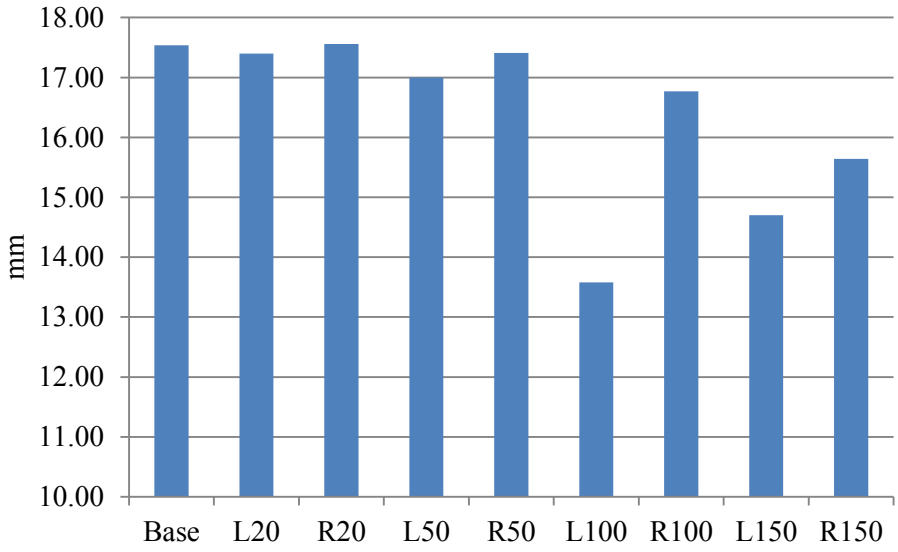

c. Mean Value of Left Rut Depth

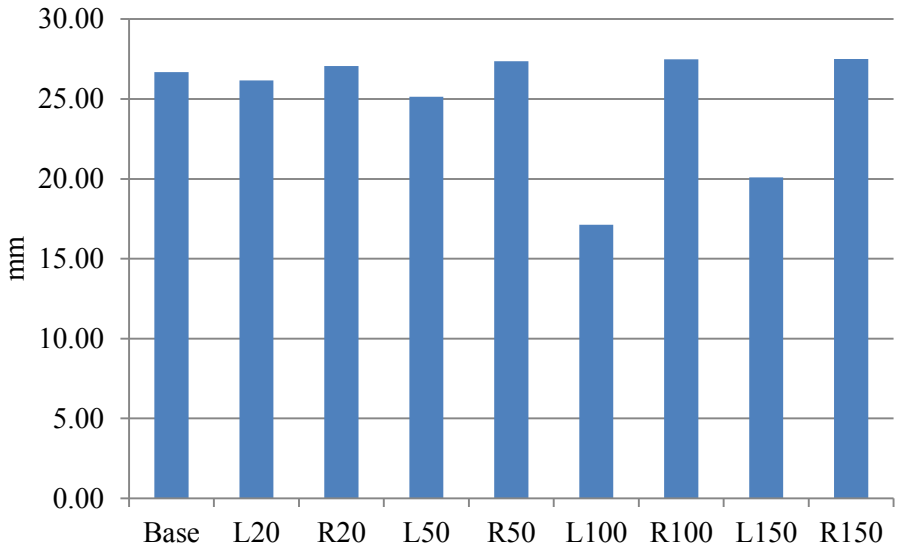

d. Mean Value of Right Rut Depth

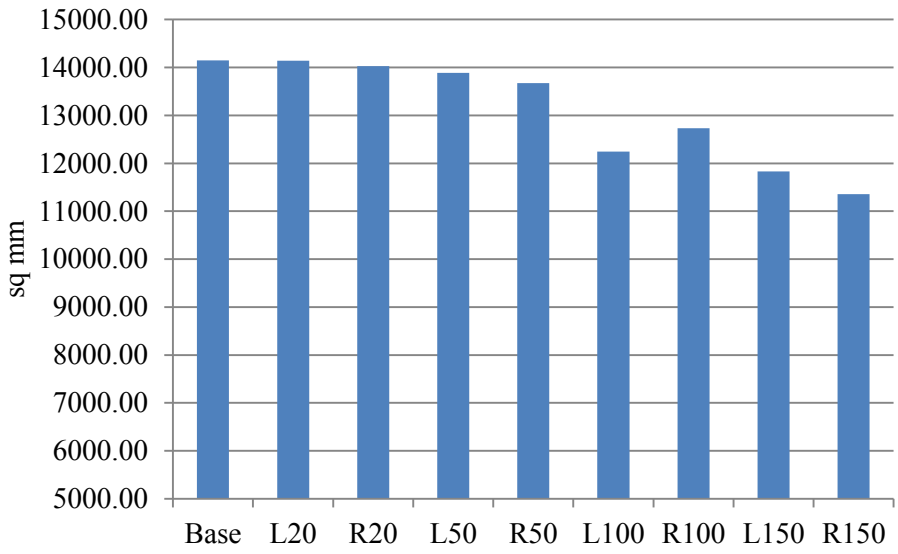

e. Mean Value of Left Rut Cross-Sectional Area

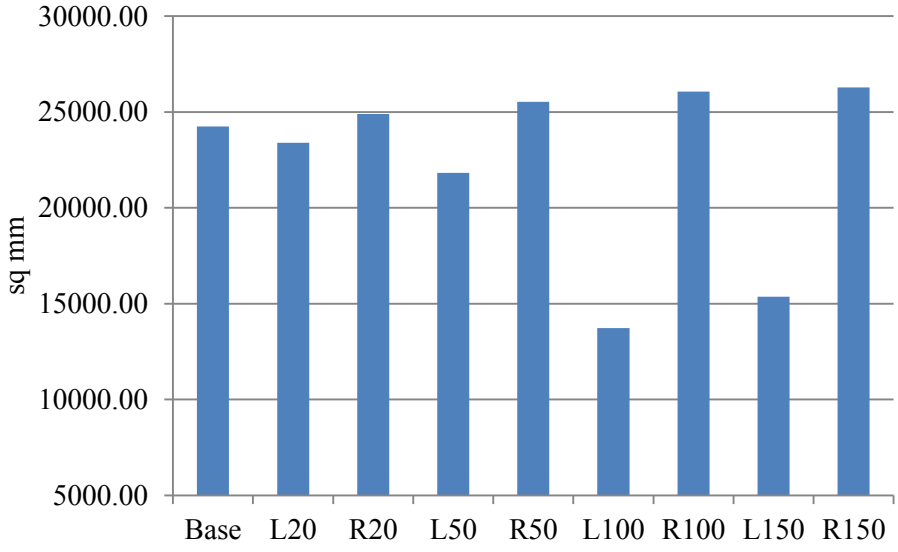

f. Mean Value of Right Rut Cross-Sectional Area

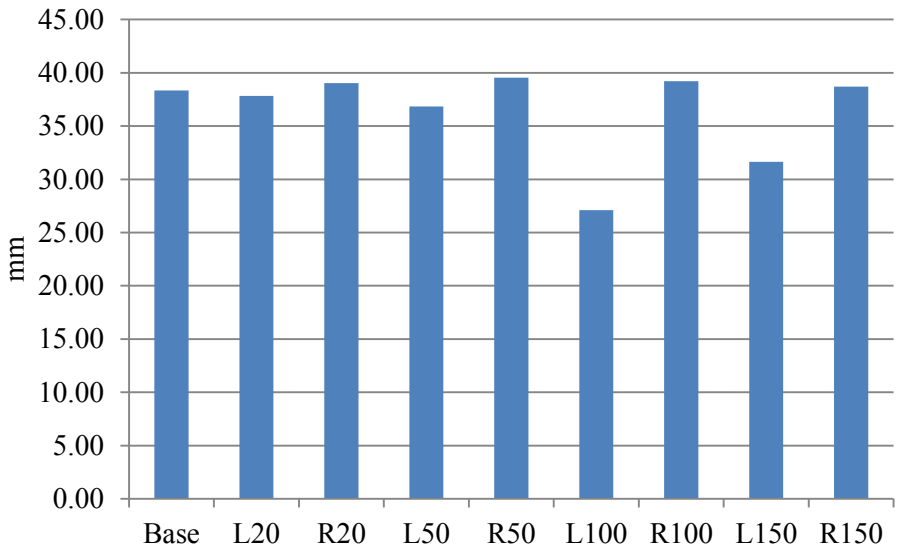

g. Mean Value of Total Water Entrapment Depth

Figure 6.5 Mean Values of Seven Attributes from Different Scenarios

6.2.3 Analysis of Results

It is determined from the data compilation that CS value decreases with the increase of left offsets but grows with the increase of the right offsets. TDP changes abruptly when the left offset is 100 mm and right offsets exceed 100 mm. For LRD and RRD, no apparent changes are observed within 50 mm offsets, either to the left or right. The changes are more evident in the left offsets than in right offsets; especially for LRD, sudden drops are found at 100 mm and 150 mm of left offsets. For LRA, it gradually decreases when the offset increases. However, left and right offsets influence RRA differently: left side offsets decrease RRA and right side offsets increase RRA. The changes of TWD are similar to those of the RRD under the same offset variations.

Hypothesis test could be used to determine the impact of offset of lane measure on the rut attributes (41). The null hypothesis H_0 is set as the mean measure of base scenario is equal to the mean of offset scenarios. The alternative hypothesis H_1 is that they aren't equal. Fifty-six two-tailed t-tests are conducted and the p-values are listed in Table 6.2. Under 95% confidence

level, a p-value less than 0.05 implies the H_0 should be rejected, which means that statistically significant differences exist between two attributes (41). It is seen that both CS and RRA reject the null hypothesis for any offset. In summary, it can be concluded that different attributes are affected at different degrees, or have different sensitivities to the lane offsets. Generally, offsets less than 50 mm would not cause significant changes to most attribute values.

Table 6.2 p-values of paired t-Test between Offset Measures and Base Measures

Offset	CS	TDP	LRD	RRD	LRA	RRA	TWD
L20	0.01	0.36	0.30	0.07	0.49	0.01	0.16
R20	0.01	0.42	0.46	0.14	0.28	0.03	0.08
L50	0.00	0.14	0.02	0.00	0.11	0.00	0.00
R50	0.00	0.41	0.31	0.03	0.01	0.00	0.01
L100	0.04	0.04	0.00	0.00	0.00	0.00	0.00
R100	0.00	0.47	0.00	0.02	0.00	0.00	0.04
L150	0.00	0.00	0.00	0.00	0.00	0.00	0.00
R150	0.00	0.00	0.00	0.01	0.00	0.00	0.23

6.3 Minimizing Effect of Lane Identification

The obtained statistics reveal that significant differences appear in most attributes if lane identification had an offset of more than 50 mm. A methodology is developed in this section to maintain accuracy of rut attributes in PP69-10.

6.3.1 Design of Experiment

This experiment is designed based on the data collected with the 3D Ultra system, which has a fixed transverse measurement width 4,096 mm. A different data set other than the previous section is used based on the need of data analysis on a successive pavement section. A pavement section of 1,646 m (1 mile) which consists of 804 successive images is selected from the pavement sections in Section 6.2. Drivers were not aware of the purpose of this study during data collection phase and therefore the vehicle wandering is assumed to be random. Semi-automated

lane extraction is applied to each image through the use of the Automated Distress Analyzer (ADA3D). The means of Left Margin (LM), Right Margin (RM), and Lane Width (LW) of the 804 images are 232 mm, 372 mm, and 3,492 mm, respectively; the standard deviations are 160 mm, 182 mm, and 48 mm, respectively. Vehicle wander is significant but lane width is relatively stable in this experimental section.

One image in 3D Ultra system contains 2,048 transverse profiles with 1 mm gap between adjacent profiles. The 1st, 501st, 1,001st, and 1,501st profile in each image are chosen to compute the actual attributes of this pavement section. 3,216 profiles are analyzed in total. The actual (true) values of seven attributes are elicited as the base value in further analysis.

Three alternatives of lane location measurement are shown in Table 6.3. For Alternative 1, the full image width is assumed to be the lane width. In other words, the LM and RM are both considered as 0 mm and the LW is 4,096 mm. For Alternative 2, the lane width measured from the first image is applied to the profiles within the entire section. This approach may be realistic as the data raters can measure the lane location at the starting point while collecting data. For this experimental section, the LM, RM, and LW of the first image are 164 mm, 387 mm, and 3,545 mm, respectively. Alternative 3 involves constructing a series of imaginary scenarios. For this experimental section, the lane width is very consistent at about 3,500 mm and the sum of LM and RM is about 600 mm. Thirteen scenarios are simulated for different combinations of LM and RM but same LW. The LMs of thirteen scenarios are from 0 mm to 600 mm with an incremental of 50 mm. Meanwhile, their corresponding RMs are from 600 mm to 0 mm. As shown in Table 6.3, the sum of LM and RM is always 600 mm in each scenario.

Table 6.3 Three Alternatives to Model the Experimental Section

	Description	Left Margin (LM) mm	Right Margin (RM) mm	Lane Width (LW) mm
Alternative 1	Full Image	0	0	4096
Alternative 2	First Image Lane Location	164	387	3545
Alternative 3	Thirteen scenarios with different LM and RM, but same LW	300	300	3496
		250	350	3496
		200	400	3496
		150	450	3496
		100	500	3496
		50	550	3496
		0	600	3496
		350	250	3496
		400	200	3496
		450	150	3496
		500	100	3496
		550	50	3496
		600	0	3496

Attributes are extracted for the three Alternatives. As abnormal values are observed in these hypothetical scenarios, data are normalized to eliminate the impact of the outliers. Scoring functions elicited in Chapter 5 are utilized to map the values within the interval [0, 1]. The piecewise functions (6.1-6.7) are used to normalize the data. For cross slope percent, it is assumed less than or equal to -12 is the 1 and greater than or equal to 12 is 0, a linear mapping is applied to the values in between. The actual attributes are normalized as well as attributes from the three alternatives.

For TDP:

$$f(x) = \begin{cases} -0.133x + 1, & 0 \leq x \leq 1.5 \quad (a) \\ 1 - \frac{1}{1+exp(-0.792x+2.575)}, & x > 1.5 \quad (b) \end{cases} \tag{6.1}$$

For LRD and RRD:

$$f(x) = \begin{cases} -0.04x + 1, & 0 \le x \le 5 \quad (a) \\ 1 - \frac{1}{1+exp(-0.185x+2.31)}, & x > 5 \quad (b) \end{cases} \tag{6.2}$$

For LRA and RRA:

$$f(x) = \begin{cases} -0.5 * 10^{-4}x + 1, & 0 \le x \le 4000 \quad (a) \\ 1 - \frac{1}{1+exp(-1.32*10^{-4}x+1.914)}, & x > 4000 \quad (b) \end{cases} \tag{6.3}$$

For TWD:

$$f(x) = \begin{cases} -0.04x + 1, & 0 \le x \le 5 \quad (a) \\ 1 - \exp(0.0396x - 1.807), & x > 5 \quad (b) \end{cases} \tag{6.4}$$

For CS:

$$f(x) = \begin{cases} -0.042x + 0.5 & -12 < x < 12 \quad (a) \\ 0 & x \ge 12 \quad (b) \\ 1 & x \le -12 \quad (c) \end{cases} \tag{6.5}$$

The attributes of the thirteen scenarios in Alternative 3 are averaged and then the values of the three alternatives are compared with the base attributes. The Error Sum of Squares (SSE) are obtained and presented in Table 6.4. Note that the SSE is calculated based on the normalized value of the attributes, which is in the 0-to-1 interval for each attribute. It can be seen that with Alternative 1, where the actual lane is substituted by the full images, has the worst performance: it has the greatest SSE in five out of seven attributes. For Alternative 2, there are two attributes performing the worst. Additionally, Alternative 2 has more accurate results than these from Alternative 3 for TDP and RRD. In other attributes, data from Alternative 3 show the least values for SSE. Overall, the analysis indicates that Alternative 3 is the best of the three alternatives to produce reasonably accurate attributes values.

Table 6.4 Error Sum of Squares (SSE) of the Three Alternatives

	Description	CS	TDP	LRD	RRD	LRA	RRA	TWD
Alternative1	Use Full Image	2.95	591.67	530.29	564.10	200.21	258.45	198.23
Alternative2	Use First Image Width	3.47	11.66	202.07	52.79	78.52	102.99	223.66
Alternative3	Average of 13 Scenarios	1.41	156.65	77.61	79.17	31.09	85.14	134.50

6.3.2 Machine Learning Techniques

Though the Alternative 3 with thirteen scenarios emerges as the best among the three alternatives, it is not the optimal method since the simple average values of the thirteen scenarios are used to calculate SSE. An attempt is made in the study to develop mathematical relationships among the actual values of attributes and the values of the thirteen imaginary scenarios. If the relationships are reliable, the actual values of the attributes should be able to be approximated through modeling the thirteen imaginary scenarios. Therefore, the attributes from the thirteen scenarios are modeled as explanatory variables or input ($x_1, x_2 \ \ldots \ x_{13}$) and the predicted values the response variables or output ($\hat{y}$) in regression-based models. Each attribute is modeled separately.

Three methodologies are adopted to establish the regression relationship between the actual values and the thirteen scenarios. The first is Multiple Linear Regression (MLR) and the latter two are machine-learning based methodologies, Artificial Neural Networks (ANN) and Random Forest (RDF) (65).

The MLR is a widely known data fitting methodology, which is introduced in Section 4.3.

The application of ANN utilizes a group of interconnected simple artificial nodes, namely "neurons", to simulate the function of biological central nervous systems. As shown in Figure 6.6,

typical ANN models contain three layers, the input, hidden and output layer, respectively. This study uses the Feedforward Backpropagation (BP) Neural Network Algorithm, which is based on sigmoid functions to transfer threshold information between neurons (66, 67). Moreover, the Steepest-Descent Minimization method is used to adjust the threshold values and weights for optimal solution (66). The output layer has only one neuron, which is the response variable. The inputs are the explanatory variables. In this research, the hidden layer has five nodes.

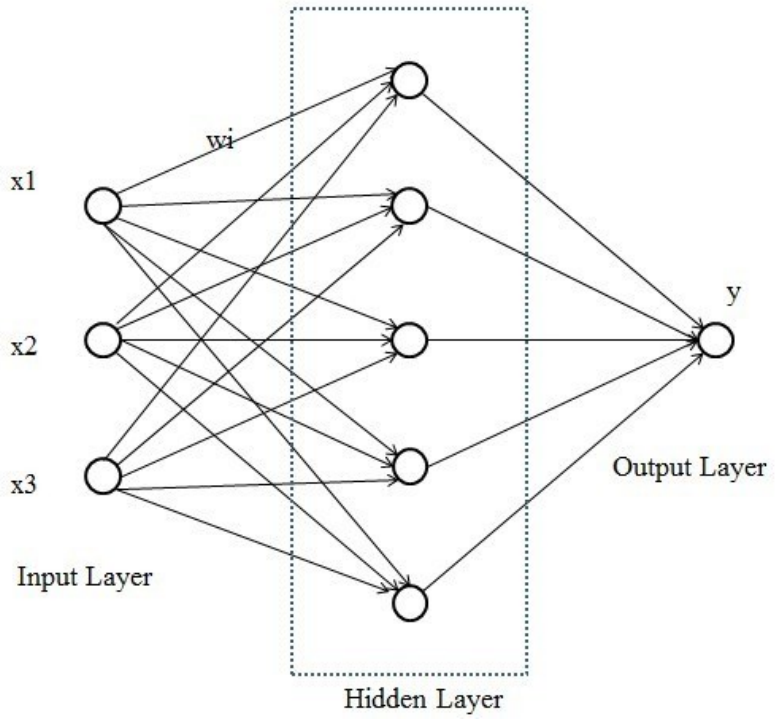

Figure 6.6 Illustration of Neural Network Principle

The foundation of RDF is the Classification and Decision Tree (CART), a visualized analytical tool (68, 69). As illustrated in Figure 6.7, in a CART, all information is concentrated at the root, and each level splits the data according to different attributes. CART can be used for classification or regression depending on the type of data. However, only applying one CART is prone to be affected by the inherent properties of the data sets and is therefore unstable. RDF is an advanced methodology developed on the basis of CART (69). It consists of a group of un-

pruned CART of randomly sampled training data (69). Like similar methodologies such as boosting and adaptive bagging, the reliability and classification rate of RDF are largely improved than ordinary CART. The most noticeable advantage of RDF is that it does not produce overfitting results (69).

Both ANN and RDF are extensively used in transportation and pavement studies (70, 71, 72, and 73). For example, Terzi used ANN in modeling the present serviceability index of the flexible pavements (70). Alsugiar et al. utilized ANN to identify appropriate maintenance and repair actions for pavements (71). Das et al. applied random forests to identify the relationship between traffic information and crash types (72). Mohammed Ali et al. developed an algorithm of RDF for vehicle classification using the inductive loop system (73).

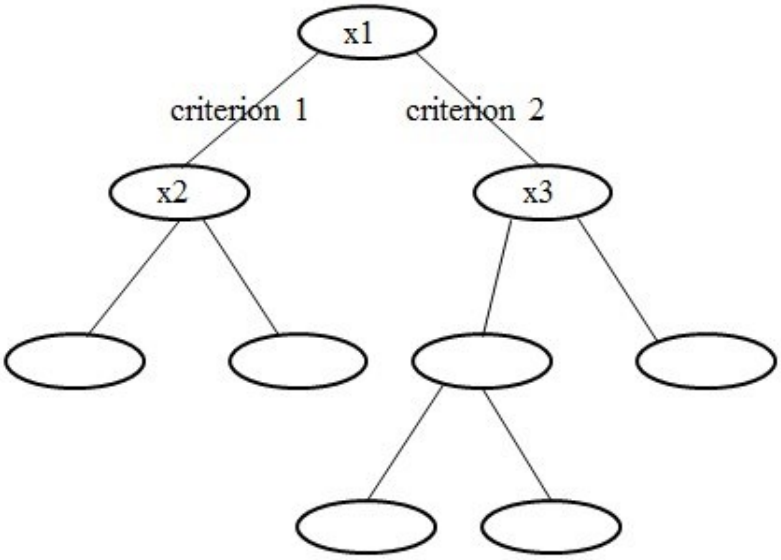

Figure 6.7 Illustration of CART

Overfitting is a commonly concerned issue in machine learning, especially in the neural networks prediction. It usually occurs on excessively complex models when there are multiple attributes involved (65). An overfitting model generally has very poor prediction performance

since it overestimates the complexity of data distribution. Due to the nature of the algorithms, the MLR and RDF would not have overfitting.

Five-fold cross validation is a conventional method to avoid overfitting and ensure robust prediction results (65, 74). By applying five-fold cross validation, the data set is randomly divided into five parts, and in each experiment four parts are used as training sets and the remaining one part used as test set. There are five experiments in total. Normalized Mean Square Error (NMSE) is used to examine the reliability of the models. As shown in Equation 6.6, if the prediction models are better than just using the mean of the explanatory data, NMSE value is smaller than 1. For the training data sets, the NMSE value is actually equal to $1 - R^2$. For both training and testing data, the smaller value of NMSE indicates a more satisfactory fitting or prediction result. It is sometimes seen that the NMSE value for training data set is small but for testing data set is large. The occurrence of this phenomenon demonstrates that the model is not very robust.

$$NMSE = \frac{\sum(y - \hat{y})^2}{\sum(y - \bar{y})^2} \tag{6.6}$$

where $\bar{y}$ is the mean of the explanatory variables;

$\hat{y}$ is the output variable of the model;

y is the actual attributes.

6.3.3 Testing Results

The *r project* is utilized to conduct the three types of machine learning based prediction analyses (42). Software packages such as *nnet* and *randomForest* are employed for these calculations (42, 75, and 76). Each attribute is modeled respectively.

Since the average values in Alternative 3 are better than the other two alternatives, any NMSE in this model less than 1 should be considered generally better than other solutions. In this five-fold cross validation, the Mean NMSE (MNMSE) from five experiments is utilized to compare the reliability of the models (74).

The MNMSE of the three methodologies are listed in Table 6.5. It is found that the RDF has the best results whereas linear regression shows the greatest MNMSE. The results of ANN stand between them. The MNMSE of test sets from Random Forest are smaller than 0.2 in all attributes except TWD, which demonstrates that the RDF is a reliable prediction model. TWD doesn't achieve a very low MNMSE with any model; however, the reliability is much improved than any other alternatives.

Table 6.5 Mean Nornamlized Mean Square Error (MNMSE) of the Three Models

		CS	**TDP**	**LRD**	**RRD**	**LRA**	**RRA**	**TWD**
Multiple Linear Regression	MNMSE Training	0.13	0.13	0.23	0.33	0.30	0.32	0.76
	MNMSE Testing	0.14	0.14	0.24	0.33	0.31	0.33	0.77
Artificial Neural Network	MNMSE Training	0.11	0.04	0.12	0.16	0.17	0.17	0.62
	MNMSE Testing	0.12	0.08	0.15	0.18	0.21	0.20	0.72
Random Forest	MNMSE Training	0.02	0.01	0.02	0.03	0.03	0.03	0.11
	MNMSE Testing	0.11	0.06	0.12	0.16	0.15	0.16	0.56

The results generated by constructing thirteen imaginary scenarios can effectively reduce the errors when actual lane measurement is not available. However, it should also be noticed that there is no direct output of numerical weights for these thirteen scenarios from the RDF and ANN. In regular regression practices, the weights or orders are meaningful as analysts need to interpret the contributions and importance of the explanatory variables. Though methodologies

have been developed to generate weights for the machine-learning techniques, it is unnecessary in this case because the thirteen scenarios are of little realistic implications. The learning results derived from the training data should be directly used to generate predictions of the actual attributes.

6.4 Summary

An experiment is designed to reveal the potential errors of pavement transverse attributes caused by offsets in lane measurement. When the offset of lane wandering reaches 50 mm or higher, most attributes in PP69-10 show significant variations from the base value based on field lane markings. To generate accurate rut attributes without lane positioning data, three methodologies are attempted to estimate the rut attributes. MNMSEs from five-fold cross validation indicate that the Random Forest (RDF) is able to perform fairly satisfactory predictions for most attributes. The proposed methodology only uses the attributes calculated from thirteen scenarios, which does not require any actual lane positioning information. However, this methodology is developed based on 3D Ultra system with a fixed transverse measurement width of 4,096 mm. Proper modification is needed before it being adopted in other profile measurement systems with different measurement width.

CHAPTER 7 CONCLUSIONS AND RECOMMENDATIONS

7.1 Conclusions

This research presents a thorough study on the measurement of pavement permanent deformation based on 1 mm 3D pavement surface model collected by PaveVision3D Ultra system. Most of the findings present in the dissertation are the first-time in research with significant potential or future applications in the coming years. Based on the new AASHTO protocol PP69-10 and PP70-10, the following tasks are undertaken in this research:

- A substantial literature review is conducted on relevant studies. Specifically, the state of art in rut measurement and characterization is reviewed. The weaknesses in current rut measurement are identified and summarized.
- Transverse profiling with 3D Ultra system is exhibited and the adaptability of the system for AASHTO standard PP70-10 is demonstrated.
- With the AASHTO new protocol PP69-10, thirteen attributes for characterizing pavement permanent deformation are derived with the data collected by 3D Ultra system and the custom program.
- The evaluation of AASHTO protocol PP69-10 is conducted.
- A geometric model is developed for identifying the abnormal deformation parameters produced from PP69-10.

- The rut depth measures based on PP69-10 are compared with traditional straightedge rut depth measures which are derived semi-automated from the same set of transverse profiles. The relationship between the two measures is established.
- The cross slope measure based on PP69-10 is compared with another two definitions of cross slope.
- A large sample of transverse profiles is analyzed. The relations between different rut measures are examined. Inferences regarding pavement performance are drawn from the statistical analysis.
- The new measures derived based on PP69-10 are predicted with rut depth measures.
- Utility theory based standard scoring functions are elicited for rut attributes based on subjective surveys of pavement engineers.
- A hierarchical evaluation system is established to comprehensively evaluate pavement permanent deformation based on Analytical Hierarchy Process, Factor Analysis and Principal Component Analysis.
- The impact of vehicle wandering on the accuracy of PP69-10 attributes is simulated and investigated.
- A methodology is proposed to reduce the errors incurred by unknown lane positions. Three machine learning techniques, multiple linear regression, artificial neural network, and random forest are introduced to realize the error reduction.

The major findings from this research are listed as follows:

- The significance of PP69-10 and PP70-10 is evident to the industry and the research field with the intention to resolve many of the issues with the current rut measurement.
    - PP70-10 specifies the detailed technical requirement for transverse profiling, which is beneficial for data collection industry.

- PP69-10 outlines specific procedures to derive rut parameters with computer programs. This process assures the uniform of data set.
- A set of rut attributes are proposed in PP69-10, which is conducive for pavement management and study.
- Generally, pavement permanent deformation parameters can be derived in a straightforward and robust manner according to PP69-10. However, a few potential improvements for PP69-10 are identified. These limitations include incomplete procedures, inconsistent definitions, and possible cause of inaccurate measures. The recommendations are made in the study to improve the reliability of PP69-10.

- The 1 mm 3D pavement surface model established with PaveVision3D Ultra system demonstrates its adequacy in transverse profiling and rut characterization.
  - It meets all technical requirements specified in PP70-10.
  - The 1 mm resolution 3D transverse profiles are apt to derive the scanning based PP69-10 rut attributes.
  - By collecting data at high speed and maintain data quality, it eliminates the gap between network level and project level data collection.
  - Simultaneous collection of 2D and 3D image provides accurate lane detection, which reduces errors in attributes derivation.
- Due to the nature of the derivation, the deformation parameter based on PP69-10 can be an indicator to identify abnormal values. Simulated geometric model suggests a deformation permillage exceeds 10 to be an abnormal value and worth further examination.
- The methodology for rut depth derivation is significantly different from the traditional straightedge rut derivation process; however, the derived measures show high

correlations. The traditionally measured rut depth in current Pavement Management System (PMS) is able to be converted to PP69-10 rut depth measures in a robust manner.

- With respect to three cross slope measurement methods, PP69-10 method and regression line method have a very strong correlation and are recommended for practical application. The edge-point method is also demonstrated an adequate alternative for cross slope estimation when data is insufficient.
- With the large sample data compilation, important inferences are drawn for pavement performance:
    - Rut data of left and right wheel-path from the large data set show significant difference. Rut depth, width, and area on the left wheel-path are generally less than those on the right wheel-path. However, the left wheel-path has more deformation than the right wheel-path.
    - The left wheel-path deformation is more likely to have more lateral deformation, which belongs to the Type 3 rut than that of the right wheel-path. The right wheel-path is possibly to have more Type 2 rut than the left wheel-path.
    - Rut cross-sectional area measures are highly correlated with rut depth measures on both wheel-paths and can be approximated with rut depth measures in a satisfactory manner.
    - Solely rut depth is insufficient to judgment the performance of pavement transverse profiles. Significant information is lost from only the single rut depth measure.
- The lane detection is critical to derive accurate rut attributes. Based on the simulated vehicle wandering models, it is identified that offsets of more than 50 mm lane detection leads to inaccurate results.

- Based on the designed thirteen scenarios, the prediction results of three machine learning based regressions, especially the random forest prediction models, demonstrate the ability to minimize the adverse impact of unknown lane position on rut measures. This methodology is significant to those agencies who are unable to adopt the latest system but are willing to practice PP69-10.

A comprehensive system for permanent deformation evaluation established in this research has the following significance:

- The construction of this system balances both subjective and objective methodologies. Retaining variations in information and engineering judgment are both considered in the development of the system.
- It is anticipated this multi-hierarchy information will facilitate the application of multiple parameters. An overall evaluation is feasible based on multiple rut attributes through the weight assigned for each parameter. Pavement rut can also be evaluated according to the three sub-objectives traffic safety, structural health, and ride quality.
- Current rut information report is very simple and fuzzy, resulting in inaccurate decisions. The standardized system provides the users a "0-to-5" scales for rut evaluation, which is a progress in rut measurement.

7.2 Recommendations

The following recommendations are proposed for future studies:

- All the studies in this research are based on two national highway systems (NHS) sections in Arkansas. A broader range of data source needs to be used for further tests.
- This study only explores the visible depression of pavement and inferences regarding pavement performance are drawn based on the interactions between different parameters.

To further examine the relations between the measured surface deformation parameters and deformations from underlying structures will be interesting and important.

- A comprehensive system for pavement study is proposed in this research. The subjective surveys are based on a limited range of expert raters. More raters will provide more robust evaluation results.
- The comprehensive system will be significant to Pavement Management System (PMS). However, this study does not provide insight into the implementation of the system. How to apply this system to agencies' practice is worth exploration.

REFERENCES

1. Simpson, A. (2001). "Measurement of rut in asphalt pavements." Dissertation presented to University of Texas at Austin in partial fulfillment of the requirements for the degree of Doctor of Philosophy.

2. Simpson, A. (2001). "Characterization of transverse profiles." FHWA-RD-01-024. Fugro-BRE, Inc. Austin, TX.

3. Highway Research Board (1962). "The AASHO road test report 1: history and description of project." National Academy of Sciences-National Research Council, Washington, D. C.

4. Highway Research Board (1962). "The AASHO road test report 5: pavement research." National Academy of Sciences-National Research Council, Washington, D. C.

5. American Association of State Highway and Transportation Officials. (2010). "Standard practice for determining pavement deformation parameters and cross slope from collected transverse profiles." AASHTO Designation: PP69-10. Washington, D.C.

6. American Association of State Highway and Transportation Officials. (2010). "Standard practice for collecting the transverse pavement profile." AASHTO Designation: PP70-10. Washington, D.C.

7. Haas, R., Hudson, W. R., and Zaniewski, J. P. (1994). "Modern pavement management." Krieger Publishing, Malabar, Fla.

8. Huang, Y. H. (2001). “Pavement analysis and design.” 2nd Ed., Prentice-Hall, Englewood Cliffs, N.J.

9. ARA, Inc. (2004). “Guide for mechanistic-empirical design of new and rehabilitated pavement structures, final report.” March 2004. National Cooperative Highway Research Program.

10. Lenngren, C.A. (1988). “Some approaches in treating automatically collected data on rutting.” Transportation Research Record: Journal of the Transportation Research Board, No. 1196, Transportation Research Board of the National Academies, Washington, D.C., pp. 20-26.

11. Obaidat, M., Al-Suleiman, T., and Abdul-Jabbar, G. (1997). “Quantification of pavement rut depth using stereovision technology.” Journal of Surveying Engineering. 123(2). pp. 55-70.

12. Naiel, A. (2010). “Flexible pavement rut depth modeling for different climate zones.” Dissertation presented to Wayne State University in partial fulfillment of the requirements for the degree of Doctor of Philosophy.

13. Miller, J., and Bellinger, Y. (2003). “Distress identification manual for the long-term pavement performance program.” FHWA-RD-03-03. Federal Highway Administration, Washington, D. C.

14. Bandini, P., and Pham, H. “Transition from manual to automatic rutting measurements: effect on pavement serviceability index values.” Report No. NM 08SAF-2.

15. Black, G., and Jackson, L. (2000). “Pavement surface water phenomena and traffic safety.” ITE journal. U.S. National Transportation Safety Board. 70(2). pp. 32-37.

16. Fwa, T., Pasindu, H., and Ong, G. (2012). ”Critical rut depth for pavement maintenance based on vehicle skidding and hydroplaning consideration.” Journal of Transportation Engineering. 138(4). pp. 423-429.

17. American Association of State Highway and Transportation Officials. (1993). “AASHTO guide for design of pavement structures.” AASHTO, Washington D.C.

18. Federal Highway Administration. (2010). “Highway performance monitoring system field manual.” FHWA. February, 2010.

19. ASTM D6433-09. (2009). “Standard practice for roads and parking lots pavement condition index surveys.” American Society for Testing and Materials.

20. Park, S. (2000). “Evaluation of accelerated rut development in unbound pavement foundations and load limits on load-zoned pavements.” Dissertation presented to Texas A&M University in partial fulfillment of the requirements for the degree of Doctor of Philosophy.

21. Omar, E. (2003). “Evaluation of rutting behavior of density-deficient asphalt mixtures.” Thesis presented to North Carolina State University in partial fulfillment of the requirements for the degree of Master of Science.

22. Ali, H., and Tayabji, S. (2000). “Using transverse profile data to compute plastic deformation parameters for asphalt concrete pavements.” Transportation Research Record: Journal of the Transportation Research Board, No. 1716, Transportation Research Board of the National Academies, Washington, D.C., pp. 89-97.

23. Al-Suleiman, T., Obaidat, M., and Abdul-Jabbar, G., Khedaywi, T. (2000). “Field inspection and laboratory testing of highway pavement rutting.” Canadian Journal of Civil Engineering. 27(6). pp. 1109-1119.

24. Yang, J., Lu, H., and Zhu, H. (2009). "Approaches to rut depth prediction in semirigid asphalt pavements," Journal of Engineering Mechanics. 135(6). pp. 510-516.

25. Wang, K. (2011). "Automated survey of pavement distress based on 2D and 3D laser images." MBTC DOT 3023.

26. Tsai, Y., Wang, Z., and Li, F. (2011). "Assessment of rut depth measurement using emerging 3D continuous laser profiling technology." Transportation Research Board 90th Annual Meeting. Transportation Research Board, Washington, D. C.

27. Huang, Y., Copenhaver, T., and Hempel, P. (2013). "Texas Department of Transportation 3D transverse profiling system for high-speed rut measurement." Journal of Infrastructure Systems. 19(2). pp. 221-231.

28. Simpson, A. (1999). "Characterization of transverse profile." Transportation Research Record: Journal of the Transportation Research Board, No. 1655, Transportation Research Board of the National Academies, Washington, D.C., pp. 185-191.

29. Chen, D., and Li, Z. (2008). "Comparisons of five computational methods for transverse profiles." Journal of Testing and Evaluation 36(5). pp. 1-8.

30. Hou, X., Ma, S., and Wang, C. (2006). "Research on measurement and evaluation of asphalt pavement rutting based-on traffic safety." Journal of Highway and Transportation Research and Development. (23)8. pp. 14-17. (Chinese).

31. Li, F. (2012). "A methodology for characterizing pavement rutting condition using emerging 3D line laser imaging technology." Dissertation presented to Georgia Institute of Technology in partial fulfillment of the requirements for the degree of Doctor of Philosophy.

32. McGhee, K.H. (2004). "Automated pavement distress collection techniques: a synthesis of highway practice." NCHRP Synthesis 334. Transportation Research Board, Washington, D.C.

33. Elkins, G. E., Schmalzer, P., Thompson, T., Simpson, A., and Ostrom, B. (2009). "Long-term pavement performance information management system pavement performance database user reference guide."

34. Sayers, M., and Karamihas, S. (1998). "The little book of profiling." The Regent of the University of Michigan.

35. Antunes, M., Brittain, S., Kokot, D., La Torre, F., Leben, B., Litzka, J., Mladenovic, G., Viner, H., and Weninger-Vycudil, A. (2008). "COST Action 354: Performance indicators for road pavements." European Cooperation in the Field of Scientific and Technical Research, FSV-Austrian Transport Research Association, Vienna, Austria.

36. ASTM E1703/E1703M-10. (2010). "Standard test method for measuring rut-depth of pavement surfaces using a straightedge." American Society for Testing and Materials.

37. American Association of State Highway and Transportation Officials. (2010). "Standard practice for determining rut depth in pavements." AASHTO Designation: R48-10. Washington, D.C.

38. Bai, Y., Schrock, S., Mulinazzi, T., Hou, W., Liu, C., and Firman, U. (2009). "Estimating highway pavement damage costs attributed to truck traffic." Transportation Research Institute, the University of Kansas, Lawrence, Kansas.

39. MathWorks Inc. (2010). "MATLAB product help." The MathWorks Inc., Natick, MA.

40. Mendenhall, W., Beaver, R., and Beaver, B. (2006)."Introduction to probability and statistics." Twelfth edition. Thomson and Brooks/Cole.

41. Johnson, D. (1998). “Applied multivariate methods for data analysts.” Duxbury Press.

42. R Development Core Team. (2012). “R: A language and environment for statistical computing.” R Foundation for Statistical Computing, Vienna, Austria. ISBN 3-900051-07-0, URL http://www.R-project.org/.

43. Su, W. (2000). “Studies in multivariate comprehensive evaluation theory.” Dissertation presented to Xiamen University in partial fulfillment of the requirements for the degree of Doctor of Philosophy. (Chinese).

44. Du. D., Pang, Q., and Wu, Y. (2008). “Methodologies and case studies for modern comprehensive evaluation.” Tsinghua University Press. (Chinese).

45. Li, Y., and Yun, J. (2009). “Synthetic research on the theory of multi-attribute comprehensive evaluation index system.” Journal of WUT (Information &Management Engineering). (31)2. pp. 305-309. (Chinese).

46. Kwangsun, Y., and Hwang, C. (1995). “Multiple attribute decision making: an introduction.” Sage University Papers Series. Sage Publications. Thousand Oaks, CA.

47. Daniel, J., Werner, P., and Bahill, T. (2001). “Quantitative methods for tradeoff analyses.” System Engineering. 4(3). pp. 190-212.

48. Gower, J. C. (1985). “Measures of similarity, dissimilarity, and distance.” Encyclopedia of Statistical Sciences, Vol. 5. S. pp. 397-405.

49. Johnson, R.A., and Wichern, D.W. (1992). “Applied multivariate statistical analysis.” 3rd Edition. Prentice Hall. Englewood Cliffs, New Jersey.

50. Wymore, W. (2000). “Model-based systems engineering: an introduction to the mathematical theory of discrete systems and to the tricotyledon theory of system design.” CRC Press.

51. Fishburn, P. (1970). “Utility theory for decision making.” Research Analysis Corporation. Publications in Operations Research No.18.

52. Zhang, Z., Singh, N., and Hudson, R. (1993). “Comprehensive ranking index for flexible pavement using fuzzy sets model.” Transportation Research Record: Journal of the Transportation Research Board, No. 1397, Transportation Research Board of the National Academies, Washington, D.C., pp. 96-102.

53. Li, Q. (2009). “Database support and modeling for the mechanistic empirical pavement design guide (MEPDG).” Dissertation presented to University of Arkansas in partial fulfillment of the requirements for the degree of Doctor of Philosophy.

54. Kirkwood, C. (1997). “Strategic decision making: multiobjective decision analysis with spreadsheets.” Duxbury Press.

55. Lamer, B. (2009). “Min-additive utility functions.” The MITRE Corporation. Bedford, MA. http://www.mitre.org/work/tech_papers/tech_papers_09/09_0383/09_0383.pdf

56. Galehouse, L., Moulthrop, J., and Hicks, G. (2003). “Principles of pavement preservation: definitions, benefits, issues, and barriers.” TR News. Transportation Research Board (TRB), National Research Council, Washington, D.C. pp. 4-15.

57. Buede, D. (2000). “The engineering design of systems: models and methods.” Wiley, New York.

58. Saaty, T.L. (1980).”The analytic hierarchy process.” New York: McGraw Hill.

59. Jolliffe, I.T. (1986). “Principle component analysis.” Springer-Verlag.

60. Ongel, A., Kohler, E., and Harvey, J. (2008). “Evaluation of effects of pavement characteristics on the OBSI levels using principal components regression.” Journal of the Acoustical Society of America. 123(5). 3390.

61. Smith, J., and Tighe S. (2006). “Analytic hierarchy process as a tool for infrastructure management.” Transportation Research Record: Journal of the Transportation Research Board, No. 1974, Transportation Research Board of the National Academies, Washington, D.C., pp. 3-9.

62. Sun, L. and Gu, W. (2011). “Pavement condition assessment using fuzzy logic theory and analytic hierarchy process.” Journal of Transportation Engineering. 137(9). pp. 648-655.

63. Xiao, X. (2012). “Risk analysis and reliability improvement of mechanistic-empirical pavement design.” Dissertation presented to University of Arkansas in partial fulfillment of the requirements for the degree of Doctor of Philosophy.

64. Federal Highway Administration. (2012). “Manual on uniform traffic control devices for streets and highways.” 2009 Edition. FHWA.

65. Conway, D., and White, J. (2012). “Machine learning for hackers.” O’Reilly Media.

66. Svozil, D., Kvasnicka, V., and Pospichal, J. (1997). “Tutorial: introduction to multi-layer feed-forward neural networks.” Chemometrics and Intelligent Laboratory Systems. 39. pp. 43-62.

67. Rumelhart, D.E., McClelland, J.L., and the PDP Research Group. (1986). “Parallel distributed processing: explorations in the microstructure of cognition.” Vol.1 and 2, MIT Press, Cambridge, Mass.

68. Breiman, L. (1984). “Classification and regression trees.” Wadsworth International Group. 1984.

69. Breiman, L. (2001). Random forests. Machine Learning. 45 (1). pp. 5-32.

70. Terzi, S. (2007). "Modeling the pavement serviceability ratio of flexible highway pavements by artificial neural networks." Construction and Building Materials, 21, pp. 590-593.

71. Alsugair, A. and Al-Qudrah, A. (1998). "Artificial neural network approach for pavement maintenance." Journal of Computing in Civil Engineering. 12(4). pp. 249-255.

72. Das, A., Abdel-Aty, M., Pande, A. (2009). "Using conditional inference forests to identify the factors affecting crash severity on arterial corridors." Journal of Safety Research. 40(4). pp. 317-327.

73. Mohammed Ali, S., Joshi, N, George, B., and Vanajakshi, L. (2012). "Application of random forest algorithm to classify vehicles detected by a multiple inductive loop system." 15th International IEEE Conference on Intelligent Transportation Systems. Anchorage, AL, USA.

74. Wu, X. (2012). "Statistical methods for complicate data sets-applications based on R." China Renmin University Press. (Chinese).

75. Venables, W. and Ripley, B. (2002). "Modern applied statistics with S." Fourth Edition. Springer, New York. 2002.

76. Liaw, A. and Wiener, M. (2002). "Classification and regression by randomForest." R News 2(3), pp. 18-22.

APPENDIX A: AASHTO Protocol PP69-10

Standard Practice for

Determining Pavement Deformation Parameters and Cross Slope from Collected Transverse Profiles

AASHTO Designation: PP 69-10

American Association of State Highway and Transportation Officials
444 North Capitol Street N.W., Suite 249
Washington, D.C. 20001

APPENDIX B: AASHTO Protocol PP70-10

Standard Practice for

Collecting the Transverse Pavement Profile

AASHTO Designation: PP 70-10

American Association of State Highway and Transportation Officials
444 North Capitol Street N.W., Suite 249
Washington, D.C. 20001

APPENDIX C: Report of Pavement Rut for the Study Sections

PP69-10 Attributes on US 65 N

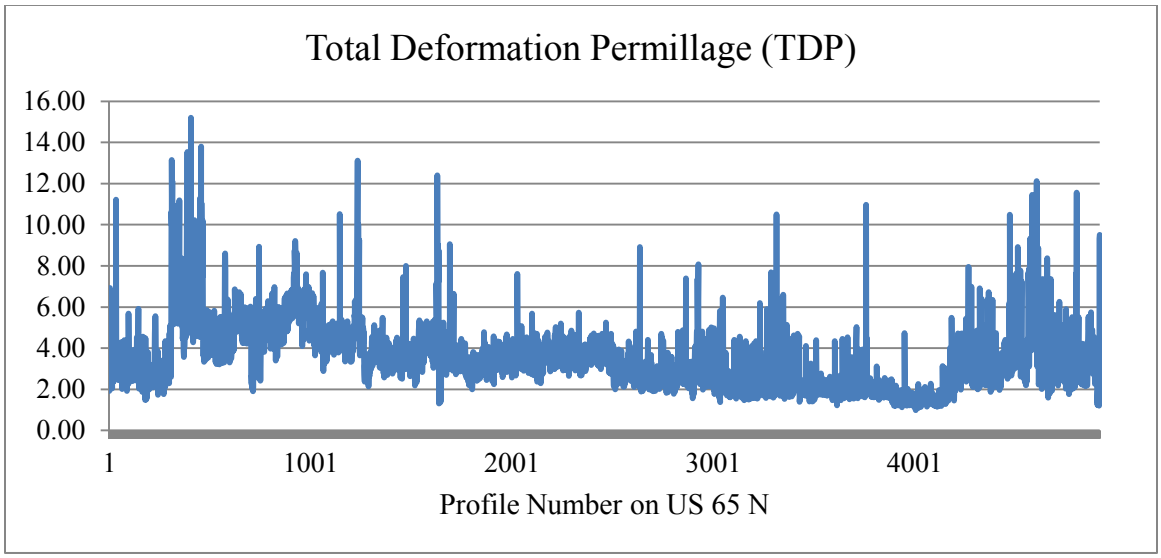

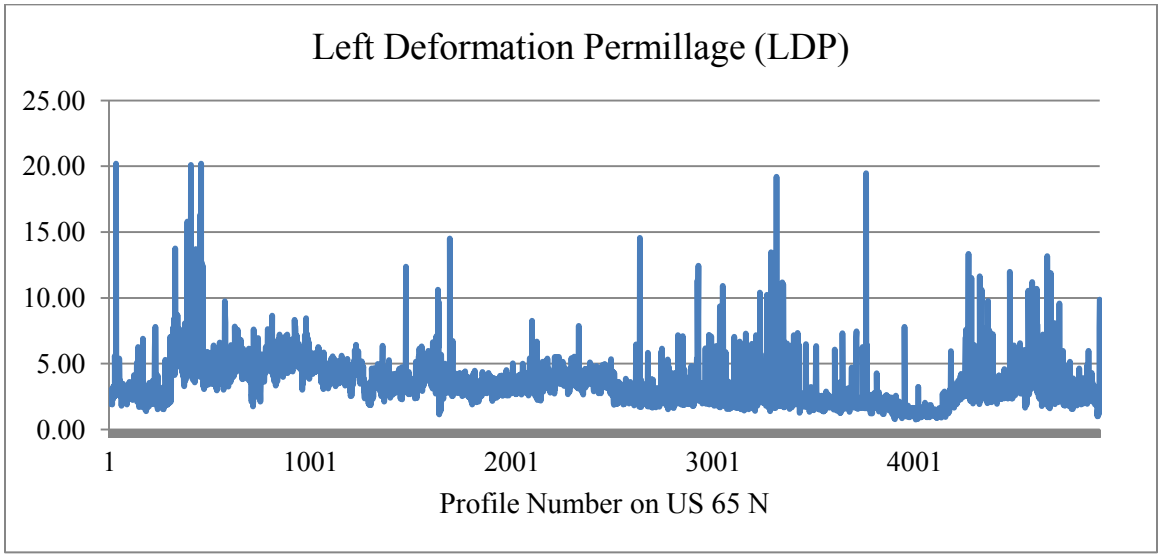

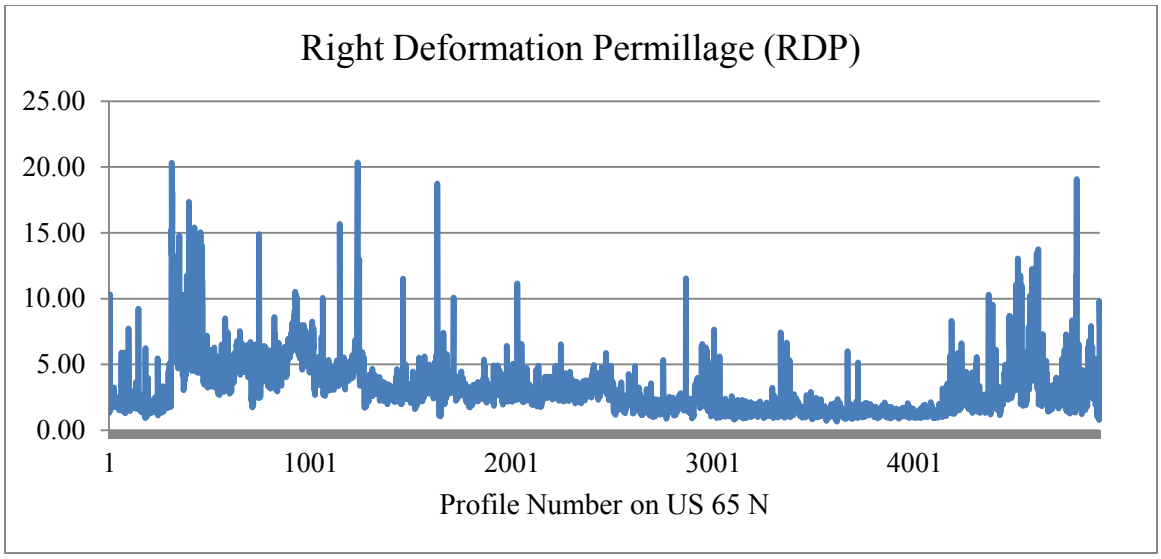
Right Deformation Permillage (RDP)
25.00
20.00
15.00
10.00
5.00
0.00
1
1001
2001
3001
4001
Profile Number on US 65 N

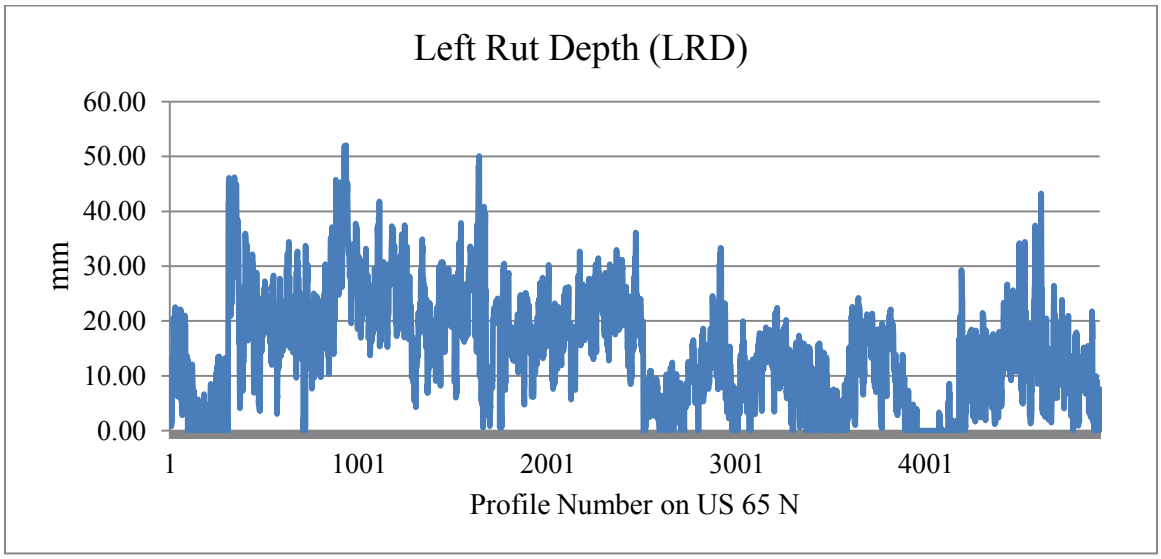
Left Rut Depth (LRD)
60.00
50.00
40.00
30.00
20.00
10.00
0.00
mm
1
1001
2001
3001
4001
Profile Number on US 65 N

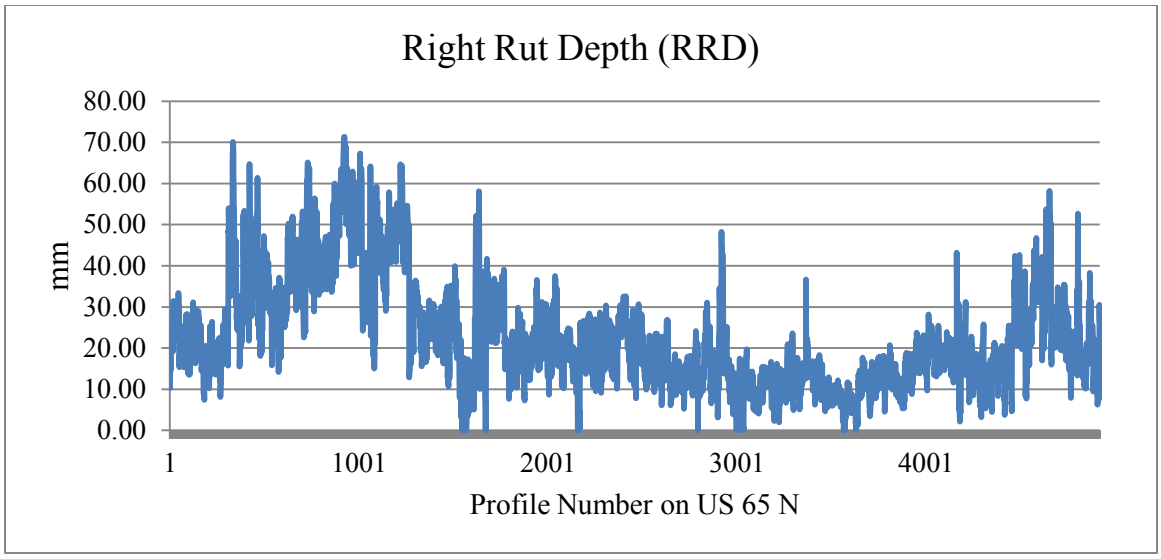
Right Rut Depth (RRD)
80.00
70.00
60.00
50.00
40.00
30.00
20.00
10.00
0.00
mm
1
1001
2001
3001
4001
Profile Number on US 65 N

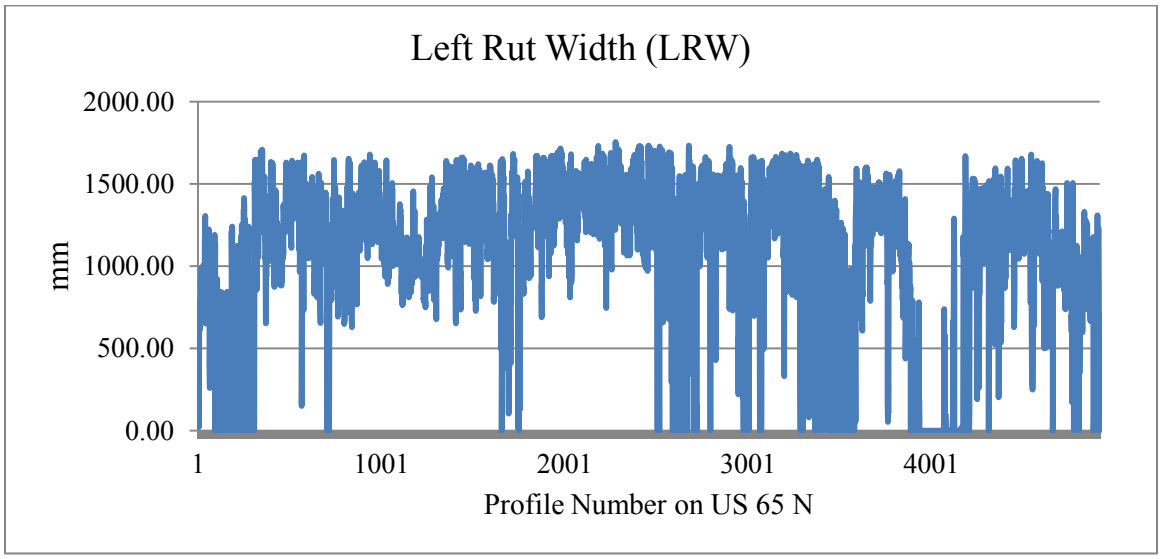
Left Rut Width (LRW)
2000.00
1500.00
1000.00
500.00
0.00
mm
1
1001
2001
3001
4001
Profile Number on US 65 N

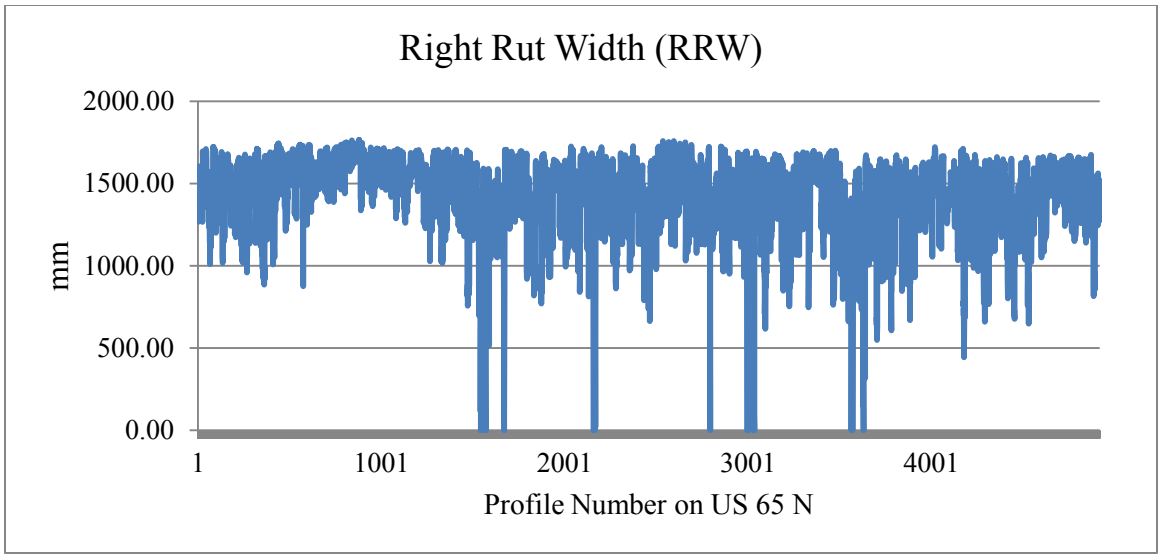
Right Rut Width (RRW)
2000.00
1500.00
1000.00
500.00
0.00
mm
1
1001
2001
3001
4001
Profile Number on US 65 N

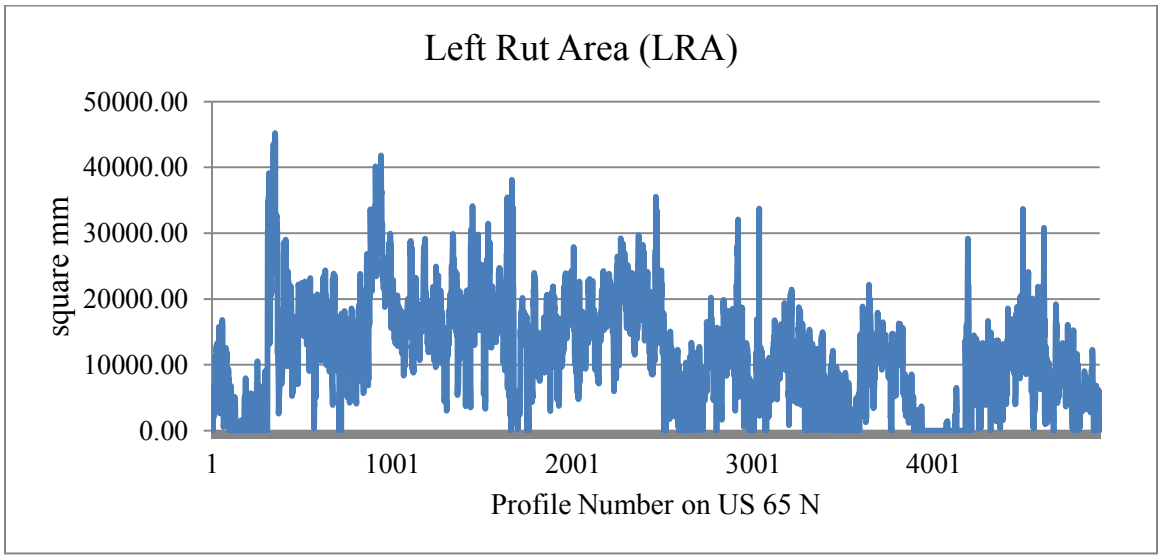
Left Rut Area (LRA)
50000.00
40000.00
30000.00
20000.00
10000.00
0.00
square mm
1
1001
2001
3001
4001
Profile Number on US 65 N

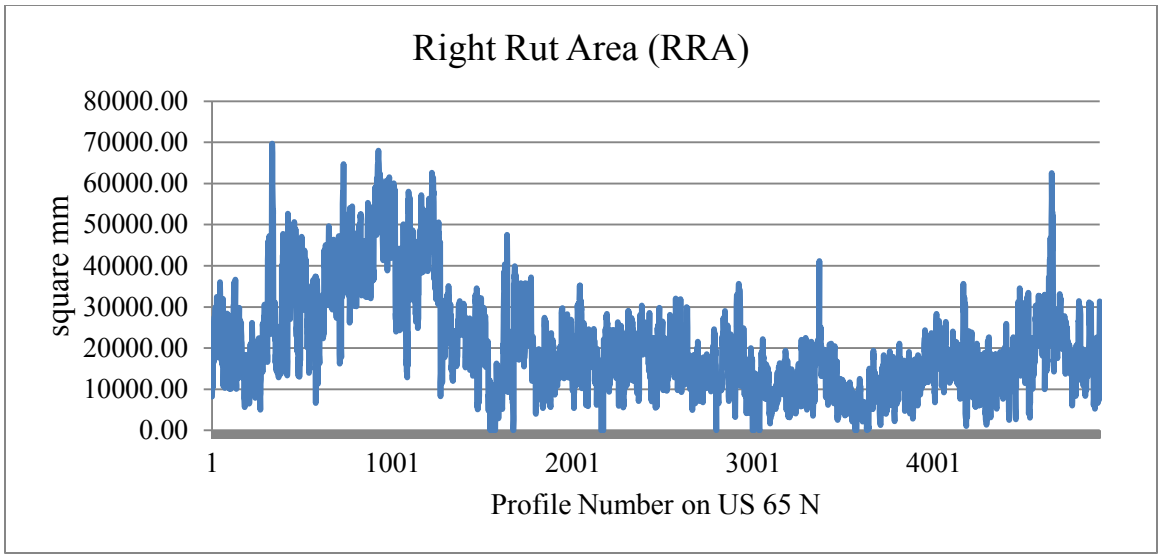
Right Rut Area (RRA)
80000.00
70000.00
60000.00
50000.00
40000.00
30000.00
20000.00
10000.00
0.00
square mm
1
1001
2001
3001
4001
Profile Number on US 65 N

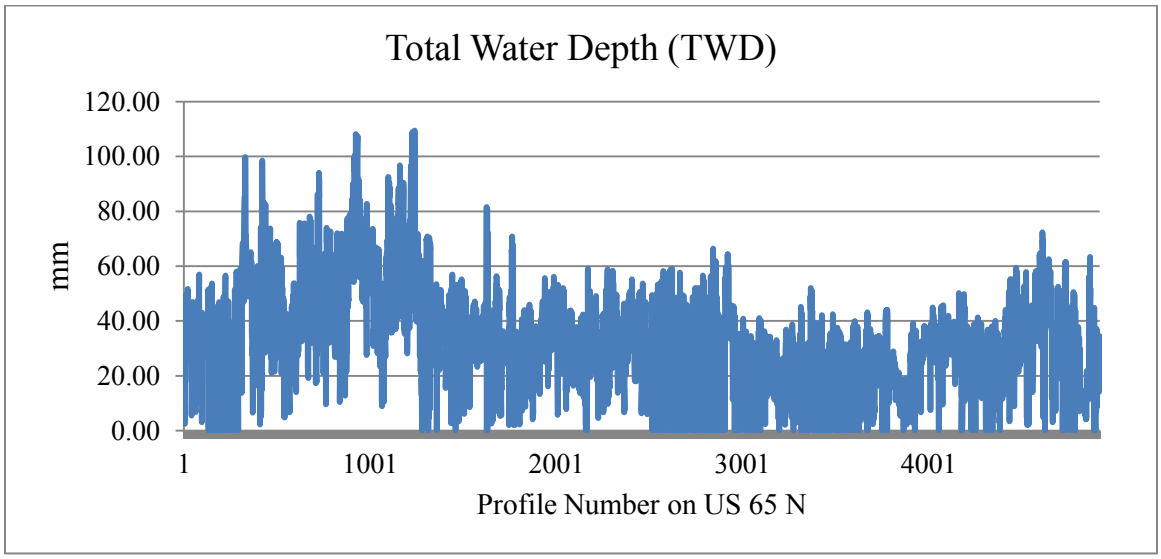
Total Water Depth (TWD)
120.00
100.00
80.00
60.00
40.00
20.00
0.00
mm
1
1001
2001
3001
4001
Profile Number on US 65 N

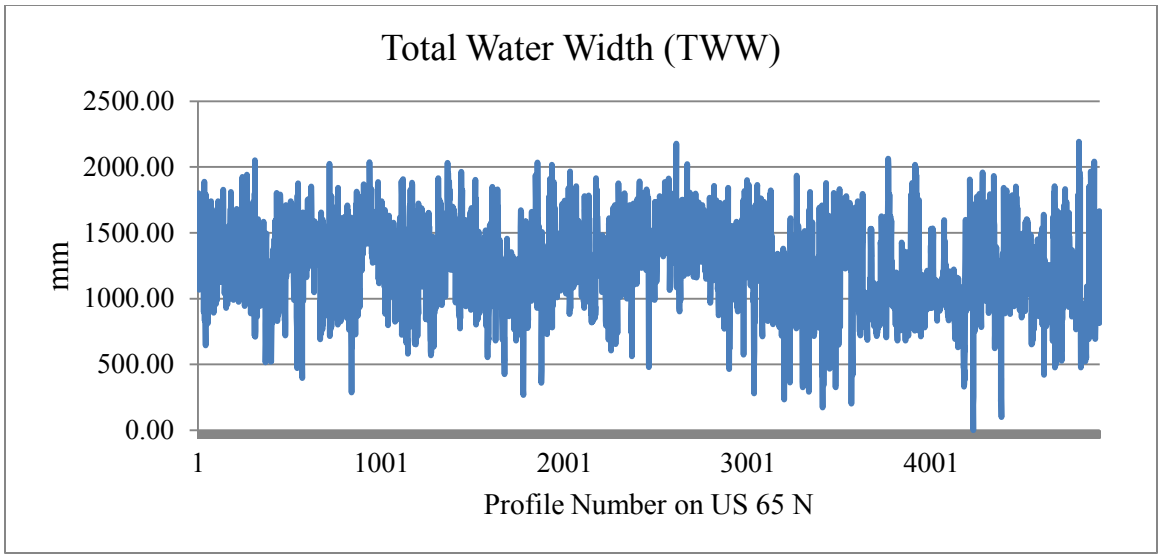
Total Water Width (TWW)
2500.00
2000.00
1500.00
1000.00
500.00
0.00
mm
1
1001
2001
3001
4001
Profile Number on US 65 N

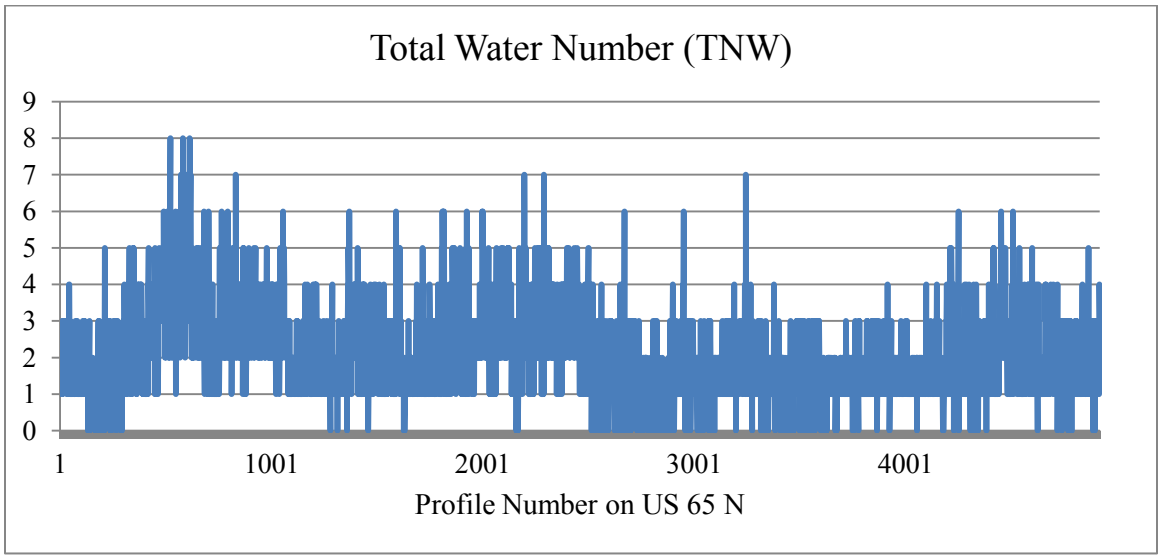
Total Water Number (TNW)
9
8
7
6
5
4
3
2
1
0
1
1001
2001
3001
4001
Profile Number on US 65 N

PP69-10 Attributes on US 70 E

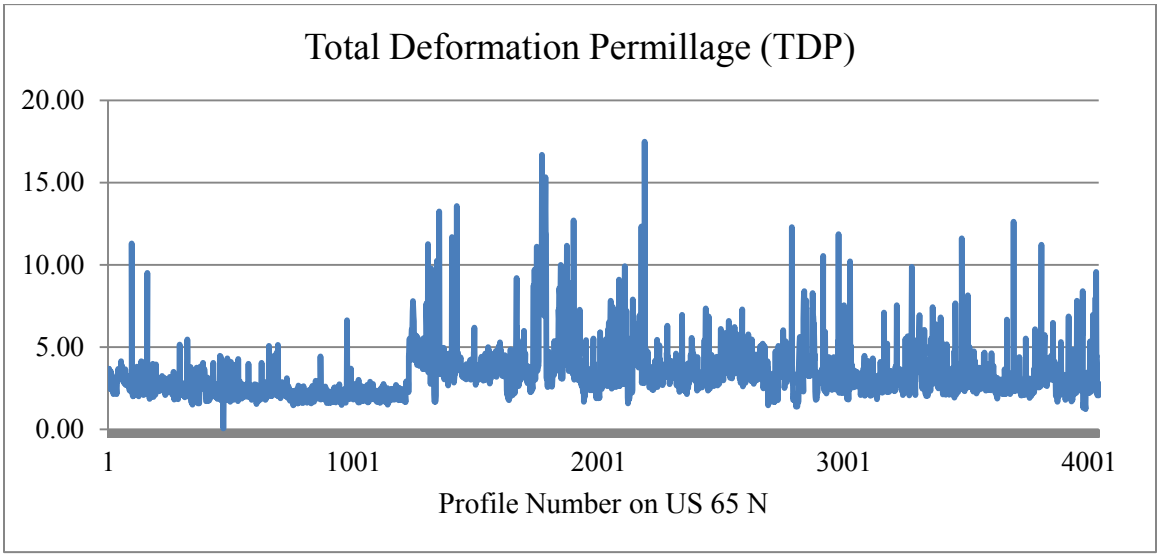

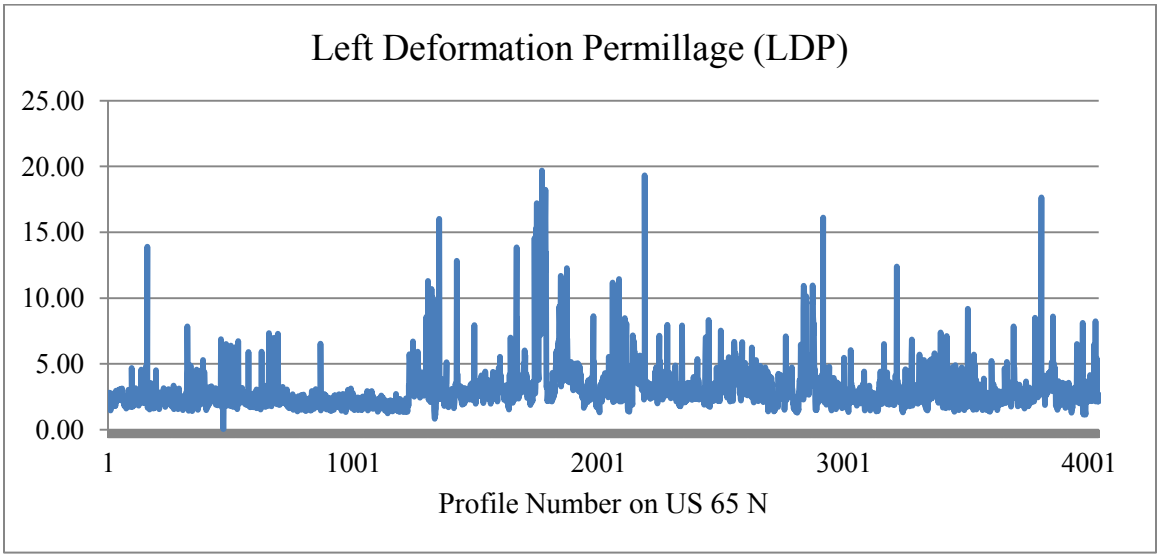

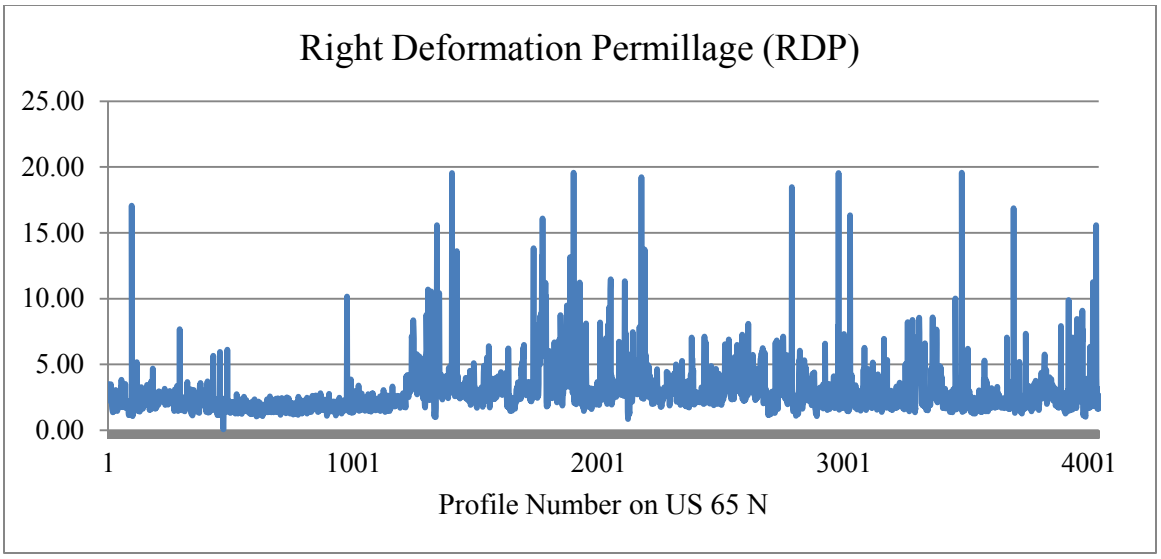
Right Deformation Permillage (RDP)
25.00
20.00
15.00
10.00
5.00
0.00
1
1001
2001
3001
4001
Profile Number on US 65 N

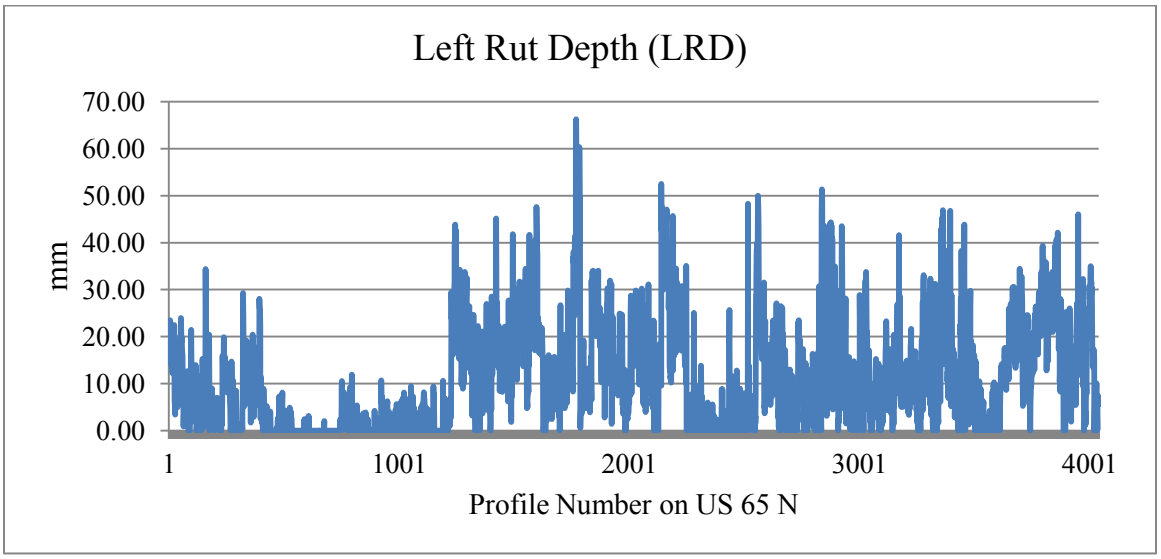
Left Rut Depth (LRD)
70.00
60.00
50.00
40.00
30.00
20.00
10.00
0.00
mm
1
1001
2001
3001
4001
Profile Number on US 65 N

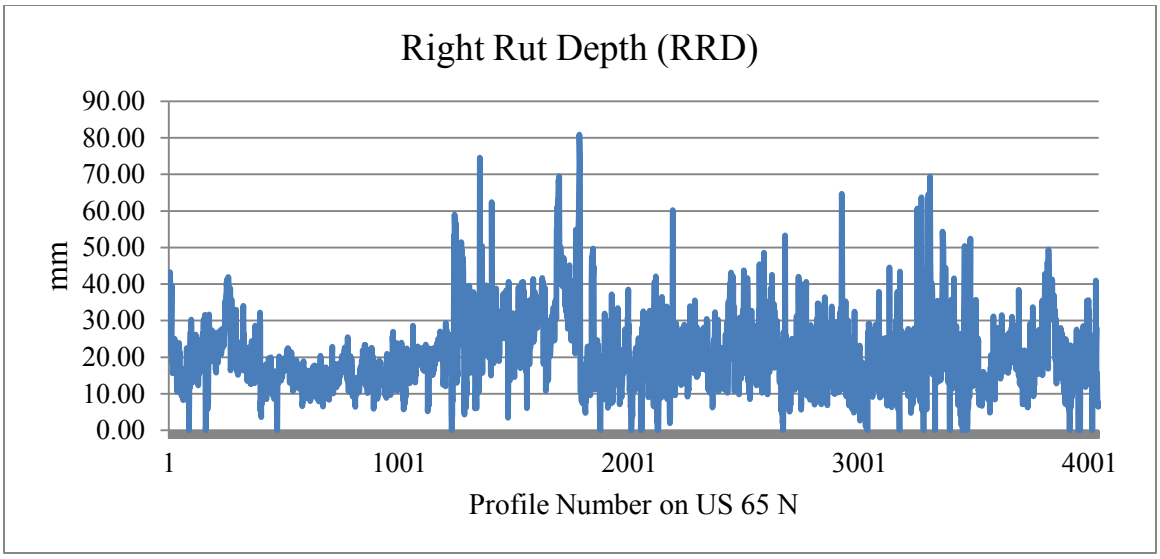
Right Rut Depth (RRD)
90.00
80.00
70.00
60.00
50.00
40.00
30.00
20.00
10.00
0.00
mm
1
1001
2001
3001
4001
Profile Number on US 65 N

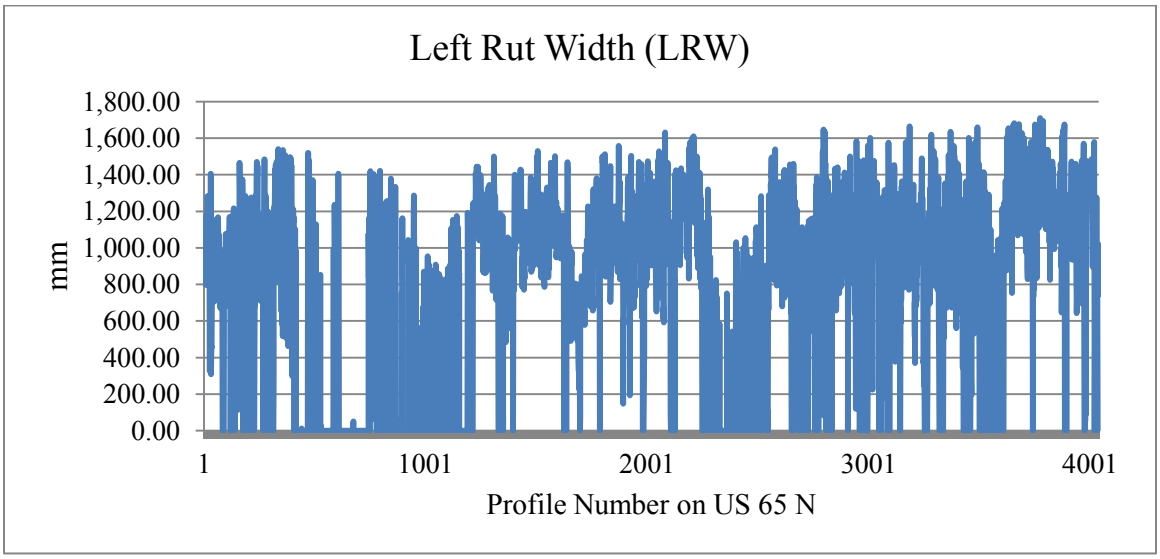
Left Rut Width (LRW)
1,800.00
1,600.00
1,400.00
1,200.00
1,000.00
800.00
600.00
400.00
200.00
0.00
mm
1
1001
2001
3001
4001
Profile Number on US 65 N

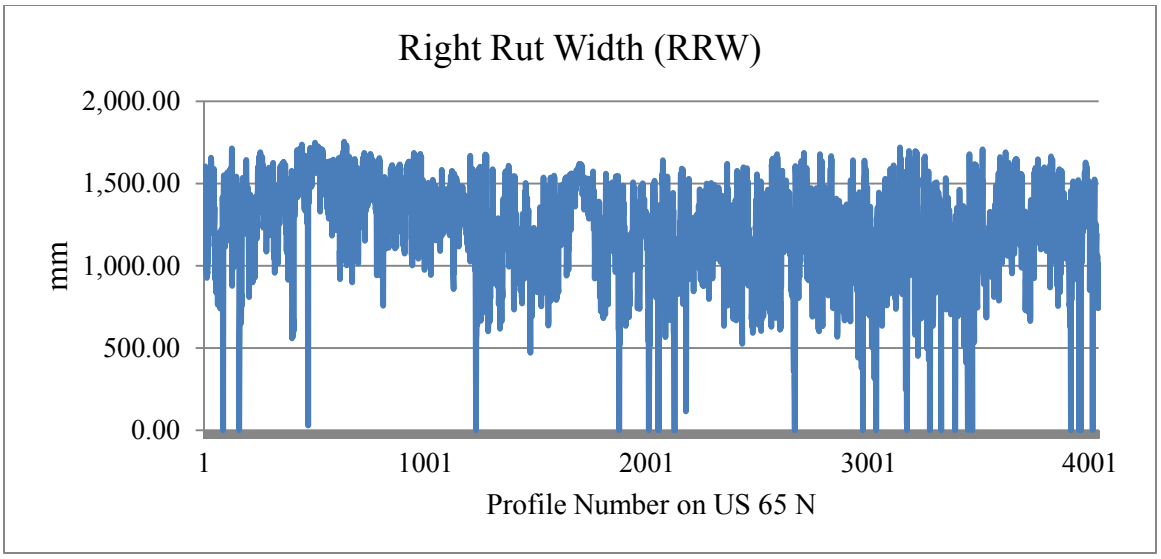
Right Rut Width (RRW)
2,000.00
1,500.00
1,000.00
500.00
0.00
mm
1
1001
2001
3001
4001
Profile Number on US 65 N

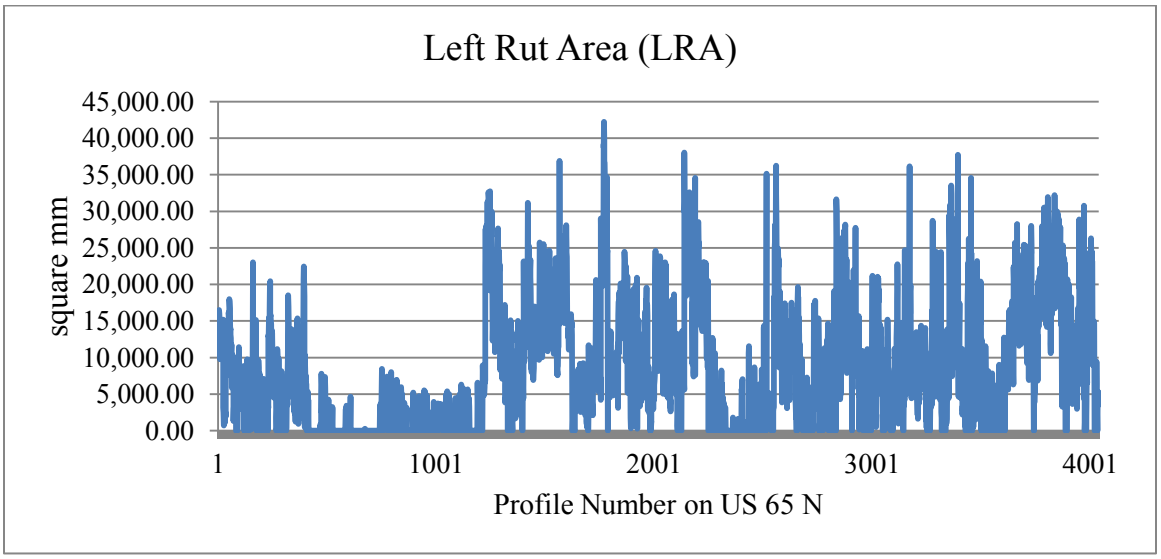
Left Rut Area (LRA)
45,000.00
40,000.00
35,000.00
30,000.00
25,000.00
20,000.00
15,000.00
10,000.00
5,000.00
0.00
square mm
1
1001
2001
3001
4001
Profile Number on US 65 N

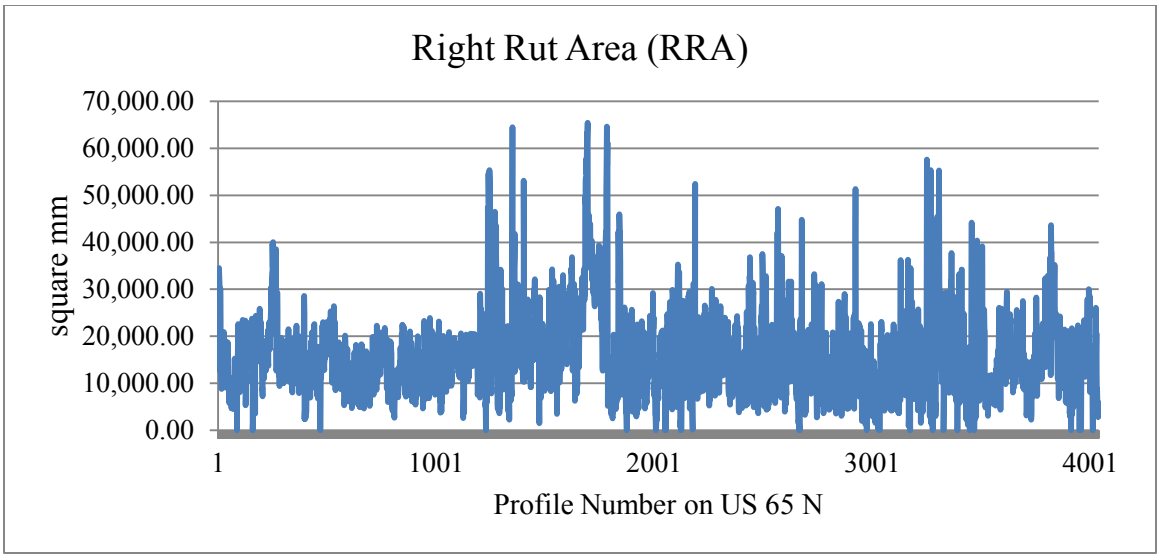
Right Rut Area (RRA)
70,000.00
60,000.00
50,000.00
40,000.00
30,000.00
20,000.00
10,000.00
0.00
square mm
1
1001
2001
3001
4001
Profile Number on US 65 N

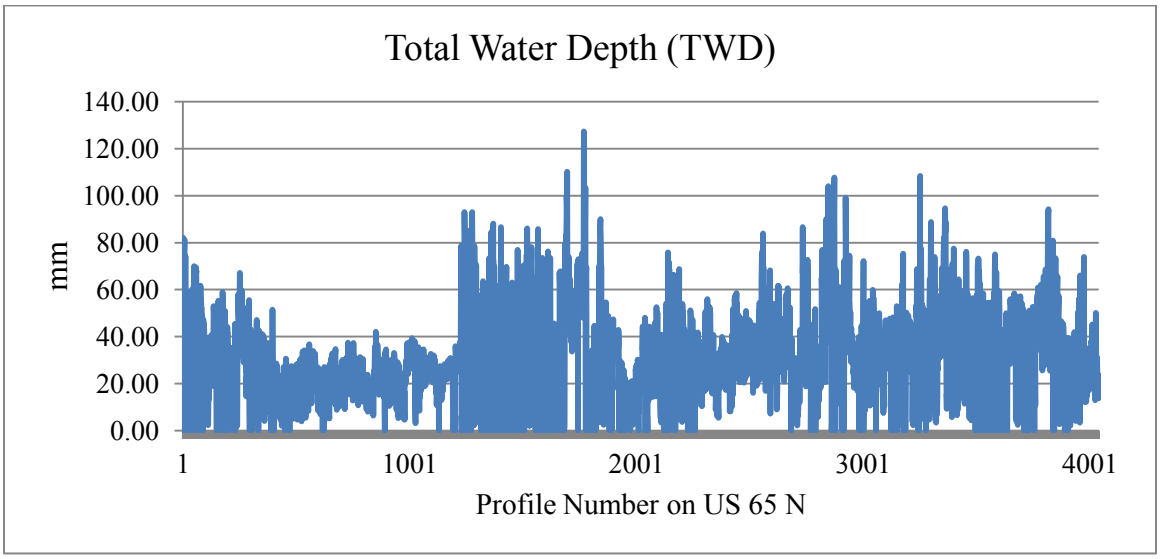
Total Water Depth (TWD)
140.00
120.00
100.00
80.00
60.00
40.00
20.00
0.00
mm
1
1001
2001
3001
4001
Profile Number on US 65 N

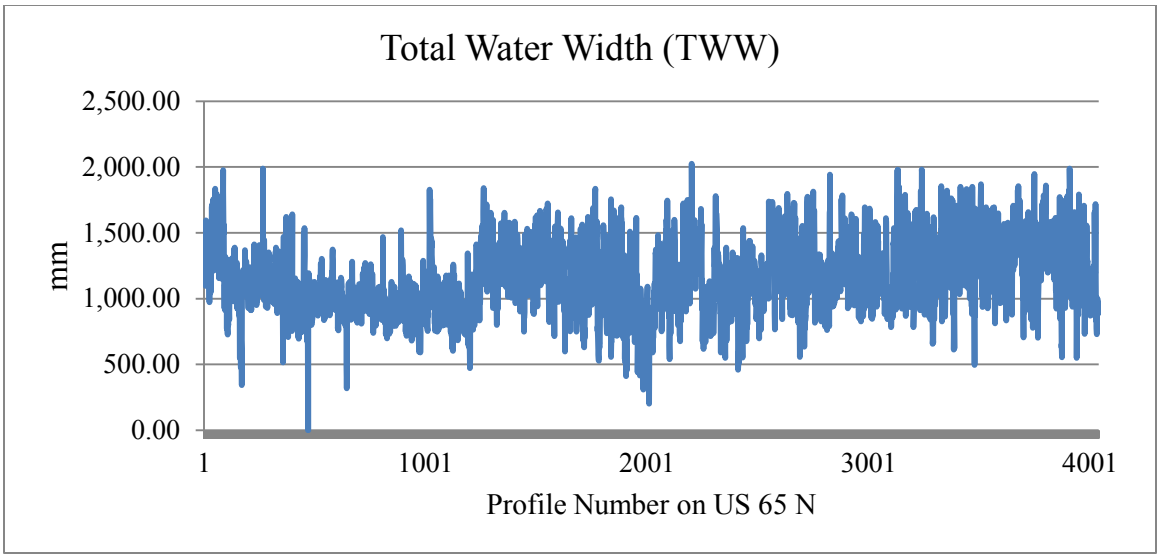
Total Water Width (TWW)
2,500.00
2,000.00
1,500.00
1,000.00
500.00
0.00
mm
1
1001
2001
3001
4001
Profile Number on US 65 N

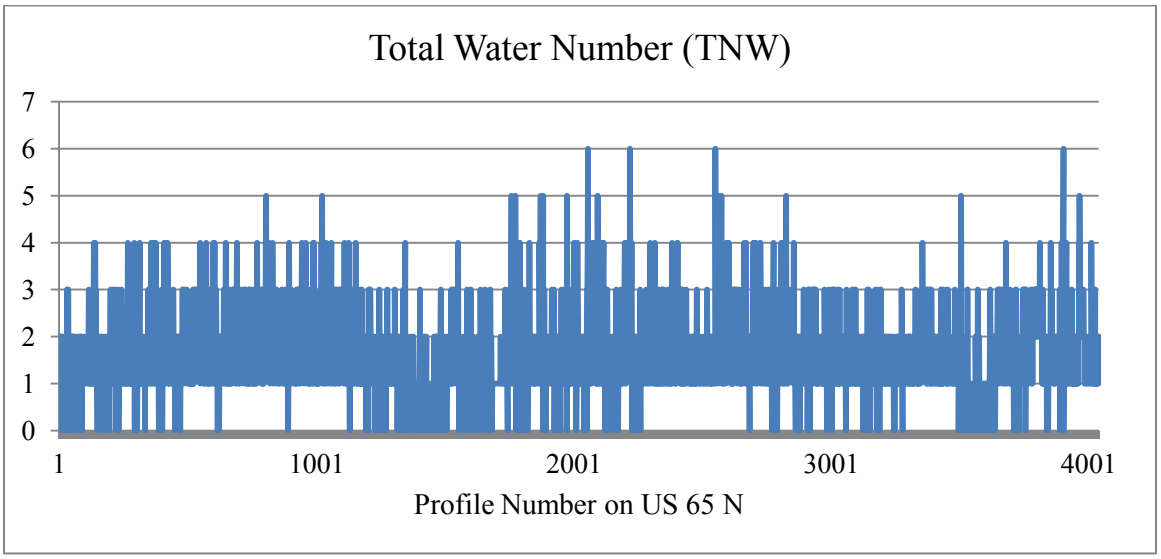
Total Water Number (TNW)
7
6
5
4
3
2
1
0
1
1001
2001
3001
4001
Profile Number on US 65 N

APPENDIX D: Phase 1 Survey Questionnaire

Comprehensive Pavement Transverse Profile Evaluation For National Highway Systems

Phase I Survey: Evaluation of Individual Attribute

Dear Professionals,

Thanks for participating in this survey. The entire evaluation is split into two phases. The purpose of Phase I survey is to collect information for eliciting utility functions of candidate attributes, respectively. Phase II survey, which is expected to conduct after results analysis of Phase I, will be assigning weights for comprehensive aggregation. Your opinions will eventually be formulized in establishing a comprehensive pavement transverse profile evaluation system.

In this study, in total 8,960 profiles were randomly selected (12 successive profiles with a longitudinal interval of about 500 mm for every approximately 200 m pavement section) for about 200 kilometers (125 miles) of US highway sections in Arkansas. Raw data were collected using PaveVision3D system engineered by WayLink System Co. with collaboration of Oklahoma State University. The attributes of which were extracted abiding by AASHTO new permanent deformation evaluation protocol PP69-10, are assumed covering most possibilities in terms of shapes of transverse profiles.

The 12 extracted attributes are:

- Total Deformation Percent
- Left Deformation Percent
- Right Deformation Percent
- Left Rut Depth
- Right Rut Depth
- Left Rut Width
- Right Rut Width
- Left Rut cross-sectional area
- Right Rut cross-sectional area
- Total Number of Water Entrapment Points
- Total Water Entrapment Depth
- Total Water Entrapment Width

It is evident that the presence of any attribute (a value of greater than zero) is undesired and considered a certain degree of deterioration. Also, any incremental quantity of an attribute decreases the pavement performance. In this survey, the basic assumption for your judgment is a five-level grading system: very good, good, fair, poor, and very poor condition. However, for the ease of this survey, you only have to give the adequate and inadequate values for the above listed attributes, based on which the researchers will later on elicit utility function. The adequate threshold distinguishes very good condition from good, in other words, if the value of the attribute exceeds the threshold value, this attribute no longer belongs to absolutely satisfied performance. Likewise, the inadequate threshold stands between poor and very poor, which means an attribute is considered a very poor status if its value exceeds this inadequate threshold. For example, in some agencies' practices, the

adequate threshold for rutting depth of primary highway is 5 mm, which indicates a depth of less than 5 mm is recognized as a very good condition. Correspondingly, the inadequate value is 20 mm, which denotes that any rutting depth more than 20 mm has fallen into very poor or failed condition.

The basic shape of the predetermined scoring function is provided in Attachment A for your reference. The adequate and inadequate threshold values will be corresponded to m and n in the graph and used to determine the parameters of the functions. The top logistic function will be used for Attribute 1-9, which are physical deformation of the surface. Attribute 10-12, the water involved attributes will use the bottom one, exponential function.

Be advised that this survey is only for national highway systems, which is usually categorized as primary roadways. Your field experience, pavement management expertise, and the statistical data attached are supposed to play important roles in this survey. Furthermore, three attachments are provided for your reference. Each attribute to be judged is literally and graphically described in Attachment B. Generally, you don't have to read through PP69-10 unless you meet with unclear statements in the Attachment B. The distribution range of the 8,960 profiles for all attributes is presented in Attachment C. Attachment D is a rutting depth evaluation provided in COST 354.

Please simply fill in two numbers for each attribute in the Attachment E spreadsheet. Feel free to let me know if there are any forms of confusions. Thanks for your time, wisdom, and cooperation.

Sincerely,

Sheldon Qiu

479-595-5009, sheldon.qiu@okstate.edu

Attachment A: Predetermined Scoring Functions

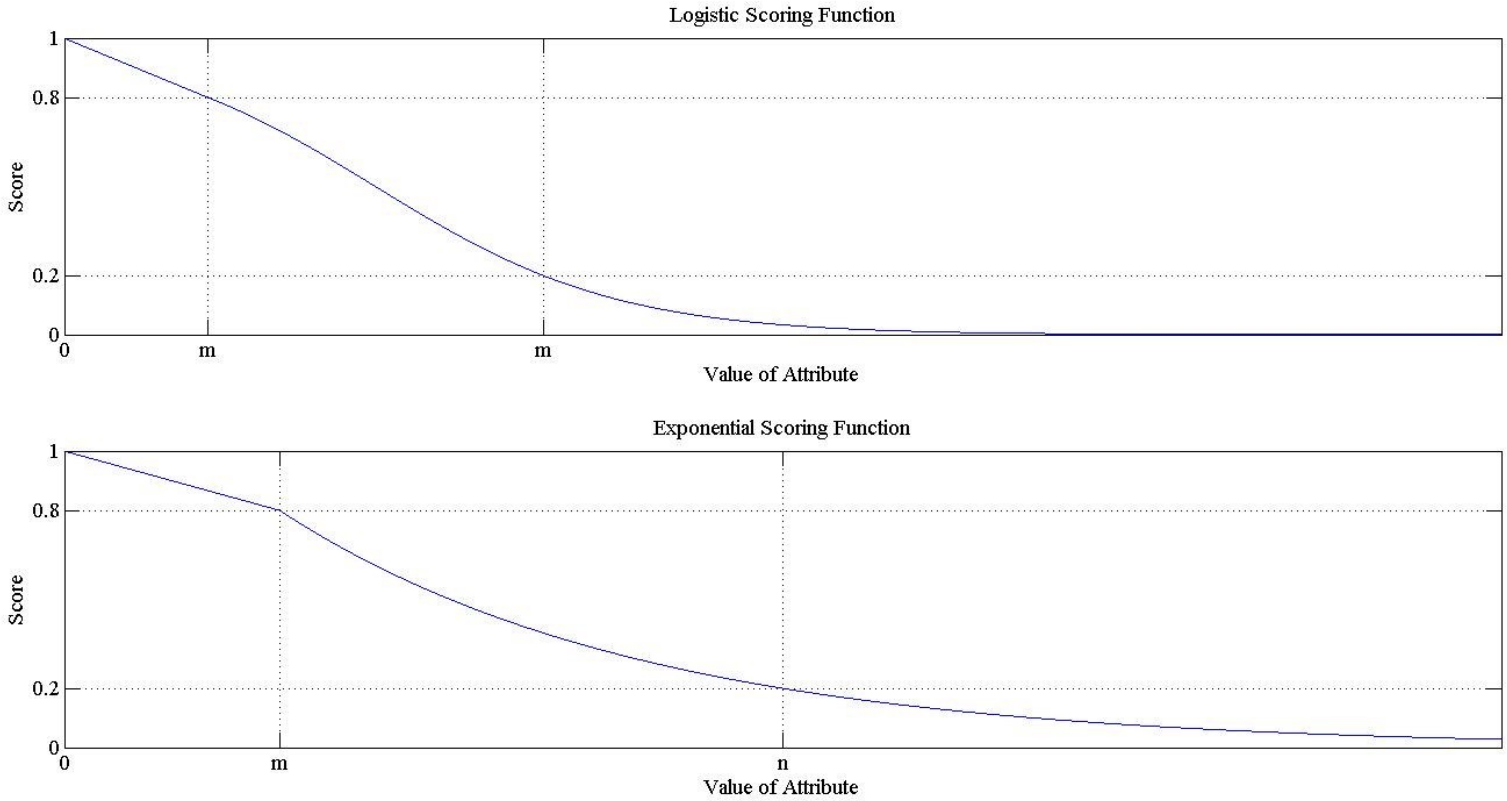

Attachment B: Illustration of Terminology

Note: the following attributes were analyzed according to PP69-10 from selected transverse profiles collecting by PaveVision3D. For deformation and rutting calculation, 50 mm moving average was applied to the original profile whereas 200 mm applied to water entrapment computation. It should be noticed that there might be information conflicting with your existing knowledge experiences, which seems non-physical (e.g. the left rutting depth determination in Figure 2). However, all procedures are executed as per requirement of PP69-10.

Deformation Percent

As illustrated in Figure 1, A and C are the inner and outer edge spots of a lane, respectively. B is the center of a lane:

Left Deformation Percent = (*Profile Length* of AB – *Straight-line Length* of AB)/ *Straight-line Length* of AB * 100

Right Deformation Percent = (*Profile Length* of BC - *Straight-line Length* of BC)/ *Straight-line Length* of BC * 100

Total Deformation Percent = (*Profile Length* of AC - *Straight-line Length* of AC)/ *Straight-line Length* of AC * 100

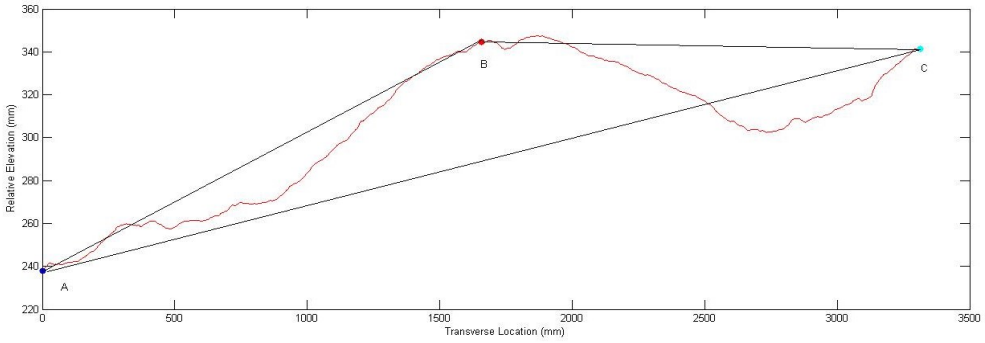

Figure 1. Illustration for Deformation Percent

Rutting Depth, Width, and Area

As illustrated in Figure 2, five spots and three profiles were identified according to PP69-10. Two wheel-paths were given for references:

Left Rutting Depth = abs (Elevation of *Spot Determining Left Rutting Depth "Light Green"*)

Right Rutting Depth = abs (Elevation of *Spot Determining Right Rutting Depth "Black"*)

Left Rutting Width = Length of *left straight-line (Purple)*

Right Rutting Width = Length of *right straight-line (Red)*

Left Rutting Area = Area between *left straight-line (Purple)* and *the profile (Black) below*

Right Rutting Area = Area between *right straight-line (Red)* and *the profile (Green) below*

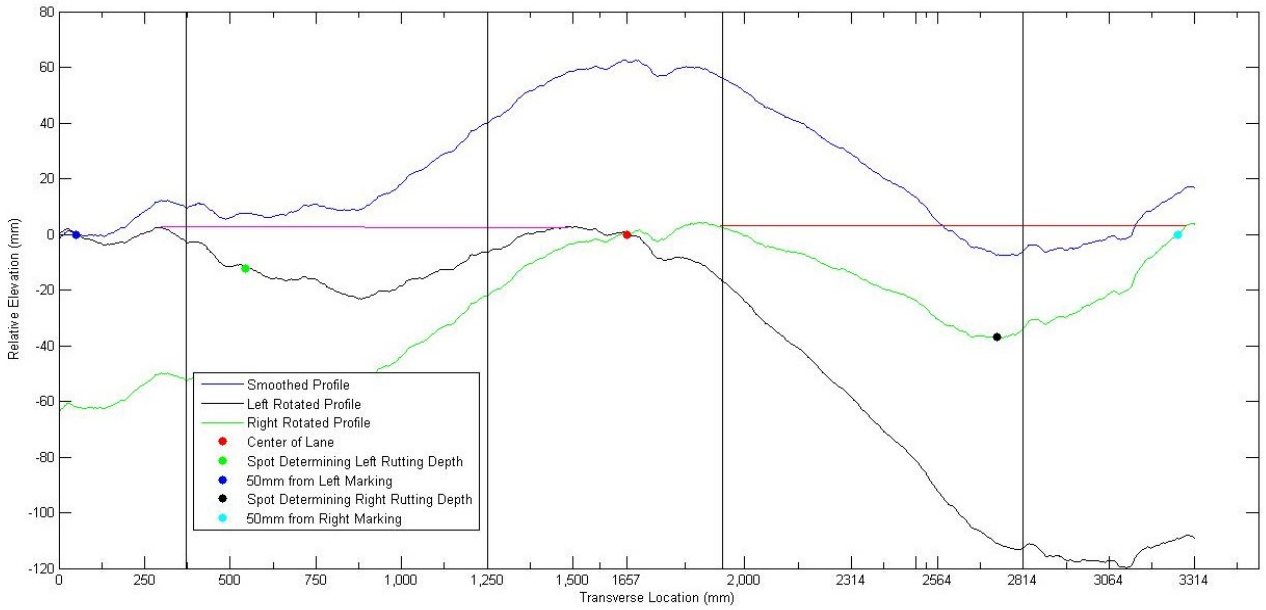

Figure 2. Illustration for Rutting Parameters

Water Entrapment

Water entrapment is graphically shown in Figure 3. The search for water entrapment point started from either left or right side depending on cross-slope. When a pair of lowest point and a lip point is encountered, a water entrapment point can be counted. The example shows only one point of water entrapment. However, there might be more than one point in other profiles.

Total Water Entrapment Number = Number of *Lowest Points* or *Water Lips*

Single Water Entrapment Depth = Elevation of *Water Lip* – Elevation of *Lowest Point*

Total Water Entrapment Depth = $\sum_1^n$ Single Water Entrapment Depth

Single Water Entrapment Width = abs (Transverse Location of *Water Lip* – Transverse Location of *Lowest Point*)

Total Water Entrapment Width = $\sum_1^n$ Single Water Entrapment Width

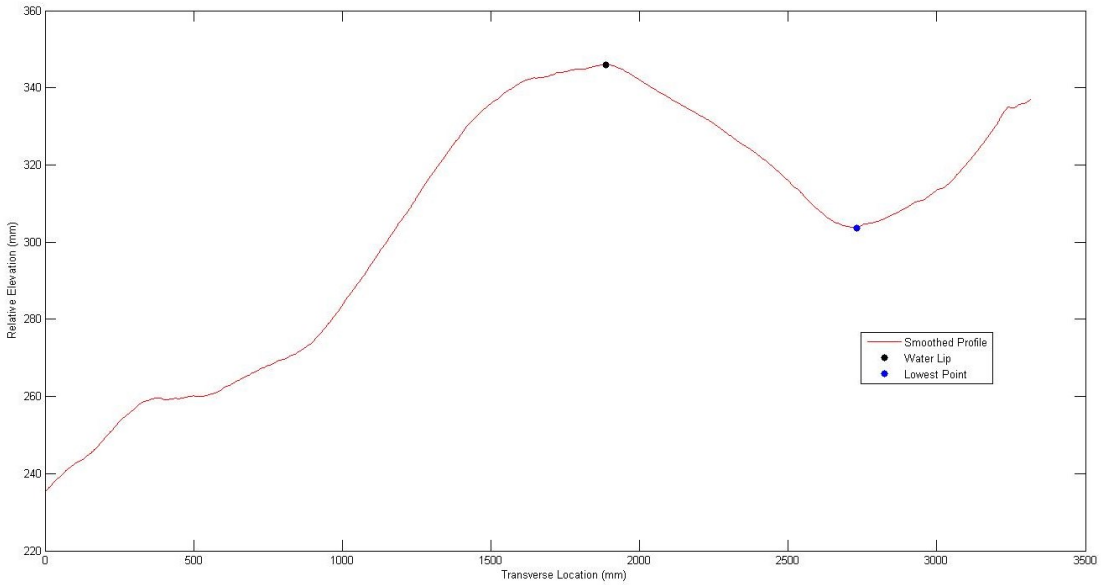

Figure 3. Illustration for Water Entrapment Parameters

Attachment C: Distribution of Sample Data

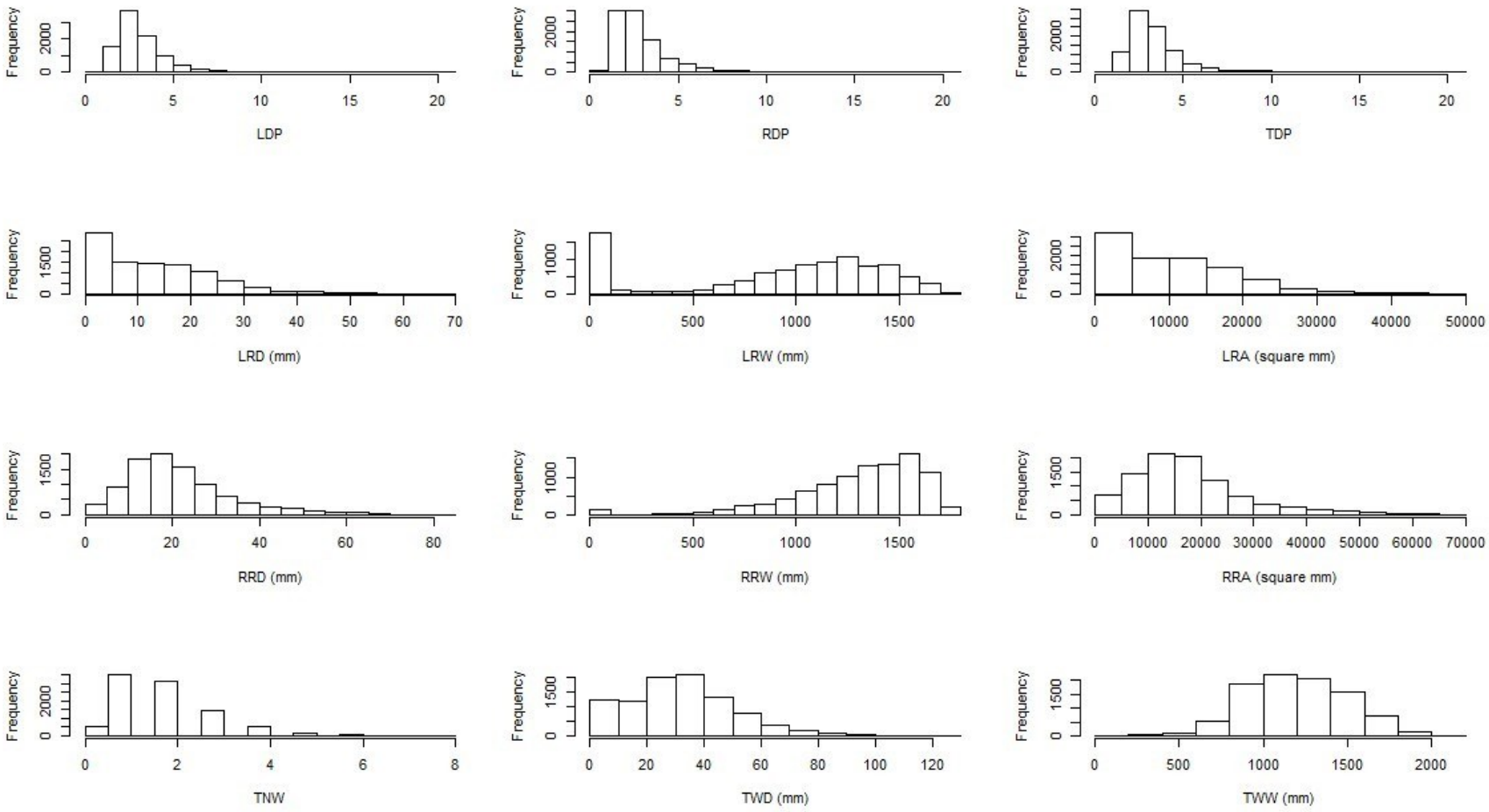

Attachment D: Examples of Rutting Depth Scoring

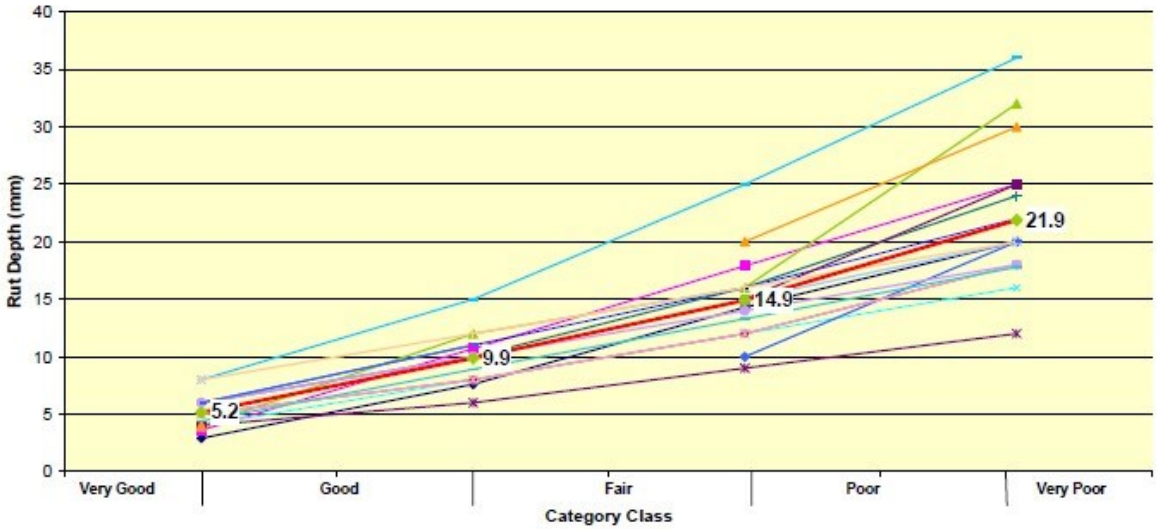

Figure 38: Limits for Technical parameter Rut Depth on Motorways and Other Primary Roads

Note: Figure adopted from COST 354, threshold values of average rutting depth by in different countries for primary roadways.

Attachment E: Spreadsheet for Results

Your Name:			
No.	**Attribute**	**Adequate Threshold**	**Inadequate Threshold**
1	Total Deformation Percent		
2	Left Deformation Percent		
3	Right Deformation Percent		
4	Left Rut Depth (mm)		
5	Right Rut Depth (mm)		
6	Left Rut Width (mm)		
7	Right Rut Width (mm)		
8	Left Rut Area (square mm)		
9	Right Rut Area (square mm)		
10	Total Number of Water Entrapment Points		
11	Total Water Entrapment Depth (mm)		
12	Total Water Entrapment Width (mm)		
Please refer to other Appendices for definition and reference			

APPENDIX E: Phase 2 Survey Questionnaire

Comprehensive Pavement Transverse Profile Evaluation For National Highway Systems

Phase II Survey: Weight Assignment for Attributes Combination

Dear Professionals,

Thanks again for your participation. As introduced previously, the purpose of this Phase II survey is to assign weights for comprehensive evaluation of performance of pavement transverse profiles.

Based on your feedback and further discussion, both threshold values for all attributes were determined, which are given in Attachment A as well as their scoring functions curves. Piecewise functions were adopted for all attributes. For all attributes except TNW (please refer to Attachment A for acronyms), linear functions were applied between the score of 0.8 and 1. For Deformation and Rut related attributes, the logistic function (Sigmoid curve) was used based on the assumption of pavement deterioration curve. For TWD and TWW, the exponential functions (Concave up, decreasing) were employed as their risks for safety. For TNW, 0, 1, 2, 3, 4 of points were corresponding to 1, 0.8, 0.6, 0.4, and 0.2, respectively. Equal and more than 5 points were graded to 0. Please also notice the units of deformation related attributes were changed to permillage due to the relative small value in percent.

In the Phase II survey, a four layer system is constructed according to Analytic Hierarchy Process (AHP) and intrinsic properties of the attributes, as shown in Attachment B. To evaluate the importance of each attribute in the entire system, you are invited to conduct a pairwise comparison of the attributes under for different layers of objectives or criteria. The instruction of the pairwise comparison and the spreadsheet for results are provided in Attachment C.

I am grateful for your cooperation. Wish you will enjoy the survey.

Sincerely,
Sheldon Qiu
479-595-5009, sheldon.qiu@okstate.edu

Attachment A: Results from Phase I and Scoring Functions and Curves

Survey Results				
No.	**Attribute**	**Acronym**	**Adequate Threshold**	**Inadequate Threshold**
1	Total Deformation Permillage	TDP	1.5	5
2	Left Deformation Permillage	LDP	1.5	5
3	Right Deformation Permillage	RDP	1.5	5
4	Left Rut Depth (mm)	LRD	5	20
5	Right Rut Depth (mm)	RRD	5	20
6	Left Rut Width (mm)	LRW	500	1500
7	Right Rut Width (mm)	RRW	500	1500
8	Left Rut Area (square mm)	LRA	4000	25000
9	Right Rut Area (square mm)	RRA	4000	25000
10	Total Number of Water Entrapment Points	TNW	0	4
11	Total Water Entrapment Depth (mm)	TWD	5	40
12	Total Water Entrapment Width (mm)	TWW	450	1500

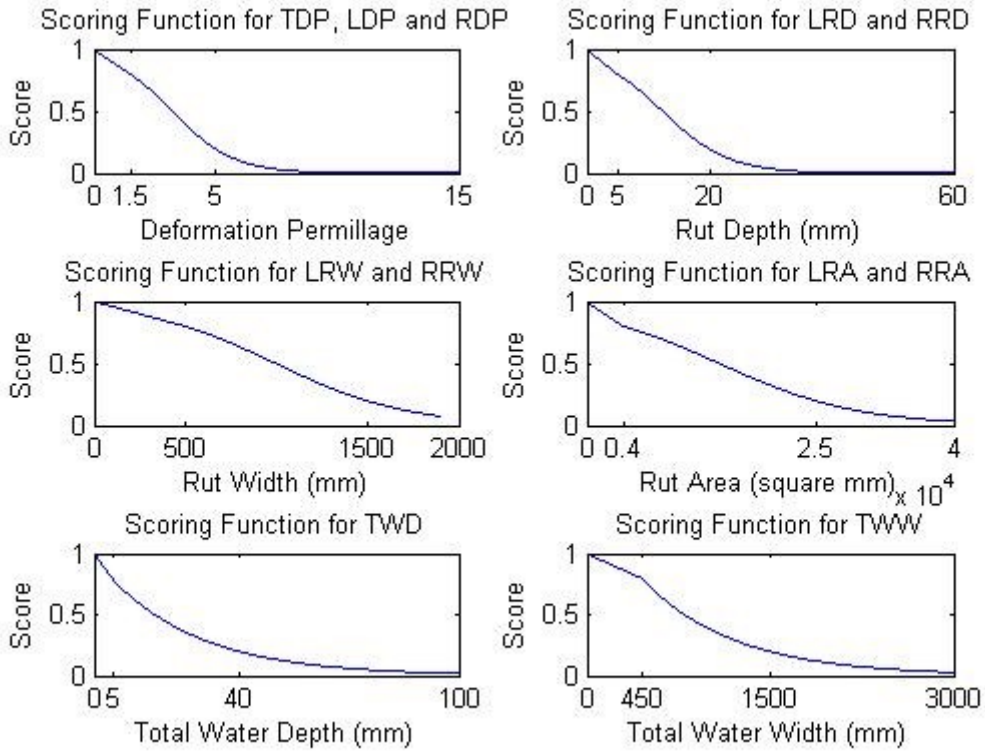

Attachment B: AHP Structure

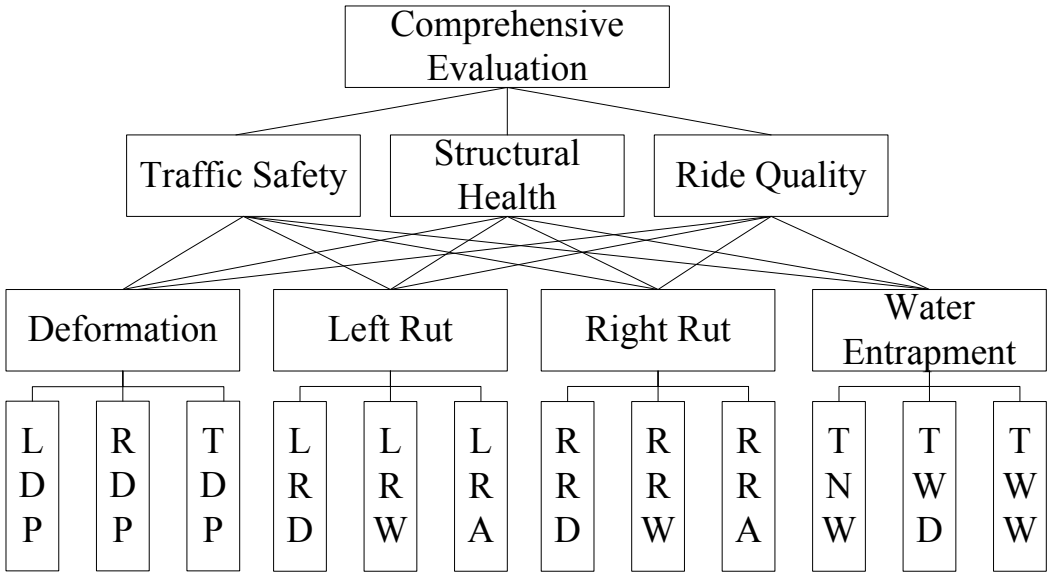

Attachment C: Pairwise Comparison Instruction

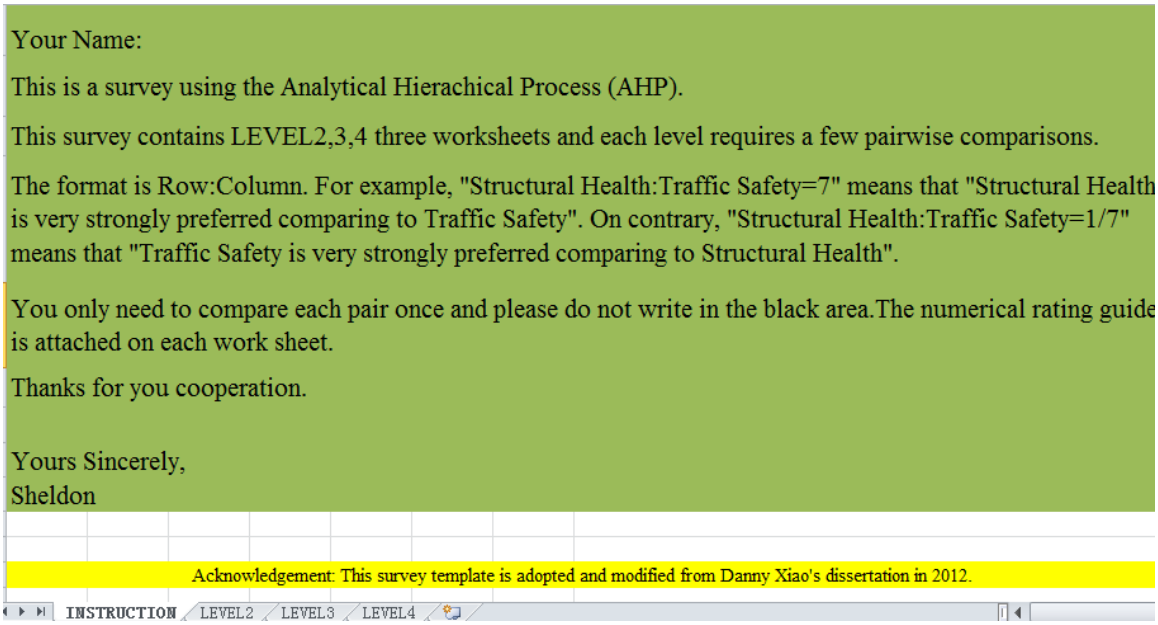

Your Name:

This is a survey using the Analytical Hierachical Process (AHP).

This survey contains LEVEL2,3,4 three worksheets and each level requires a few pairwise comparisons.

The format is Row:Column. For example, "Structural Health:Traffic Safety=7" means that "Structural Health is very strongly preferred comparing to Traffic Safety". On contrary, "Structural Health:Traffic Safety=1/7" means that "Traffic Safety is very strongly preferred comparing to Structural Health".

You only need to compare each pair once and please do not write in the black area.The numerical rating guide is attached on each work sheet.

Thanks for you cooperation.

Yours Sincerely,
Sheldon

Acknowledgement: This survey template is adopted and modified from Danny Xiao's dissertation in 2012.

INSTRUCTION LEVEL2 LEVEL3 LEVEL4

Comprehensive	Traffic Safety	Structural Health	Ride Quality
Traffic Safety	1		
Structural Health		1	
Ride Quality			1

Numerical Rating	Definition
9	Extremely Preferred
7	Very Strongly Preferred
5	Strongly Preferred
3	Moderately Preferred
1	Equally Preferred

2, 4, 6, 8 can also be used to represent the preferences between odd numbers.

Traffic Safety	Deformation	Left Rut	Right Rut	Water Entrap
Deformation	1			
Left Rut		1		
Right Rut			1	
Water Entrap				1

Structural Health	Deformation	Left Rut	Right Rut	Water Entrap
Deformation	1			
Left Rut		1		
Right Rut			1	
Water Entrap				1

Ride Quality	Deformation	Left Rut	Right Rut	Water Entrap
Deformation	1			
Left Rut		1		
Right Rut			1	
Water Entrap				1

Deformation	LDP	RDP	TDP
LDP	1		
RDP		1	
TDP			1

Left Depth	LRD	LRW	LRA
LRD	1		
LRW		1	
LRA			1

Right Depth	RRD	RRW	RRA
RRD	1		
RRW		1	
RRA			1

Water Entrap	TNW	TWD	TWW
TNW	1		
TWD		1	
TWW			1

VITA

Shi Qiu

Candidate for the Degree of

Doctor of Philosophy

Thesis: MEASUREMENT OF PAVEMENT PERMANENT DEFORMATION BASED ON 1 MM 3D PAVEMENT SURFACE MODEL

Major Field: Civil (Transportation) Engineering

Biographical:

Education:

Completed the requirements for the Doctor of Philosophy in Civil Engineering at Oklahoma State University, Stillwater, Oklahoma in December, 2013.
Completed the requirements for the Master of Science in Management Science and Engineering at Beijing Jiaotong University, Beijing, China in 2009.
Completed the requirements for the Bachelor of Science in Logistics Management at Beijing Jiaotong University, Beijing, China in 2007.

Experience:

May 2012- present (Part-time): Research Assistant, Department of Civil and Environmental Engineering, Oklahoma State University
April 2012- present (Part-time): Program Assistant, Office of International Students and Scholars, Oklahoma State University
March 2009- December 2009 (Full-time): Coordinator, Tiananmen Square Background Department, The Celebration Preparatory Committee of the 60th National Day of People's Republic of China (PRC)
June 2009- June 2010 (Full-time): Executive President, Beijing Students Federation
July 2007- October 2008 (Full-time): Logistics Assistant, National Indoor Stadium of the Beijing Organizing Committee for the Games of the XXIX Olympiad (BOCOG)